Implications of GRACE Satellite Gravity Measurements for Diverse Hydrological Applications

by

Sitotaw Yirdaw-Zeleke, M.Sc., P.Eng.

A Thesis submitted to the Faculty of Graduate Studies of
The University of Manitoba
in partial fulfillment of the requirements of the degree of

DOCTOR OF PHILOSOPHY

Department of Civil Engineering
University of Manitoba
Winnipeg, Manitoba
CANADA

January 2010

©2010 - Sitotaw Yirdaw-Zeleke
All rights reserved

Thesis Advisor:

Dr. Kenneth R. Snelgrove
Faculty of Engineering and Applied Science, Memorial University of Newfoundland
Adjunct Professor, Department of Civil Engineering, University of Manitoba

Examining Committee:

Dr. Allan D. Woodbury, Department of Civil Engineering, University of Manitoba
Dr. Peter F. Rasmussen, Department of Civil Engineering, University of Manitoba
Dr. John M. Hanesiak, Centre for Earth Observation Science, University of Manitoba
Dr. Masaki Hayashi, Department of Geoscience, University of Calgary (External)

Abstract

Soil moisture plays a major role in the hydrologic water balance and is the basis for most hydrological models. It influences the partitioning of energy and moisture inputs at the land surface. Because of its importance, it has been used as a key variable for many hydrological studies such as flood forecasting, drought studies and the determination of groundwater recharge. Therefore, spatially distributed soil moisture with reasonable temporal resolution is considered a valuable source of information for hydrological model parameterization and validation. Unfortunately, soil moisture is difficult to measure and remains essentially unmeasured over spatial and temporal scales needed for a number of hydrological model applications.

In 2002, the Gravity Recovery And Climate Experiment (GRACE) satellite platform was launched to measure, among other things, the gravitational field of the earth. Over its life span, these orbiting satellites have produced time series of mass changes of the earth-atmosphere system. The subsequent outcome of this, after integration over a number of years, is a time series of highly refined images of the earth's mass distribution. In addition to quantifying the static distribution of mass, the month-to-month variation in the earth's gravitational field are indicative of the integrated value of the subsurface total water storage for specific catchments. Utilization of these natural changes in the earth's gravitational field entails the transformation of the derived GRACE geopotential spherical harmonic coefficients into spatially varying time series estimates of total water storage. These remotely sensed basin total water storage estimates can be routinely validated against independent estimates of total water storage from an atmospheric-based water balance approach or from well calibrated macroscale hydrologic models. The hydrological relevance and implications of remotely estimated GRACE total water storage over poorly gauged,

wetland-dominated watershed as well as over a deltaic region underlain by a thick sand aquifer in Western Canada are the focus of this thesis.

The domain of the first case study was the Mackenzie River Basin wherein the GRACE total water storage estimates were successfully inter-compared and validated with the atmospheric based water balance. These were then used to assess the WATCLASS hydrological model estimates of total water storage. The outcome of this inter-comparison revealed the potential application of the GRACE-based approach for the closure of the hydrological water balance of the Mackenzie River Basin as well as a dependable source of data for the calibration of traditional hydrological models.

The Mackenzie River Basin result led to a second case study where the GRACE-based total water storage was validated using storage estimated from the atmospheric-based water balance $P-E$ computations in conjunction with the measured streamflow records for the Saskatchewan River Basin at its Grand Rapids outlet in Manitoba. The fallout from this comparison was then applied to the characterization of the Prairie-wide 2002/2003 drought enabling the development of a new drought index now known as the Total Storage Deficit Index (TSDI). This study demonstrated the potential application of the GRACE-based technique as a tool for drought characterization in the Canadian Prairies.

Finally, the hydroinformatic approach based on the artificial neural network (ANN) enabled the downscaling of the groundwater component from the total water storage estimate from the remote sensing satellite, GRACE. This was subsequently explored as an alternate source of calibration and validation for a hydrological modeling application over the Assiniboine Delta Aquifer in Manitoba. Interestingly, a high correla-

tion exists between the simulated groundwater storage from the coupled hydrological model, CLM-PF and the downscaled groundwater time series storage from the remote sensing satellite GRACE over this 4,000 km^2 deltaic basin in Canada.

Contents

Title Page i

Abstract iii

Table of Contents vi

List of Figures xi

List of Tables xvii

Citations xix

Acknowledgments xx

Dedication xxiii

1 Introduction **1**

1.1 Background 1

1.2 Hypothesis 6

1.3 Objectives of the Research 6

1.4 Contributions to Scientific Research 10

2 Methodology **12**

2.1 GRACE (Gravity Recovery And Climate Experiment) 12

2.1.1 Background 12

2.1.2 Literature Review 15
2.1.3 GRACE Gravity Model 17
2.1.4 Equivalent Water Thickness 18
2.1.5 Data Source 19
2.2 Atmospheric and Hydrologic Water Budget 21
2.2.1 Background 21
2.2.2 Literature Review 22
2.2.3 Water Balance Description 25
2.2.4 Divergence 27
2.2.5 Hydrologic-based Terrestrial Water Storage Anomalies 31
2.3 Downscaling of GRACE Total Water Storage 33
2.3.1 Background 33
2.3.2 Literature Review 34
2.3.3 Artificial Neural Network (ANN) 36
2.3.4 ANN Model Training 39
2.4 Modeling of the Assiniboine Delta Aquifer 40
2.4.1 Background 40
2.4.2 Variably Saturated Groundwater Flow (ParFlow) 41
2.4.3 Common Land Model (CLM) 43
2.4.4 Shallow Overland Flow 46
2.4.5 The Assiniboine Delta Aquifer (ADA) of Manitoba 48

3 Assessment of the WATCLASS Hydrological Model Result of the Mackenzie River Basin Using the GRACE Satellite Total Water

Storage Measurement **53**

3.1 Introduction 54

3.2 Methodology 58

3.2.1 Site Descriptions 59

3.2.2 GRACE-Based Moisture Storage 60

3.2.3 Atmospheric-based Water Balance 62

3.2.4 Numerical Simulation from WATCLASS 68

3.3 Results and Discussions 71

3.4 Conclusions 81

4 GRACE Satellite Observations of Terrestrial Moisture Changes for Drought Characterization in the Canadian Prairies **84**

4.1 Introduction 85

4.2 Methods and Datasets 89

4.2.1 GRACE-Based Terrestrial Water Storage 89

4.2.2 Hydrological Storage 90

4.2.3 Dataset 94

4.3 Results and Discussion 95

4.4 Conclusions 104

5 Regional Groundwater Storage from GRACE Over the Assiniboine Delta Aquifer (ADA) **108**

5.1 Introduction 109

5.2 Methodology 113

5.2.1 Site Descriptions 114
5.2.2 Measured Groundwater Storage 115
5.2.3 GRACE-based Moisture Storage 117
5.2.4 Artificial Neural Network (ANN) Model Training 118
5.3 Result and Discussion 119
5.4 Conclusions 127

6 Modeling of the Assiniboine Delta Aquifer of Manitoba 129
6.1 Introduction 129
6.1.1 Geology 130
6.1.2 Topography and Surface Water Features 131
6.1.3 Climate 135
6.2 Coupled Model Setup 136
6.2.1 Aquifer Stratigraphy 136
6.2.2 Hydraulic Conductivity 136
6.2.3 Storativity and Specific Yield 138
6.2.4 Groundwater level 138
6.2.5 Land Cover 141
6.2.6 Initial and Boundary Condition 142
6.2.7 North American Regional Reanalysis (NARR) Data 143
6.3 Results and Discussions 147
6.3.1 Calibration 147
6.3.2 Groundwater Storage Anomalies 154
6.3.3 Groundwater Head 161

6.3.4 Unsaturated Soil Moisture Profile 164

6.3.5 Moisture Fluxes 170

6.4 Summary 174

6.5 Future Modeling Work 177

7 Summary and Conclusions **179**

References **185**

List of Figures

2.1 GRACE satellites (Source: http://www.csr.utexas.edu/grace/gallery/) 14

2.2 GRACE Satellite-to-Satellite Tracking Technique (After: Abart, 2005) 20

2.3 Schematic diagram of the hydrologic and atmospheric water budget. . 26

2.4 Vector Cross Product 29

2.5 Boundary of Mackenzie River Basin with sample moisture flux vectors 32

2.6 A schematic diagram describing the downscaling approach. The GRACE scale (top) overlain on the measured groundwater locations in the ADA (bottom). 34

2.7 Typical architecture of an artificial neural model and for a full connected feed-forward neural network (After Govindaraju, 2000) 37

2.8 Schematic of the conductance concept (left) with an interface of thickness m' , which is represented by the conductance coefficient λ in theoretical models. The more general overland flow boundary is shown on the right side (After Kollet and Maxwell, 2006). 47

2.9 Approximate location of the Assiniboine Delta Aquifer (ADA) indicated by the circle (Source: Manitoba Conservation) 49

2.10 Map of the Assiniboine Delta Aquifer (ADA) (Source: http:// www.townof carberry.ca /PDFfiles/Neepawa.pdf, Accessed on June 2005) 50

2.11 The Assiniboine Delta Aquifer Sub-basins (Source: Manitoba Conservation) 51

2.12 Assiniboine Delta Aquifer Monitoring Stations (Source: Manitoba Conservation) 52

3.1 Location of the study area (Mackenzie River Basin and its sub basins) with locations of upper air stations (circle) 60

3.2 Land cover from the CCRS-II classification (After Soulis and Seglenieks, 2007) 70

3.3 Terrestrial water storage anomalies in cm of water equivalent thickness relative to the mean storage for March 2004 (top) and October 2004 (bottom) 72

3.4 Total water storage anomalies derived from GRACE, atmospheric-based water balance technique and WATCLASS for the Mackenzie River Basin 74

3.5 Total water storage anomalies derived from GRACE, atmospheric-based water balance techniques and WATCLASS for the different Mackenzie River sub basins 80

4.1 Schematic diagram of the hydrologic and atmospheric water budget. . 91

4.2 Saskatchewan River Basin showing the Grand Rapids outlet and locations of upper air stations (circle). 95

4.3 Terrestrial water storage anomalies in cm of water equivalent thickness relative to the mean storage for October 2003 (top) and November 2003 (bottom). 96

4.4 (a) Total water storage anomalies derived from GRACE and the atmospheric-based water balance techniques with the corresponding estimated relative uncertainties in the two methods for the Saskatchewan River Basin. (b) Trends in measured monthly average precipitation and streamflow at the Grand Rapids outlet for the Saskatchewan River Basin in conjunction with the monthly computed GRACE total water storage anomalies. 98

4.5 Cumulative Total Storage Deficit (TSD) for the Saskatchewan River Basin derived from GRACE-based total water storage. 103

4.6 Total Storage Deficit Index (TSDI) computed from Equation 4.14. . . 105

4.7 Cumulative Total Storage Deficit Index (TSDI) for the Saskatchewan River Basin. 106

5.1 Location of the study area (ADA) along with the sub-basins of the aquifer and the location of the observation wells (triangle) and rain gauges (circle) superimposed over the DEM (elevation units of meters) 115

5.2 The average groundwater head (meter) distribution interpolated from the measured pizometric head for December of 2006. 116

5.3 Terrestrial water storage anomalies in cm of water equivalent thickness relative to the mean storage for April 2006 (top) and May 2006 (bottom) 120

5.4 Comparison between GRACE total water storage anomalies and measured and downscaled groundwater storage anomalies at pizometric location of G05MH048 122

5.5 Comparison between GRACE total water storage anomalies and measured and downscaled groundwater storage anomalies at pizometric location of G05MH053 123

5.6 Comparison between GRACE total water storage anomalies and measured and downscaled groundwater storage anomalies averaged over the ADA 124

5.7 Average monthly measured and downscaled groundwater storage anomalies for the months of (a) April 2003, (b) September 2005 and (c) March 2006 over the ADA 126

6.1 Geology of the Assiniboine Delta Aquifer: (a) Surficial Deposits of the Assiniboine Delta Aquifer, (b) the 3D plate of the geological units (After Frost and Render, 2002) 132

6.2 Shaded relief of the Assiniboine Delta Aquifer in conjunction with the locations of the observation wells (triangle) and the rain gauges (circle) 134

6.3 The various sub basins of the Assiniboine Delta Aquifer 135

6.4 Measured groundwater head at observation well G05LL057 within the Assiniboine Delta Aquifer 139

6.5 Measured groundwater head at observation well G05MH052 within the Assiniboine Delta Aquifer 140

6.6 Average groundwater head (m) distribution of the Assiniboine Delta Aquifer interpolated from the measured pizometric head for December 2006 140

6.7 Land cover of the Assiniboine Delta Aquifer 141

6.8 Measured and NARR Temperature within the Assiniboine Delta Aquifer for the year 1999 145

6.9 Monthly Measured and NARR Precipitation within the Assiniboine Delta Aquifer for the year 1999 145

6.10 Daily Measured and NARR Precipitation within the Assiniboine Delta Aquifer for the year 1999 146

6.11 Cumulative Measured, Adjusted and NARR Precipitation within the Assiniboine Delta Aquifer 146

6.12 Calibrated Hydraulic Conductivity (K in m/hr) values over the Assiniboine Delta Aquifer sub basins 149

6.13 Average Modeled and Downscaled Groundwater Storage of the ADA during Model Calibration 150

6.14 Modeled and Downscaled Groundwater Storages at four observation well locations in the ADA during Model Calibration 152

6.15 Simulated Vs. measured groundwater head from daily results from 15 wells (January to December 2003) 153

6.16 Spatial Distribution of Groundwater Storage Anomalies in units of cm over the ADA for the month of April 2003 155

6.17 Average Groundwater Storage Anomalies over the ADA 157

6.18 Groundwater Storages at four observation well locations in the ADA 160

6.19 Spatial Distribution of Groundwater Head (m) over the ADA for the month of May 2000 162

6.20 Groundwater Head at Selected well Locations in the ADA: Part 1 . . 165

6.21 Groundwater Head at Selected well Locations in the ADA: Part 2 . . 166

6.22 Time series Vertical Soil Saturation Profile at a Particular Location (99.31^{o}W, 49.81^{o}N) 167

6.23 Vertical Soil Saturation Profile at a Particular Location (99.31^{o}W, 49.81^{o}N) 169

6.24 Simulated surface runoff over the ADA and measured streamflow records for the Pine Creek at its outlet near Melbourne 172

6.25 Monthly moisture fluxes (Precipitation from NARR, Evapotranspiration, Surface Runoff and Groundwater Storage) over the ADA 173

6.26 Annual moisture fluxes (Precipitation from NARR, Evapotranspiration, Surface Runoff and Groundwater Storage) over the ADA 174

List of Tables

3.1 Sub basins gross drainage area of the Mackenzie River Basin as reported by Mackenzie River Basin Board (MRBB) 59

3.2 The correlation (R) of the total water storage estimates between the GRACE (G) and the Atmospheric-based water balance computation (A), the GRACE and the WATCLASS (H: hydrologic model) and the WATCLASS and the Atmospheric-based water balance computation . 77

3.3 Statistical test results (p-values) for the difference of means of the GRACE (G) and the Atmospheric-based water balance computation (A), the GRACE and the WATCLASS (H: hydrologic model) and the WATCLASS and the Atmospheric-based water balance computation . 78

3.4 Statistical test results (p-values) for the equality of variances of the GRACE (G) and the Atmospheric-based water balance computation (A), the GRACE and the WATCLASS (H: hydrologic model) and the WATCLASS and the Atmospheric-based water balance computation . 78

6.1 Average Transmissivity (T), Saturated Thickness (S) and Hydraulic Conductivity (K) of the Assiniboine Delta Aquifer sub basins 137

6.2 Calibrated and Initial Hydraulic Conductivity (K) values of the Assiniboine Delta Aquifer sub basins 148

6.3 Annual moisture fluxes (Precipitation (P) from NARR, Evapotranspiration (ET), Groundwater Storage (GWS) and Surface Runoff (R) and its percentage with respect to precipitation over the ADA 175

Citations

Large portions of Chapters 3, 4, 5 and 6 and some sections of Chapter 2 have appeared in the following papers and proceedings:

Yirdaw, S. Z., K. R. Snelgrove, F. R. Seglenieks, C. O. Agboma and E. D. Soulis, 2009: Assessment of the WATCLASS Hydrological Model Result of the Mackenzie River Basin Using the GRACE Satellite Total Water Storage Measurement. Hydrological Processes, 23:23, 3391-3400.

Agboma, C. O., **S. Z. Yirdaw** and K. R. Snelgrove, 2009: Intercomparison of the Total Storage Deficit Index (TSDI) over two Canadian Prairie Catchments. J. Hydrology, 374:3-4, 351-359.

Yirdaw, S. Z., K. R. Snelgrove and C. O. Agboma, 2008: GRACE Satellite Observations of Terrestrial Moisture Changes for Drought Characterization in the Canadian Prairie. J. Hydrology, 356:1-2, 84-92.

Yirdaw, S. Z. and K. R. Snelgrove, 2008: Regional Groundwater Storage from GRACE over the Assiniboine Delta Aquifer (ADA) of Manitoba. To be submitted to Water Resour. Res.

Yirdaw, S. Z. and K. R. Snelgrove, 2007: Modeling of the Assiniboine Delta Aquifer (ADA) of Manitoba using the Groundwater Storage from GRACE, Eos Trans. AGU, 88(52), Fall Meet. Suppl., Abstract H33D-1615.

Yirdaw, S. Z. and K. R. Snelgrove, 2007: Groundwater Storage from GRACE Over the Assiniboine Delta Aquifer (ADA) of Manitoba: Early Result, CMOS-CGU-AMS joint congress (H01-2DP.14), St. Johns, Canada (May 28 - June 1, 2007).

Yirdaw, S. Z. and K. R. Snelgrove, 2006: Validation of Regional Precipitation Minus Evaporation Using a Coupled GRACE Driven Moisture Storage and Measured Basin Runoff, Eos Trans. AGU, 87(52), Fall Meet. Suppl., Abstract GC41A-1031.

Snelgrove, K. R., **S. Z. Yirdaw**, E. D. Soulis and F. R. Seglenieks, 2005: GRACE (Gravity Recovery And Climate Experiment) Measurements For Drought Monitoring. Conference for Predicting Drought on Seasonal to Decadal Time Scales, University of Maryland, MD, (May 17-19, 2005).

Snelgrove, K. R., **S. Z. Yirdaw** and E. D. Soulis, 2004: GRACE (Gravity Recovery And Climate Experiment) Measurements of the Mackenzie River Basin Water Balance. Eos Trans. AGU, 85(47), Fall Meet. Suppl., F780.

Acknowledgments

Looking back, completing this doctoral work has been a wonderful and often overwhelming experience. For any starter, it is often difficult to know what a Ph.D. programme in engineering would entail and especially how smooth or tortuous the learning experience would be. Myriad of thoughts cloud ones mind as to what to expect or accomplish within a specific time frame, or grappling with how to write a journal article, deliver a coherent presentation, work peaceably in a team, develop a smart piece of algorithm, recover a crashed hard drive and tunnel through volumes of materials from dawn to dusk. In all these, I wish to express my unreserved gratitude to the Almighty God who has made this path so smooth, rewarding and exciting and for the great opportunity to have brought this work to a successful end. Without HIM, it would have been impossible to complete this work.

I am very grateful to my supervisor, Dr. Kenneth R. Snelgrove for his supervision, invaluable guidance, and for all the time spent reviewing and improving my manuscript. His comments and constructive criticism has enhanced this thesis in no small way. My thanks goes to my advisory committee members Dr. Allan D. Woodbury, Dr. Peter F. Rasmussen and Dr. John M. Hanesiak and my external examiner Dr. Masaki Hayashi for their time, excellent feedbacks and comments which enabled me to complete this thesis. Moreover, I wish to extend my profound and unreserved thanks to Dr. Reed Maxwell of the Lawrence Livermore National Laboratory, for the kind assistance and making me his guest at the University of Berkeley, California whilst training on the use of the coupled groundwater-surface water code. My colleague Clement Agboma is worthy of my thanks and appreciation for his time and effort in reading through and providing worthwhile feedback on this thesis. I am also

very thankful to all my friends for their support and encouragement during the whole period of my study.

Moreover, I am sincerely grateful to the University of Manitoba for awarding me the University of Manitoba Graduate Fellowship (UMGF) which enabled me to successfully complete my studies. My gratitude goes to the Prairie Adaptation Research Collaborative (PARC) for the generous award that enable me to undertake a good proportion of my Ph.D. ressearch. Many thanks go to the Atlantic Computational Excellence Network (ACEnet) team for the access and assistance with the usage of the high performance computing (HPC) facility, without which it would have been a challenge running the computationally expensive model used for my research. Immense thanks go to the staff of the Manitoba Conservation for the numerous data access they provided whilst undertaking the groundwater modeling research over the Assiniboine Delta Aquifer (ADA).

Finally, my mother, Manasib Wondie (I will always call you, "Tatye") who is worthy of my heartfelt appreciation and unparalleled gratitude for all the support from my childhood till date, you are undoubtedly the best mother anyone could possibly hope for. Your endless love and care coupled with the ceaseless prayers have honed me into the man that I am today and I am glad that I did not let down the trust you had invested in me and your dream to see me succeed academically. Mom, to say that you are the strength of my life is by all means an understatement and I will always remain indebted to you. To my beloved wife, Belaynesh Ayine, you know that you are my rock and without your patience, love and encouragement, this journey would not have been completed, I would only hope that I could reciprocate

all the love you had showered on me during my ordeal as a Ph.D. student. My brothers and sisters (Muche, Mullu, Missa, Amanuale, Birhanu, Bayu, Bethlehem and Eyerusalem), you have given me your unequivocal support throughout this study period for which my mere expression of thanks does not suffice.

Dedicated to:

my late father Yirdaw Zeleke

and

my late sister Banchamlack Yirdaw

Chapter 1

Introduction

1.1 Background

Modeling river basin hydrologic processes can be an enormous challenge especially under conditions of complex geography and topography. These are exacerbated by poorly available or absent dataset needed for modeling purposes. Most existing distributed hydrologic and land surface models require an extensive array of datasets to drive them, calibrate their internal parameters and validate their simulated outputs. As a result, the degree of a model's parameterization and complexity is heavily constrained by data availability. In light of this, new methods of generating high-quality dataset to drive highly distributed hydrologic models has become an issue of paramount importance. Within most hydrologic modeling communities, the traditional means of model calibration was essentially through intercomparison of model simulated streamflow from a specific basin outlet with the available measured streamflow record. Assessing the performance and reliability of any hydrological model solely

on a visual match of the observed and simulated streamflow records or quantitatively via performance test statistics alone might lead to flawed conclusions. This appears logically correct since it is often possible to incorrectly simulate internal state variables from a hydrologic model whose errors may cancel themselves out and yet result in correct streamflow simulations. A simple example would help to corroborate this; an incorrect hydrological model simulation that led to an overestimation of snowmelt runoff could be compensated for by an overestimation of evapotranspiration resulting in an accurate or near-accurate streamflow simulations, yet for the incorrect reasons.

Recently, a new global dataset has become available for the calibration and validation of hydrologic models. This dataset is the measured total water storages from the Gravity Recovery And Climate Experiment (GRACE) remote sensing satellite (Tapley et al., 2004a). The GRACE mission satellite platform was launched in March 2002 to measure, among other things, the gravitational field of the earth. It is the first remote sensing satellite mission that has the ability to measure integrated subsurface moisture storage under all types of terrestrial conditions. Throughout its life span, these orbiting satellites have been generating time series of mass changes of the earth-atmosphere system. Upon mission completion, this time series will be averaged to yield a highly refined picture of the earth's gravitational field which are indicative of the distribution of global mass. Usually, for hydrological applications, the emphasis is on capturing the month-to-month variation in earth's gravity which are then transformed into integrated values of watershed total water storage. The GRACE geopotential spherical harmonic coefficients, generated from raw satellite data, are subsequently converted to produce a basin's spatially varying time series of

integrated mass change. These spatial estimates of mass are then converted to water equivalent amounts and compared with monthly estimates of basin total water storage derived from traditional in-situ measurements and hydrological model outputs.

The usefulness of GRACE-derived data becomes apparent if the internal variables simulated from a hydrological model can be shown to compare well with alternative data sources such as the total water storage. This inter-comparison will enhance the confidence in the model's ability to reproduce streamflow patterns over the basin. Additionally, it is imperative to compare model results with independent data sources since model-to-model comparisons can lead to incorrect conclusions. Therefore, spatially distributed total water storage with reasonable temporal resolution is considered a valuable information source for model parameterization and validation. Moreover, spatially distributed total water storage is a vital hydrological variable that can be used for drought studies since drought characterization becomes possible if stored moisture can be measured or accurately estimated. Unfortunately, the estimation of moisture storage via watershed modeling can be challenging and sometimes yield incorrect storage estimates since these models typically transfer moisture and energy between model stores, using physically based transfer laws and conservation equations to produce streamflow hydrographs. Judging by the problem of non-uniqueness in the generation of model hydrographs, it has become increasingly imperative to ensure the representativeness of a model's output (Beven and Freer, 2001). Similarly, it is well known that total water storage is difficult to measure and remains essentially unmeasured over spatial and temporal scales needed for hydrological model applications and drought studies.

Traditionally, there are two possibilities to measure total water storage over the basin: namely, in-situ measurements and through remote sensing techniques. In-situ measurements have been used to obtain total water storage information at the point scale. These techniques provide accurate total water storage estimates but hydrological models require total water storage data that effectively represents large spatial areas. This data requirement can be realized using remote sensing techniques. In the 1970s, scientists began to hypothesize and test the potential of aircraft and satellite based remote-sensing systems for measuring hydrologically and meteorologically significant phenomena. Since then, remote sensing systems have offered the potential for measurement of soil moisture over various space and time scales. Remarkable efforts have been made to obtain soil moisture data from these techniques (Njoku and Kong 1977; Jackson et al., 1999; Wagner et al., 1999). However, most retrieval methods remain experimental because of the strong interference of vegetation and surface roughness on measurements.

In addition to the challenges in retrieving total water storage from remote sensing measurements, the techniques generally only measure unsaturated zone moisture within the first few centimeters (5-10 cm in general) of the soil profile. These measurements are meant to determine the root zone soil moisture that can interact with the atmosphere on short time scales. Most vegetation has deeper roots than 5-10 cm, at least for most of the growing season. It is only in the first few weeks of growth that root zone depth is limited to 5-10 cm. As a result, groundwater and other surface storages are difficult to retrieve using these traditional remote sensing methods. Direct measurement of integrated watershed storage via GRACE could serve

as a surrogate for the deficiencies that arises from the determination of this storage from traditional remote sensing methods and hydrological modeling. Subsequently, storages from different reservoirs (snow pack, soil moisture, groundwater and lake storage) can be used to characterize droughts that frequently affect water availability needed to support agricultural, urban, human as well as environmental water needs.

This GRACE-based total water storage measurement has potential applications in a number of environmental and hydrological studies such as those presented in this thesis. The first study, explored in Chapter 3, entails the application of the GRACE-based technique in assessing the variation in terrestrial water storage in large river basins such as the Mackenzie and Saskatchewan River Basins in Canada. Chapter 4 explores the application of the GRACE technique as a tool for drought characterization as it relates to the 2002-2003 Canadian Prairie drought. The applicability of the downscaled groundwater component from the GRACE remote sensing satellite and its utility as an alternate calibration and validation data source for a regional groundwater study over a deltaic aquifer is assessed in Chapter 5. Interestingly, one of the main science questions being addressed by this thesis is: Does the GRACE remote sensing satellite output have any potential application in regional hydrological studies? In response to this question, Chapter 6 will use GRACE total water storage results for small-scale hydrological modeling using a downscaling approach over the Assiniboine Delta Aquifer (ADA) in Manitoba where a detailed case study was undertaken.

1.2 Hypothesis

Introducing gravity measurements into hydrological studies will be accomplished by estimating the total water storage from the GRACE remote sensing satellite and validating this dataset with independent estimates of total water storage from hydrological models. Once the relationship between gravity measurement and water storage has been established, a number of hydrological applications will be demonstrated. By introducing gravity information into hydrologic studies, this thesis aims to test the following: "In an era where the parameterization of distributed hydrologic models have become rather complex and data intensive, it is anticipated that the total water storage retrieved from the GRACE remote sensing satellite would have utility as an alternate or additional data source for hydrologic applications".

1.3 Objectives of the Research

This thesis will pioneer some of the most pertinent applications of the GRACE remote sensing satellite for hydrological studies over a number of Canadian catchments of varying spatially scales. Hence, the following are the key objectives of this study;

- To estimate total water storage employing the atmospheric-based water balance technique in the Mackenzie and Saskatchewan River Basins for subsequent use in the validation of the GRACE-based total water storage estimates.

- To retrieve the total water storage from the GRACE remote sensing gravity measurements and validate it with that computed from the atmospheric-based water balance technique.

- To assess the applicability of GRACE-based total water storage in evaluating the WATCLASS hydrological model driven over the Mackenzie River Basin.

- To assess the potential use of the GRACE-derived total water storage for drought characterization in the Canadian Prairie sub-basins.

- To evaluate the utility and quality of the downscaled regional scale groundwater storage dataset from the large scale GRACE-derived terrestrial moisture storage dataset over a small deltaic aquifer.

- To drive a coupled groundwater-surface water distributed hydrological model known as CLM-PF (Common Land Model ParFlow; Maxwell and Miller, 2005) over the Assiniboine Delta Aquifer using the downscaled GRACE total water storage as a data source for coupled model calibration and validation.

The first task in this research is to estimate the total water storage using the atmospheric-based water balance approach for the Mackenzie River Basin. This approach relies on the estimation of precipitation less evaporation in conjunction with the measured runoff given at the catchment's outlet to determine the total water storage for that specific catchment. The results obtained will enable the comparison and validation of the GRACE-derived and the hydrologically-based total water storage estimates of the Mackenzie River Basin and its sub-basins. The hydrologically-based total water storage estimates were obtained from the WATCLASS (a coupled WATFLOOD (Kouwen et al., 1993) hydrological model and CLASS (Verseghy, 1991) land surface scheme) simulated over the Mackenzie River Basin. Once completed, the method will be used in the Saskatchewan River Basin, where measured streamflow

at the Grand Rapids outlet is used, to determine the basin total water storage. This will thereafter be utilized in the validation of the GRACE-based total water storage.

The next task will be centered on the evaluation of the change in total water storage from the GRACE gravity measurements similar to the approach employed by Heiskanen and Moritz (1967) and Wahr et al. (1998). This will require detailed knowledge of the many factors contributing to the gravity changes, and successful validation of the GRACE estimate with hydrological model results to identify the gravity changes in the hydrological reservoirs. The potential of the GRACE technique to monitor variations in the total water storage (groundwater, soil water, surface waters and snow) over a basin will be assessed and the result obtained will be used to characterize the recent Canadian Prairie drought.

The application of GRACE measurements in assessing regional groundwater storage will also be investigated. The significance of this storage will be explored by downscaling efforts using the measured groundwater storage available in the region. The third task therefore will be to obtain and evaluate the local groundwater storage information from coarse resolution GRACE total water storage estimates. Results of several such experiments will be tested with the storage from the measured observation well data to evaluate the performance of the downscaling scheme.

Once the total water storage validation and downscaling of the GRACE terrestrial moisture storage are completed, a groundwater hydrological model that will assess the applicability of GRACE total water storage for regional hydrological model calibration will be driven over the ADA. Finally, the calibrated model will be validated independently using the measured groundwater level data. This validation will hope-

fully provide a better explanation for the underlying reasons for the differences in model simulations and measurements. This will identify some of the key assumption and uncertainties in predicting groundwater storage, and highlight topics for further discussion and research.

To accomplish the above-mentioned objectives, this sandwich thesis is organized as follows:

- Chapter 2 details the methodologies used in this study and background literature of each method mentioned in this chapter.

- Chapters 3, 4, 5 and 6 have been generated from the published works, submitted and yet-to-be submitted articles for publication as well as papers in conference proceedings. Chapters 3 and 4 focus respectively on the validation of the GRACE total water storage over the Mackenzie River Basin and its sub basins and the application of the GRACE total water storage anomalies for drought studies in the Canadian Prairie specifically on the Saskatchewan River Basin. Finally, the downscaling of the GRACE total water storage into regional groundwater storage and the modeling of the ADA using the coupled groundwater-surface water hydrological model will be discussed in Chapters 5 and 6.

- The last Chapter (Chapter 7) offers conclusions from the different studies undertaken in catchments over Canada and summarizes the usefulness of the GRACE dataset for hydrologic applications.

1.4 Contributions to Scientific Research

The originality and scientific contributions of this research are as follows:

- A methodology for comparison of the GRACE (Gravity Recovery And Climate Experiment) total water storage with the atmospheric- and hydrologic-based water balances was developed in this thesis. This will help to address a criticism associated with the comparison of the atmospheric- and hydrologic-based water balance estimates. Moreover, it will help to guide the user on the use of the GRACE total water storage estimates for future hydrologic studies in other river basins where measured data is limited.

- The 2002 - 2003 Canadian Prairie Drought was characterized by employing the GRACE total water storage anomalies estimated over the Saskatchewan River Basin. This method will be useful for any other river basins globally where soil moisture availability is spare or non-existent thereby making such drought assessment impossible.

- The GRACE total water storage was further downscaled to local groundwater storage for use in regional hydrological studies. A hydroinformatic approach based on artificial neural network (ANN) methods was used to downscale the GRACE total water storage into local groundwater storage. This study is the first to investigate the GRACE total water storage for regional hydrological studies and signals a very promising prospect for the use of gravity data in the hydrologic community.

- The application of the GRACE gravity information for hydrological model calibration was explored over a deltaic aquifer in Manitoba. This pioneers the use of such downscaled groundwater storages for regional hydrological model parameterization.

- A coupled land surface scheme and groundwater model (CLM-PF) was used to simulate the Assiniboine Delta Aquifer. This study is the first of its kind in this area and will help to address sustainability issues of water resource on regional scales and increased our understanding of groundwater storage and soil moisture within the aquifer.

Chapter 2

Methodology

2.1 GRACE (Gravity Recovery And Climate Experiment)

2.1.1 Background

In physics, gravitation or gravity is the tendency of massive objects to accelerate toward each other. Earth's gravitational attraction keeps the moon and satellites in orbit around the Earth. The gravitational force exerted between two objects can be determined using Newton's law of gravity as given in Equation 2.1.

$$F = K\frac{m_1 \times m_2}{r^2} \tag{2.1}$$

where F is the magnitude of the gravitational force between the two objects, K is the universal gravitational constant ($6.6726 \times 10^{-11} Nm^2kg^{-2}$), m_1 is the mass of object 1 in kg, m_2 is the mass of a second object 2 in kg and r is the distance between the

two objects in m. The force of gravity is weak compared with other forces in nature, such as electric and magnetic forces, but gravity's influence is the most far-reaching and dramatic. Gravity controls many phenomena from ocean tides to the expansion of the universe. Therefore, the precise measurement of gravity is very important for geodetic applications and of a number of important aspects for global change. GRACE provides the greatest detail of measurement of the gravity field distribution over the earth that has ever been available (Tapley et al., 2004a). Since its launch in March 2002, GRACE has mapped the variation in gravity over the surface of the earth. The mission is a joint effort between the National Aeronautics and Space Administration (NASA) in USA and Deutsches Zentrum fur Luft und Raumfahrt (DLR) in Germany.

The GRACE mission makes use of two identical spacecraft flying approximately 220 km apart in a polar orbit at an altitude of 400-500 km (Figure 2.1). These spacecrafts use microwave range detectors to continually monitor their separation distance (Swenson and Wahr, 2003). The two satellites do not carry science instruments themselves but essentially become the science instrument that monitor gravity changes over the uneven distribution of mass inside the Earth (Tapley et al., 2004b). Gravity variations that GRACE detects include mass changes associated with surface and deep ocean currents, soil and groundwater storage on land, ice sheet and glaciers distribution, air and water vapor within the atmosphere and variations of mass within the solid Earth (Wahr et al., 1998). Promising results from GRACE gravity measurements are also making a significant contribution to global climate change studies (Ramillien et al., 2004). From a hydrological perspective, the GRACE remote sens-

ing satellite provides accurate estimates of changes in terrestrial water storage within large watersheds. It has the potential to monitor the variations in total water storage (ground water, soil water, surface waters (lakes, wetlands, rivers), water stored in vegetation, snow and ice) but fails to separate these components, making detailed hydrological interpretation a challenge (Rodell and Famiglietti, 2001 & 2002). The next sections of this thesis will review the recent progress towards the application of the GRACE data for hydrological studies, the challenges in the interpretation of this data and the methods used to extract the total water storage from the GRACE satellite remote sensing measurements.

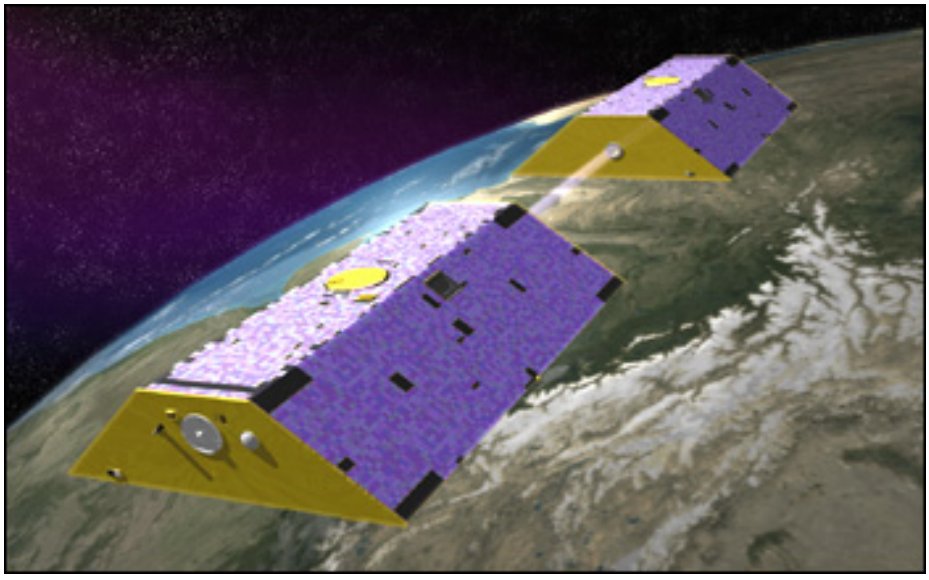

Figure 2.1: GRACE satellites (Source: http://www.csr.utexas.edu/grace/gallery/)

2.1.2 Literature Review

The time-varying gravity information from the GRACE satellite has increased our understanding of mass distribution on Earth. Understanding how Earth's mass varies over time is an important component necessary in the study of changes in global sea level, polar ice mass, deep ocean currents, as well as depletion and recharge of continental aquifers. The GRACE satellite also can assist in tracking global changes in soil moisture, an important factor in the hydrological cycle that influences climate change (Tapley et al., 2004b). Prior to and after its launch, a number of studies have been published detailing the origin and application of the Gravity Recovery and Climate Experiment (GRACE) satellite remote sensing mission. Wahr et al. (1998) noted that GRACE would provide estimates of variations in water storage to within 2 cm water thickness over land on a monthly basis. Similarly, Rodell and Famiglietti (1999) demonstrated the potential utility of these data for hydrologic studies, including its application in large ($\geq$150,000 km^2) watersheds; and they further discussed the potential of GRACE for constraining water storage in land surface models. Similar studies by Swenson and Wahr (2003) have concluded that the capability of the GRACE satellite gravity measurements for estimating monthly change in total water storage is within an accuracy of 1 cm of water thickness for regions larger than 4×10^5 km^2.

Following the release of the GRACE satellite remote sensing gravity data, the accuracy of the GRACE total water storage estimate was found to be less than expected prior to launch. As a result, new spatial smoothing or filtering techniques have been applied for noise removal. Prior to its launch, it was expected that users would apply

smoothing techniques to recover the total water storage from the GRACE dataset. For example, Wahr et al. (1998) recommended that the signal-to-noise characteristics of the GRACE gravity measurement would require averaging over large spatial domains when recovering water storage changes in specific hydrological basins. Therefore, smoothing or filtering of noise associated with GRACE errors is first required in order to make it useful for hydrological studies. Some of the studies that demonstrated the use of such smoothing techniques are described below.

Wahr et al. (2004b) pointed out that the accuracy of the GRACE total water storage estimate is 40% worse than the excepted when smoothed over a 750 km radius. They further showed GRACE's ability to recover monthly changes in water storage, both on the land and ocean to accuracies of 1.5 cm of water thickness when smoothed over 1000 km. Andersen et al. (2005a) also demonstrated the use of the GRACE data to capture the change in groundwater on inter-annual scales with an accuracy of 0.9 cm water thickness on spatial scales longer than 1300 km. Similar studies by Rodell et al. (2004) estimated that the uncertainty of the change in moisture storage is approximately 2.5 cm for a 800 km radius. Their study suggested that the initial comparisons between the GRACE gravity field solutions and water storage simulations from the Global Land Data Assimilation System (GLDAS) provide reasonable detection of global-scale changes in terrestrial water storage resulting from hydrological processes. Generally, such studies found that the water storage estimates for hydrological study need to be smoothed using a Gaussian averaging radius such as the one employed by Chen et al. (2005a) or any other filtering techniques that would help to recover the hydrological signal from GRACE. The smoothing method

suggested by Chen et al. (2005a) provides a reasonable trade-off between GRACE instrument errors that increase at shorter length scales, and smoothing and leakage errors (mass change signals originating outside of the basin) that increase with larger radii. Processing of GRACE signals continues to advance with improved noise reduction methods and extraction of non-hydrologic mass variations.

2.1.3 GRACE Gravity Model

The gravitational potential of the earth has been modeled with the Laplace equation in spherical coordinates, which is given in Equation 2.2.

$$\nabla^2 N = \frac{1}{r^2}\frac{\partial}{\partial r}\left(r^2\frac{\partial N}{\partial r}\right) + \frac{1}{r^2\sin\theta}\frac{\partial}{\partial\theta}\left(\sin\theta\frac{\partial N}{\partial\theta}\right) + \frac{1}{r^2\sin^2\theta}\frac{\partial^2 N}{\partial\phi^2} = 0 \tag{2.2}$$

where N is the gravitational potential, r is the distance from the origin of the coordinate system, θ is the latitude, and ϕ is the longitude. The gravitational potential of the earth is commonly described in terms of the shape of the geoid. A geoid, often referred to as a close representation or physical model of the earth's shape, is an equipotential surface which approximately coincides with the mean ocean surface. Outside of the attracting masses, the geoid shape (N) can be expanded into a series of spherical harmonics (Heiskanen and Moritz, 1967). This expansion is expressed as:

$$N(t) = a\sum_{l=0}^{l_{max}}\sum_{m=0}^{l} P_{lm}(\cos(\theta))\left[C_{lm}(t)\cos(m\phi) + S_{lm}(t)\sin(m\phi)\right] \tag{2.3}$$

where a is the mean radius of the Earth, θ and ϕ are latitude and longitude and $C_{lm}(t)$ and $S_{lm}(t)$ are time dependent dimensionless harmonic coefficients, the coefficients provided to GRACE users at monthly time steps. Variables l and m are the harmonic

degree and order, respectively, while l_{max} is the maximum harmonic degree used to compute the geoid. P_{lm} is the normalized Legendre function required for the solution (Heiskanen and Moritz, 1967).

The time varying geoid anomaly aids the study of fluid contributions to the gravity field. The anomaly can be determined from the monthly geoid $N(t)$ measured by GRACE satellite compared to the static mean component N_0 (Ramillien et al., 2004) (Equation 2.4).

$$\Delta N(t) = N(t) - N_0 \tag{2.4}$$

Several months or years of average GRACE measurements or any accurately determined gravity model could be used as the static mean component (N_0). Generally, it characterizes the main contribution to the gravity field as the solid part of the Earth.

2.1.4 Equivalent Water Thickness

The observed gravity from GRACE satellite is commonly expressed in geoid coefficients. The monthly changes in mass can be thought of as concentrated in a very thin layer of water on the geoid surface, whose thickness changes in time. Much of this monthly change in gravity is due to changes in total water storage in hydrologic reservoirs such as groundwater, unsaturated soil moisture, surface water (lakes and rivers), snow accumulation and atmospheric moisture storages. As a result, it is useful to express the mass change from the GRACE measurements in terms of equivalent water thickness. Wahr et al. (1998) determined the surface density mass as the surface of the Earth in terms of equivalent water thickness. They found a simple relation between the surface density coefficients and its equivalent water thickness as shown

in Equation 2.5.

$$C^w_{lm}(t) = W_l \times C_{lm}(t)$$

$$S^w_{lm}(t) = W_l \times S_{lm}(t) \tag{2.5}$$

where

$$W_l = \frac{\rho_{avg}}{3\rho_w}\frac{2l+1}{1+k_l}$$

Combining Equations 2.4 and 2.5 results in Equation 2.6 that expresses the change in surface mass in terms of equivalent water thickness ($N^w(t)$).

$$N^w(t) = \frac{a\rho_{avg}}{3\rho_w}\sum_{l=0}^{l_{max}}\sum_{m=0}^{l} P_{lm}(\cos(\theta))\frac{2l+1}{1+k_l}\left[C_{lm}(t)\cos(m\phi) + S_{lm}(t)\sin(m\phi)\right] \tag{2.6}$$

where ρ_{avg} is the average density of the earth (5517 kg/m^3), ρ_w is the density of water (1000 kg/m^3) and k_l is the Elastic Love Number (ELN). The ELNs describe the underling solid earth. These deformations yield additional geoid contribution in addition to the direct gravitational attraction of the surface mass. ELN values were taken directly from Wahr et al. (1998).

2.1.5 Data Source

As mentioned in the previous sections, the GRACE satellite vehicles are the science instrument used to monitor the gravity change from an uneven distribution of mass inside the earth. It measures gravity through a Satellite-to-Satellite Tracking (SST) technique. The technique is based on the highly precise measurement of the range between two satellites. One satellite follows the other on the same orbital track (Figure 2.2), separated by some 220 km, which is measured with very high precision.

This high precision measurement of separation and its rate of change is achieved through the use of a microwave K-Band ranging system that links the two satellites. A SuperSTAR accelerometer is also housed on both satellites in order to measure nonconservative accelerations like air drag, solar radiation pressure, etc., acting on the satellites (Reigber et al., 2005). This helps to obtain a precise gravity field model of the earth. The other major component of the GRACE satellite is the Global Positioning System (GPS) receiver. This component determines precise orbital data, which is fundamental for gravity field determination and is also responsible for time tagging all payload data.

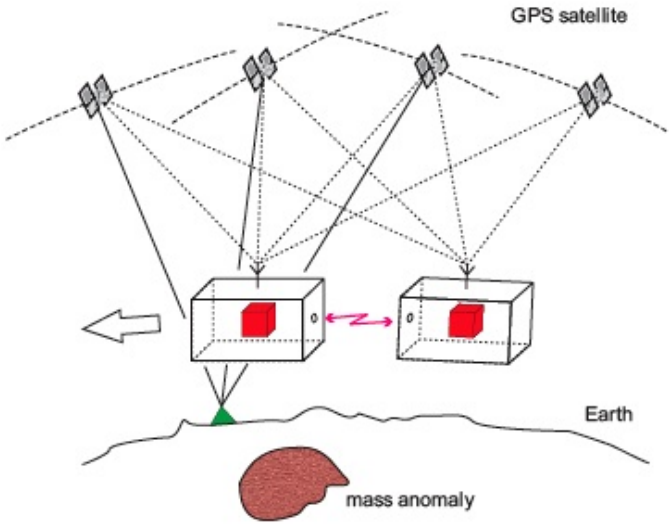

Figure 2.2: GRACE Satellite-to-Satellite Tracking Technique (After: Abart, 2005)

The GRACE research teams at UTC (University of Texas Center for space research), GFZ (GeoForschungsZentrum Potsdam) and JPL (Jet Propulsion Laboratory) use all these data sources to separately process the gravity harmonic coefficients

($C_{lm}(t)$ and $S_{lm}(t)$) into a product that is known as level 2 data. These data sets are provided for GRACE users free of charge.

2.2 Atmospheric and Hydrologic Water Budget

2.2.1 Background

Atmospheric-based water balance is often used to evaluate watershed moisture storages, land-atmosphere interactions, groundwater recharges, and droughts. It is the moisture change in a large region determined by monitoring the moisture flux across the boundaries of a region. Vertically, a region is bounded by the earth's surface at the bottom and the top of the atmosphere from above (defined at a specified atmospheric pressure) and horizontally by an arbitrary polygon (i.e. a state, country or a river basin boundary) extending from the earth's surface to the top of the atmosphere. In general, the atmospheric water balance is the inflow and outflow of water vapor flowing over a region, coupled to the rate at which liquid water is being added to or removed from the atmosphere by means of evaporation and precipitation (Reed et al., 1997). Similarly, the hydrologic water balance is the amount of water entering and leaving the land surface plus the change in water stored in the land surface. The main components in the hydrological water balance are precipitation, evaporation, storage of water in deeper portions of the soil not accessible to plants, runoff from the ground surface, snow storage, and moisture stored in unsaturated soil. These two water balance computational methods (Atmospheric and Hydrologic) equate to precipitation less evaporation at the land surface.

By estimating the precipitation minus evaporation from the atmospheric-based water balance and coupling this estimate with the measured streamflow at the outlet of the basin, it is possible to quantify the change in basin total water storage. Similarly, the basin total water storage can be estimated from traditional hydrological models using evaporation estimated from the model, precipitation used as an input to the model and runoff estimated from the model or measured at the outlet of the basin. The comparison of the basin total water storage estimated from these two independent techniques help to better understand mechanisms associated with global water circulation and water balance of a particular basin. For areas where measured data is limited or sparse, this serves as a dataset for calibration and validation of hydrological models that simulate basin streamflow and other hydrological variables such as moisture stored in the soil. Furthermore, the total water storage estimated from the atmospheric-based water balance approach helps to validate the GRACE-based total water storage estimates, which is one of the focuses of this thesis. The following sections present a detailed review of these two techniques and the methodology associated with the mathematical comparison of the total water storage estimated from these two approaches with that of GRACE-based estimate.

2.2.2 Literature Review

The simulation of the water balance of the atmosphere and the land surface is very important for many hydrological and atmospheric studies. It is used to evaluate land-atmosphere interactions, evaluate the regional and global water circulation and balance (Milly, 1994; Milly and Dunne, 1994), estimate groundwater recharge, vali-

date Global Circulation Model (GCM) grid scale hydrological models, and interpret model forecasts for water resources and climate change assessment. Therefore, it is important to estimate the water balance of the atmosphere and the land surface with acceptable accuracy, as it is a fundamental aspect of the hydrological cycle. Currently, there are many documented studies that seek to observe or estimate evaporation and precipitation over large spatial scales using radar or satellite remote sensing techniques. These approaches complement traditional methods of estimating the water balance using observed data at the ground surface. However, it is still difficult to obtain reliable estimates. On the other hand, water balance estimation using atmospheric data is becoming less problematic due to the increasing availability of high-resolution atmospheric data (Oki et al., 1995).

A number of studies have been undertaken detailing the use and uncertainties of estimating the hydrological fluxes at river basin, continental, and global scales (Rasmusson, 1967; Brubaker et al., 1994; Oki et al., 1995; Hu and Feng, 2001; Bosilovich and Schubert, 2002; and Alberto et al., 2005). For example, Rasmusson (1967) and Hu and Feng (2001) analyzed the characteristics of total water vapor flux fields over North America and the seas of Central America. A similar study by Brubaker et al. (1994) observed vapor flux transport at sub-monthly time scales and noted a significant pole-ward eddy flux transport from the Gulf of Mexico, particularly during winter months. Their study further concluded that the use of monthly-averaged or sparse data might significantly underestimate the eddy flux component of vapor transport. Bosilovich and Schubert (2002) identified alternate sources of moisture transported into the central United States, including evaporation from the Gulf of Mexico, the

Caribbean Sea, and the tropical Atlantic Ocean east of the Caribbean. A more recent study by Alberto et al. (2005) quantified the uncertainties of calculated moisture flux divergence due to the design of the boundary of an area, mathematical algorithms, as well as spatial and temporal resolutions using high resolution observations. These observations were obtained from the NCEP (National Centers for Environmental Prediction) Eta high-resolution regional analysis, and the NCEP/NCAR (National Centers for Atmospheric Research) coarse-resolution global reanalysis data.

Some studies use water balance approaches to evaluate the interaction between the atmospheric- and hydrologic-based water budgets. Kite et al. (1994) used the outputs (precipitation, temperature, and evaporation) from a GCM as input to a hydrological model to generate streamflow from the Mackenzie River and to verify the performance of the GCM. Kite and Haberlandt (1999) also compared hydrological model output using data from various atmospheric models such as GCM and Numerical Weather Prediction (NWP) models for a number of river basins and examined the use of archived atmospheric model data to force hydrologic models. Strong et al. (2002) made a more realistic comparison of the land surface water budget using the atmospheric-based water budget together with the streamflow record. They demonstrated significant advances towards monthly closures of the water balance compared to previous studies. However, the comparison using observed discharge suffers primarily from errors due to undetected diurnal component in the atmospheric data. This resulted in a +21% bias of average annual difference between atmospheric- and hydrologic-based estimates of the precipitation less evaporation. Individual monthly differences of precipitation less evaporation occasionally varied between 30 - 50%

of hydrologic precipitation less evaporation. Such studies can benefit from inter-comparisons with independently measured or estimated hydrological variables similar to the GRACE-based total water storage. The GRACE-based terrestrial water storage mentioned in the previous section (Section 2.1) will help to overcome the criticism of lack of validation data for atmospheric- and hydrologic-based water balance estimates.

2.2.3 Water Balance Description

Atmospheric water budget studies (Strong et al., 2002; Walsh et al., 1994) attempt to calculate the evaporation (E) $[m/s]$ less precipitation (P) $[m/s]$ based on the net advection of the atmospheric moisture through a closed atmospheric volume. From an atmospheric perspective this is expressed as:

$$\frac{\partial W}{\partial t} + \nabla \cdot Q = -(P - E) \tag{2.7}$$

where W $[m]$ is the water content in an atmospheric column, $\nabla \cdot Q$ is the divergence or net outflow of water vapour across the side of the atmospheric column, and Q $[m/s]$ is the vertically integrated flux of specific humidity derived from wind and humidity measurements. The divergence measures the difference between inflow and outflow to a region, in other words, it measures the rate at which fluid is being transported into or out of the region at any given point in time. A positive divergence means that outflow is greater than inflow, and a negative divergence (or convergence) means that inflow is greater than outflow.

Similarly, the land surface water balance can be compared with the atmospheric water balance by formulating a similar equation. From the land surface perspective

the water balance can be expressed in a similar fashion as:

$$\frac{\partial S}{\partial t} + R = P - E \tag{2.8}$$

S $[m]$ is the depth of liquid water stored in the basin, R $[m/s]$ is the water that leaves the basin as surface or subsurface runoff, E $[m/s]$ is the evaporation, and P $[m/s]$ is the precipitation. Combining Equations 2.7 and 2.8 yields the expression given in Equation 2.9 with a graphical presentation shown in Figure 2.3.

$$-\left(\frac{\partial W}{\partial t} + \nabla \cdot Q\right) = \left(\frac{\partial S}{\partial t} + R\right) = (P - E) \tag{2.9}$$

Therefore, the negative of the divergence combined with the precipitable atmospheric

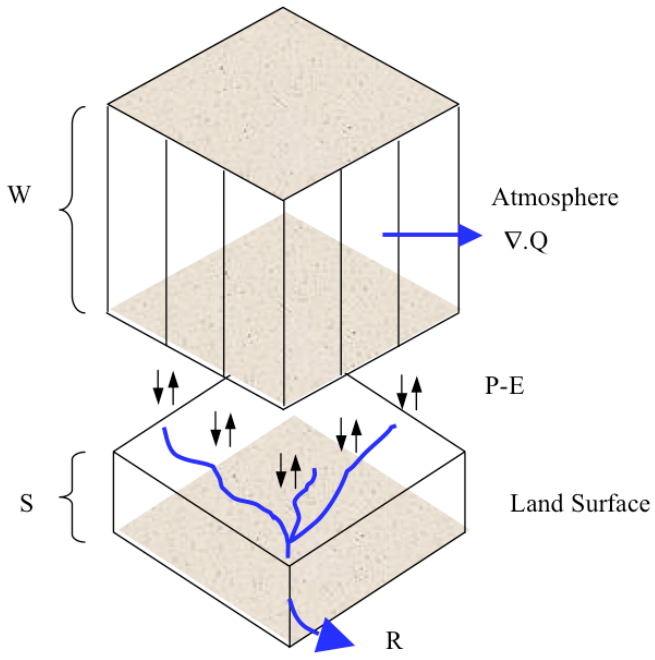

Figure 2.3: Schematic diagram of the hydrologic and atmospheric water budget.

water provides an estimate of the change in water storage in the basin and the measured or modeled runoff. This is equivalent to the precipitation minus evaporation over the basin. The precipitable atmospheric water content is computed as:

$$W = \frac{1}{\rho g} \int_{p_s}^{p_t} q dp \tag{2.10}$$

where q is the specific humidity $[kg/kg]$, p is the pressure $[kg \times m/(s^2 m^2)]$, g is the gravitational constant $[m/s^2]$ and ρ is the density of water (kg/m^3). The limits of integration are the surface pressure (p_s) and the pressure at the top of the atmosphere (p_t). The computation of the divergence in Equation 2.9 is detailed in the following section.

2.2.4 Divergence

There are two methods that can be used to compute the divergence or the atmospheric flux that is used for estimating the atmospheric water balance. The methods are direct computation and flux integration approaches. They use the same input data but approach the solution in a different fashion. Utilizing these two approaches will help to illustrate results obtained before using Equation 2.9. The following equations are used to compute the divergence in Cartesian and Spherical coordinates.

$$\nabla \cdot Q = \frac{\partial Q_u}{\partial x} + \frac{\partial Q_v}{\partial y} \tag{2.11}$$

$$\nabla \cdot Q = \frac{1}{R_e \cos\phi} \left(\frac{\partial Q_\lambda}{\partial \lambda} + \frac{\partial (Q_\phi \cos\phi)}{\partial \phi} \right) \tag{2.12}$$

The vertically integrated vapour fluxes Q_u and Q_v are estimated from Equations 2.13 and 2.14.

$$Q_u = -\frac{1}{\rho g}\int_{p_s}^{p_t} qudp \tag{2.13}$$

$$Q_v = -\frac{1}{\rho g}\int_{p_s}^{p_t} qvdp \tag{2.14}$$

Q_u and Q_v are the east-west and north-south components of vapor flux in $[m^2/s]$, respectively, and u and v are the zonal and meridian components of wind velocity $[m/s]$. R_e is the mean earth radius $[6.3712 \times 10^6\ m]$, Q_λ and Q_ϕ are the zonal and meridional components of vapor flux $[kg/(ms)]$, and λ and ϕ are the longitude and latitude in radians. Kreyszig (1993) developed a methodology to derive the spherical form of the divergence equation. The following center difference approximation is used to calculate divergence directly from gridded data.

$$\nabla{\cdot}Q(i,j) = \frac{1}{R_e\cos(\phi_j)}\left(\frac{Q_{\lambda(i+1,j)} - Q_{\lambda(i-1,j)}}{\lambda_{(i+1)} - \lambda_{(i-1)}} + \frac{\cos(\phi_{j+1})Q_{\phi(i,j+1)} - \cos(\phi_{j-1})Q_{\phi(i,j-1)}}{\phi_{j+1} - \phi_{j-1}}\right) \tag{2.15}$$

The second method of calculating the moisture flux across line segments that make up a basin boundary is called flux integration approach. This method estimates the flux across any arbitrarily boundary using an important theorem in vector analysis known as the Divergence theorem or the Gauss theorem (Kreyszig, 1993, p. 545, 551). The theorem states that the flux of a vector field on a surface is equal to the triple integral of the divergence of the region inside the surface. Intuitively, it states that the sum of all sources minus the sum of all sinks gives the net flow out of a region. Similarly, a three dimensional problem can be reduced into a two dimensional problem through vertical integration of the vapor flux. Therefore, the Divergence

theorem in two dimensions can be written as:

$$\nabla \cdot Q = \frac{1}{A} \oint Q \cdot n_i dl \tag{2.16}$$

Variable n is the normal vector in the i dimension. The vector dot-product of Equation 2.16 (the right hand side) can be evaluated by applying a vector cross-product to each border segment and summing the result for each segment to determine the net flux into the atmosphere (Reed et al., 1997). This concept is illustrated in Figure 2.4.

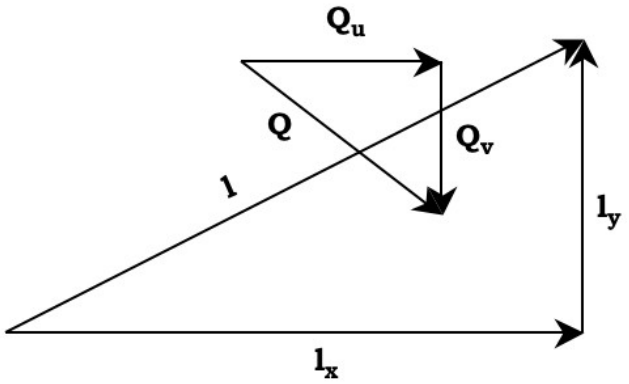

Figure 2.4: Vector Cross Product

The cross product of the two vectors l and Q is denoted by $l \times Q$. It is defined as the vector which is perpendicular to both l and Q with a magnitude equal to the area of the parallelogram they span. The vector $l = (l_x, l_y)$ defines the boundary line in $[m]$ whereas the vector $Q = (Q_u, Q_v)$ defines the atmospheric moisture flux in $[kg/(ms)]$. The vector cross product in Equation 2.17 determines the mass flow rate across a boundary segment in $[kg/s]$.

$$Q_l = l \times Q = k(l_x Q_v - l_y Q_u) \tag{2.17}$$

To calculate the moisture flux vectors that are represented in Figure 2.4, the boundary segments, which make up the border, are defined so that they all point in clockwise directions; the interior of the region is to the right of each boundary vector and the exterior of the region is to the left of each boundary vector. From the right hand rule, the result of the vector cross product is a vector oriented in the vertical direction. The outflow and inflow of the moisture flux from and to the basin are determined based on the sign of the vector. If the vector is positive, this indicates moisture is leaving the region and if this vector is negative, this indicates moisture is entering the region. The total outflow is determined by summing the magnitudes of all Q_l vectors pointing in the positive k direction whereas the total inflow is determined by summing the magnitudes of all Q_l vectors pointing in the negative k direction. The net flux or divergence is outflow minus inflow of the resulting vector Q_l.

Degrees of latitude are parallel so that the distance between each degree remains virtually constant. However, degrees of longitude are farthest apart at the equator and converge at the poles so that their distance varies greatly with latitude. Therefore, the geographic space and the geometric relationship between the flux vectors and border segments are determined in geographic space. The lengths of the border components $|l_x|$ and $|l_y|$ correspond to the length of these segments as measured along the surface of the earth and are estimated from the given latitude and longitude of segment endpoints. The length of a radian of longitude and a radian of latitude on the earth's surface with the earth represented as an ellipsoid were multiplied by the difference between the longitude and latitude of the two segment endpoints as shown in Equations 2.18 and 2.19.

$$|l_x| = \frac{a \times \cos\phi}{(1 - e^2 \sin^2\phi)^{15}} \triangle\lambda \tag{2.18}$$

$$|l_y| = \frac{a(1 - e^2)}{(1 - e^2 \sin^2\phi)^{15}} \triangle\phi \tag{2.19}$$

where a is the radius of curvature for the ellipse in the plane of the equator ($a = 6378206.4\ m$), e is the eccentricity ($e = 0.000045815$), and $\triangle\lambda$ and $\triangle\phi$ $[radians]$ are the longitudinal and latitudinal difference between segment end points, respectively.

The outline of the region, the land surface and the top of the atmosphere define the control volume over which the physical laws can be applied. Required are the boundary conditions to define an atmospheric column for vapor flux calculations. This boundary is often chosen as a river basin generalized by dividing it into straight segments, each with a length of approximately l_x and l_y. The watershed boundary is extended vertically from the surface to the top pressure level of the atmosphere (usually 10 mb). An example showing the extent of the boundary of the Mackenzie River basin over which the divergence was calculated using the flux integration approach is presented in Figure 2.5. The arrows are the zonal moisture flux vectors explained above.

2.2.5 Hydrologic-based Terrestrial Water Storage Anomalies

Hydrologists often deal with measured quantities of the water budget in terms of their time variant quantities; therefore one can express Equations 2.8 and 2.9 in hydrologic units as:

$$\frac{\Delta S}{\Delta t} = P - E - R$$

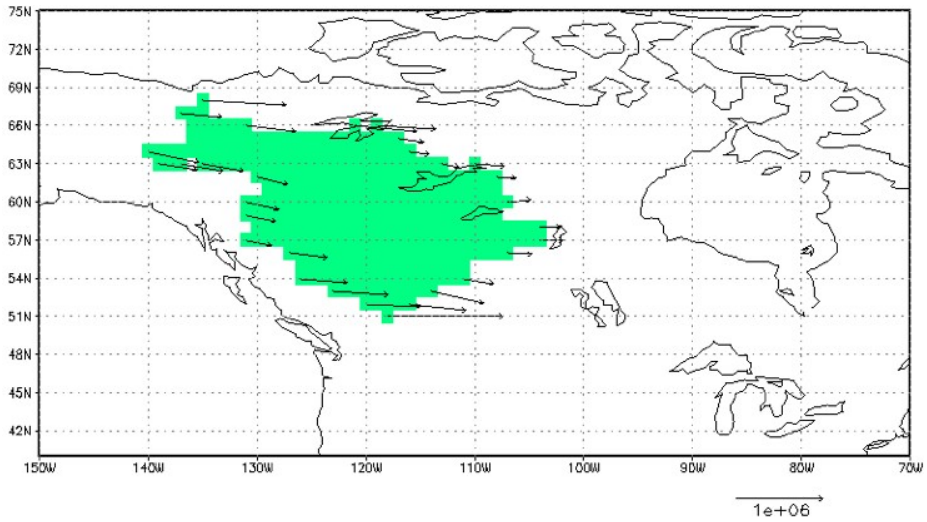

Figure 2.5: Boundary of Mackenzie River Basin with sample moisture flux vectors

$$\frac{\Delta S}{\Delta t} = -\left(\frac{\partial W}{\partial t} + \nabla \cdot Q\right) - R \tag{2.20}$$

where ΔS is the change in water content over a given time interval (Δt). The runoff (R) incorporates the surface as well as the baseflow components. It is worthwhile emphasizing at this point that $\frac{\Delta S}{\Delta t}$ which is of key interest to hydrologists is not the direct resultant of GRACE measurement, but rather storage anomalies that require further differentiation with time to form the desired result. Hence, in order to compare the total water storage anomalies from the GRACE-based and atmospheric- or hydrologic-based approaches, the total water storage anomaly in a hydrologic reservoir should be computed as:

$$S_n = S_{n-1} + \left(\frac{\triangle S}{\triangle t}\right)_n \tag{2.21}$$

where S_n is the storage anomaly for the current time (month, week or day), S_{n-1} is the storage anomaly for the previous time and $\frac{\Delta S}{\Delta t}$ is the average moisture storage for the current time obtained from Equation 2.20. These anomalies are equivalent to storage anomalies from GRACE, which are averaged over approximately one month periods and used for comparison with storages estimated from the other two methods (GRACE-based and hydrologic- or atmospheric-based total water storages).

2.3 Downscaling of GRACE Total Water Storage

2.3.1 Background

Downscaling is based on the view that larger, continental or even planetary scales condition regional information. This information cascades down from larger to smaller scales (Figure 2.6). In general, it can be defined as the disaggregation of spatial information with a change from macro-scale or mesoscale to a finer scale (Becker and Braun 1999). There are a number of downscaling techniques that can be used for different applications, but in practice two major classifications can be identified, namely deterministic and statistical procedures. Deterministic procedures are based on the distribution of spatial patterns whereas statistical procedures use stochastic distribution functions based on empirical relationships of features between the two scales (Hay and Clark, 2003). The following sections present a literature review on various downscaling techniques that can be used for such studies.

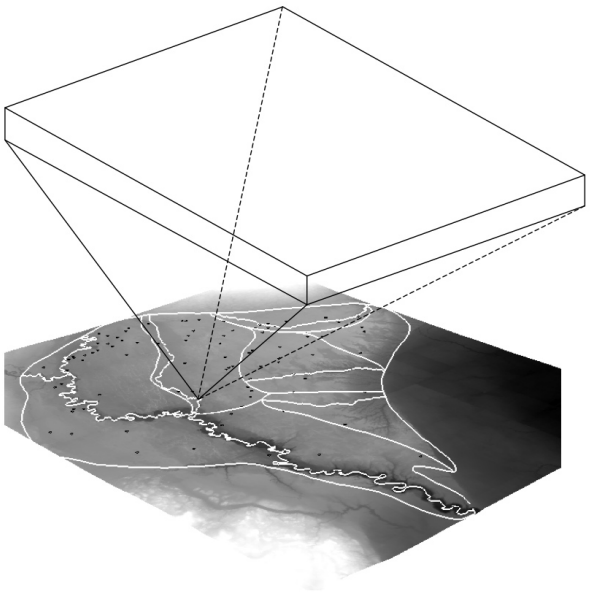

Figure 2.6: A schematic diagram describing the downscaling approach. The GRACE scale (top) overlain on the measured groundwater locations in the ADA (bottom).

2.3.2 Literature Review

Traditionally, downscaling methods have been used in the fields of climatology and meteorology to obtain regional information (precipitation, temperature, etc.) from remotely sensed data and coarse resolution climate model output. However, only a few studies, including Reichle et al. (2001), Kim and Barros (2002), Pellenq et al. (2003) and Lavado et al. (2006) have dealt with the feasibility of disaggregating low resolution soil moisture to a finer scale. For a successful application of a downscaling method, the above studies have determined relationships between the large-sacle and local-scale characteristics. For example, Reichle et al. (2001) investigated the possibility of simulating high resolution soil moisture from lower resolution passive microwave measurements using data assimilation techniques. The applied downscaling

method used in their study showed that soil moisture can be satisfactorily estimated at scales finer than the resolution of the passive microwave images, provided that micrometeorological, soil texture, and land cover input data are available at the finer scale. Their study essentially mapped large scale information onto finer scale features.

Other studies by Kim and Barros (2002) examined the downscaling potential of large scale remotely sensed soil moisture data in order to determine the temporal and spatial variability of soil moisture. Their study demonstrated that the downscaling method used captured all the basic statistical and scaling behavior of soil moisture at the higher resolution for a wide range of environmental conditions (wet and dry soils). Pellenq et al. (2003) also applied a similar method to disaggregate soil moisture data. Their downscaling algorithm used topography and soil depth to successfully downscale soil moisture data. Lavado et al. (2006) used an alternate approach for downscaling near surface soil moisture using digital terrain modeling and artificial neural networks. Their approach used digital models of topography and land cover as inputs and a series of soil moisture measurements as training data. Their study further suggested that artificial neural network techniques provide an efficient analytical data procedure for elucidating the spatial pattern of non-linear processes such as those related to near-surface soil moisture. In general, such studies suggested that fine scale moisture storage can be estimated from low-resolution soil moisture provided that other high resolution environmental and geophysical data are available. Because of the ability of artificial neural networks to resolve non-linear processes, this thesis proposes to use a hydroinformatic approach based on artificial neural networks (ANN) to downscale GRACE-based moisture storages to regional groundwater storage.

2.3.3 Artificial Neural Network (ANN)

The basic principle behind the artificial neural network (ANN) method is that many different processing elements are utilized by creating intertwined connections in a similar fashion to communication between single neurons in a biological brain (Haykin, 1994). These elements represent highly simplified mathematical models of neural networks. Each neuron may receive tens of thousands of input signals with only a single output signal being produced using an internal weighting system. This output may then be sent as input to another neuron. Neurons are interconnected and organized into a series of layers. For instance, the input layer receives raw inputs while the output layer produces the processed output. Usually one or more hidden layers are distributed between the input and output layers similar to those shown in Figure 2.7. They are widely used as an effective approach for handling non-linear and noisy data and are especially useful in situations where physical processes are not fully understood. They are particularly well suited for modeling complex systems on a real-time basis.

Mathematically, ANN can be expressed as follows: if the input vector to a layer is $X = (x_1, ..., x_i, ...x_n)$ and the weight vector is $W_j = (w_{1j}, w_{ij}, ...w_{nj})$, then the output vector becomes:

$$y_j = f\left(X.W_j - b_j\right) \tag{2.22}$$

where b_j is the bias associated with the neuron j, and f is an activation function of each node in the hidden layers which determines the response of a node to a total input signal.

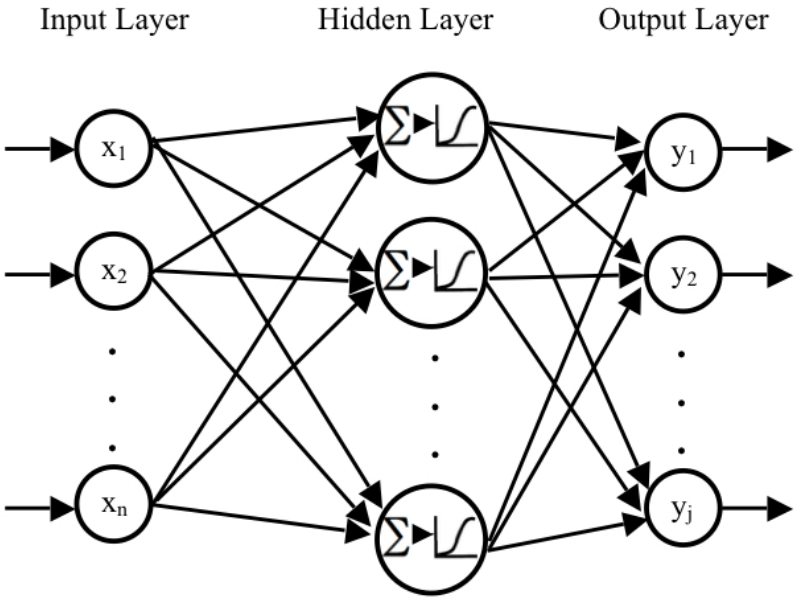

Figure 2.7: Typical architecture of an artificial neural model and for a full connected feed-forward neural network (After Govindaraju, 2000)

The most commonly used activation function is a sigmoid function given by

$$f_j\left(t+1\right) = \frac{1}{1+e^{-(\sum w_{ij} o_i(t) - b_j)}} \tag{2.23}$$

where $f_j\left(t+1\right)$ is the activation function of neuron j in layer L at time step $(t+1)$, w_{ij} is the weight of connection between unit i in the previous layer $(L-1)$ and unit j in layer L, o_i is the output of unit i in layer $(L-1)$, and b_j is the bias of unit j in layer L. This function enables a network to map nonlinear processes. Once established, the network is trained using an observed dataset $[X^n\ t^n]_{n=1}^N$ through the adjustment of network parameters (weights and biases) to minimize an error function such as,

$$E = \sum_{n=1}^{N} \left(y^n\left(x^n; w; b\right) - t^n\right)^2 \tag{2.24}$$

where t^n is a component of the desired output T; y^n is the corresponding ANN output.

Normally, the network training starts with an initial set of weights and biases and ends with a single best set of weights and biases through an iterative optimization process. The manner in which the nodes of an ANN are structured is closely related to the algorithm used to train the model. For this thesis, a feed-forward algorithm is used to train the model.

ANN can be characterized as computational models with properties including the ability to learn from examples, to generalize, or to cluster, to organize data, to adapt solutions, and process information rapidly (Jain et al., 2004). Because of these advantages, the method has been used to represent complex functions in various fields of application including pattern recognition, forecasting, classification, speech recognition, and control systems. In hydrology, ANN have been successfully used for rainfall runoff modeling (Khan and Coulibaly, 2006), reservoir inflow prediction (Jain et al., 1999), unsaturated soil hydraulic properties estimation (Jain et al., 2004), and reference crop evaporation prediction (Kumar et al., 2002).

Furthermore, ANN have been widely applied in downscaling of coarse resolution data to a finer scales. For example, it has been used to downscale global climate models (GCMs) output for hydrological studies (Weichert and Burger, 1998; von Storch et al., 2000; Schoof and Pryor, 2001; and Dibike and Coulibaly, 2006). The basic premise of this approach is to convert GCM outputs to simulated localized meteorological observations at the watershed scale. In general, downscaling of GCM output using ANN requires predictor variables derived from GCMs, such as wind speed and geopotential height as inputs and local meteorological observations as outputs during model training and validation.

ANN addresses many of the non-linearities in physical systems described above and therefore, will be used to downscale GRACE total water storage into local groundwater storage. Although previous studies indicate that ANN are useful in downscaling coarse resolution variables, some disadvantages have been documented as well. Large quantities of data are required for successful use of ANN. This requirement cannot always be met, as measured variables often lack sufficient observation history. In addition, the relationship between input and output does not take advantages of the user's judgment. As a result, ANN models tend to be viewed as black box or input/output table driven without physical basis.

2.3.4 ANN Model Training

As was mentioned in Section 2.3.3, the approach taken in this thesis is to train the ANN model using the GRACE total water storage as input and to use measured groundwater storage as output. In doing so, the ANN model "learns" the mapping of the low resolution GRACE total water storages into the point (measured) groundwater storages. Once trained, the ANN model will replicate the measured patterns of the groundwater storage. More than 100 piezometric measurement locations are available over the Assiniboine Delta Aquifer. However, only those measurements that contain continuously recorded data are used to downscale the GRACE total water storage. A total of 59 piezometers that have continuous records of groundwater head data from April 2002 to December 2006 are used for downscaling of the GRACE measurements. Once identified, the GRACE total water storage is downscaled to each piezometric or point groundwater storage and then interpolated spatially. Missing

GRACE data, during the months of May, June, and July 2002 are not considered for training or validation. As a result, a total of 46 monthly GRACE total water storage estimates are considered for the ANN modeling. Among these measurements, the first 30 months of measured groundwater storages are used for model training, the following 8 months are used for model validation and the remaining 8 months are used for model testing.

2.4 Modeling of the Assiniboine Delta Aquifer

2.4.1 Background

To assess the application of the downscaled GRACE-based total water storage for model calibration and validation, a hydrological model is developed over the Assiniboine Delta Aquifer (ADA). A Land Surface Model (LSM) simulates moisture and heat transfer through the unsaturated zone, and a groundwater model simulates flow in the saturated zone over the ADA area. The coupled LSM-groundwater model that has been identified for this study is the CLM-PF (Maxwell and Miller, 2005) hydrological model. This model is physically based and dynamically coupled surface and groundwater model that uses a hybrid version of the Common Land Model (Dai et al., 2003) and a 3D groundwater model know as ParFlow (Ashby and Falgout, 1996). The dynamics of this formulation hinges on the interaction between the LSM soil column and a deeper groundwater model. In addition to the LSM, the model is also coupled with surface hydrologic flow equations that do not rely on a conductance concept (Kollet and Maxwell, 2006). The overland flow equation used in this coupled

model is the kinematic wave approximation (Chow et al., 1988). This formulation reduces the initial value problem of variably saturated groundwater flow to an overland flow boundary condition. This boundary condition takes into account the free surface of water ponded on the land surface. A detailed description of this coupled model is given in Maxwell and Miller (2005) and Kollet and Maxwell (2006). Only a brief description of the groundwater model, the LSM and the shallow overland flow equations is given in this section of the thesis.

2.4.2 Variably Saturated Groundwater Flow (ParFlow)

The variably saturated groundwater flow model, ParFlow, is a groundwater flow code developed at Lawrence Livermore National Laboratory (Ashby and Falgout, 1996). A parallel, multigrid-preconditioned conjugate gradient solver for steady-state, fully saturated groundwater flow problems and a parallel, globalized Newton method coupled to the multigrid-preconditioned linear solver for the transient, variably saturated flow are used to solve the flow equations in ParFlow. Use of both methods provide a very robust solution (i.e., computationally accurate and efficient) of water pressure (hydraulic head) in the subsurface and excellent parallel scaling of solver performance (Ashby and Falgout, 1996; Jones and Woodward, 2001, Maxwell and Miller, 2005) and thus provide a solution of large (3D, with many computational nodes) subsurface flow systems with heterogeneous parameters.

Like most hydrological models, an external boundary condition is used to force the transient, variably saturated flow. Similarly, initial and boundary conditions (specified as water pressure or flux) are required to initialize and define the groundwater

simulations. From these, the pressure head in the subsurface and resulting saturation fields are computed over time. There is no parameterization scheme involved for estimating the water table depth, rather the saturation field is calculated from the pressure field. A water table depth is calculated for regions where subsurface water pressure is greater than zero and saturation is 100%.

ParFlow solves the well-known Richard's (1931) equation of variably saturated groundwater flow, given as:

$$S_S S_W \frac{\partial \psi_p}{\partial t} + \phi \frac{\partial S_W(\psi_p)}{\partial t} = \nabla \cdot q + q_s + \frac{q_e}{m'} \tag{2.25}$$

$$q = -k(x)\, k_r(\psi_p)\, \nabla(\psi_p - z)$$

where S_S is the specific storage coeffcient (L^{-1}), S_W is the degree-of-saturation ($-$), ψ_p is the subsurface pressure head (L), ϕ is the soil porosity ($-$), $k(x)$ is the saturated hydraulic conductivity (LT^{-1}), k_r is the relative permeability ($-$) that is a function of hydraulic head, z is the depth below the surface (L) with the negative z-axis pointing downward, q_s is a general source/sink term (T^{-1}), q_e is the exchange rate with the surface (LT^{-1}) and m' is the thickness of an interface separating the surface and subsurface domains (L).

The saturation-pressure and relative permeability in ParFlow is determined following the van Genuchten (1980) relationships given in Equations 2.26 and 2.27:

$$S_w(\psi_p) = \frac{S_{sat} - S_{res}}{(1 + (\alpha\psi_p)^n)^{\left(1-\frac{1}{n}\right)}} + S_{res} \tag{2.26}$$

$$k_r\left(\psi_p\right) = \frac{\left(1 - \frac{(\alpha\psi_p)^{n-1}}{(1+(\alpha\psi_p)^n)^{\left(1-\frac{1}{n}\right)}}\right)^2}{\left(1+(\alpha\psi_p)^n\right)^{\frac{\left(1-\frac{1}{n}\right)}{2}}} \tag{2.27}$$

where S_{sat} and S_{res} are the respective relative saturated water content and the relative residual saturation $(-)$ while α (L^{-1}) and n $(-)$ are fitted soil parameters.

Like many traditional groundwater modes, ParFlow uses a simplified upper boundary condition that is explicitly specified and is intended to represent fluxes of water related processes such as infiltration and evapotranspiration. These fluxes are often simplified, uncoupled, and may be averaged in time and space, possibly missing key dynamics of important land surface processes (Maxwell and Miller, 2005). In addition, they do not account for frozen soil and ice processes, or any traditional land-surface-type processes such as runoff or evaporation. To overcome these deficits, Parflow has been coupled with the CLM (Section 2.4.3) and the shallow overland flow equation (Section 2.4.4), and the coupled model has been successfully applied in a number of studies (Maxwell and Miller, 2005; Kollet and Maxwell, 2006, 2008; Maxwell et al., 2007).

2.4.3 Common Land Model (CLM)

As reported in Dai et al. (2003), the Common Land Model (CLM) is based on three well known Land Surface Models (LSM): the LSM of Bonan (1996), the Biosphere-Atmosphere Transfer Scheme (BATS) of Dickinson et al. (1993), and the 1994 version of the Chinese Academy of Sciences Institute of Atmospheric Physics LSM (IAP94) (Dai and Zeng, 1997). The model simulates the water and energy balances in a multi layer soil and snow structure. In the moisture category these include

canopy water storage, snow depth, snow mass, snow water equivalent (SWE), and soil moisture content. In the energy category these include the temperature of the canopy, soil and snow layers, as well as momentum, latent heat, sensible heat, and ground heat fluxes, surface albedo and outgoing long-wave radiation. Together, conservation of energy and moisture provides accurate simulations over a wide variety of timescales. CLM has also been designed to simulate many land surface combinations required for global modeling including land cover type, soil and vegetation parameters, model initialization, and atmospheric boundary conditions (Dial et al., 2003). Land surface characteristics (land cover type, soil texture and soil color) are based on the International Geosphere Biosphere Programme (IGBP) or University of Maryland (UMD) classification system. These require percentages of sand and clay to define soil texture. CLM can be forced by observed atmospheric data or reanalysis, or it can be fully coupled with an atmospheric model. Required atmospheric inputs include wind speed, air temperature, and specific humidity all measured at the same height above the ground. In addition, precipitation rate, incoming short-wave and long-wave radiation and atmospheric pressure measured at the surface are required.

The water balance expression in the soil layers that is used to couple the groundwater in ParFlow with the unsaturated zone in CLM is presented next. Detailed descriptions and coupling procedures are explained in Dial et al. (2003) and Maxwell and Miller (2005), respectively. The change in liquid and ice water content in the soil in CLM is expressed as:

$$\frac{\partial w_{liq,j}}{\partial t} = [q_{j-1} - q_j] - f_{root,j} E_{tr} + [M_{il} \triangle z]_j \tag{2.28}$$

$$\frac{\partial w_{ice,j}}{\partial t} = [q_{j-1,ice} - q_{j,ice}] - f_{root,j} E_{tr} + [M_{il} \triangle z]_j \tag{2.29}$$

where $w_{liq,j}$ and $w_{ice,j}$ are the masses of the liquid and ice in each of the j soil layers, expressed as $(\rho_{liq}\theta_l \triangle z)_j$ and $(\rho_{ice}\theta_i \triangle z)_j$ respectivey; ρ is the density, θ is the volumetric soil moisture content, l is liquid and i is the ice, q is the flux at each layer interface, $f_{root,j}$ is the root fraction in each j layer, E_{tr} is the transpiration, M_{il} is the mass rate of melting (positive) or freezing (negative) of soil ice, and $\triangle z$ is the vertical discretization of the soil column. The vertical water moment or flux within the soil layers is described by Darcy's law;

$$q = -K \left(\frac{\partial \psi}{\partial z} - 1 \right) \tag{2.30}$$

Here, the hydraulic conductivity (K) and the soil matric potential (ψ) in CLM are based on the Clapp and Hornberger (1978) and Cosby et al. (1984) relationships. However, these formulations were replaced by van Genuchten (1980) relationships (Equations 2.26 and 2.27) in the coupled CLM-PF model. These two models are dynamically coupled at the land surface and in the first ten soil layers by replacing the soil moisture formulation of the CLM with the ParFlow formulation so that continuous hydrological processes can be achieved in the coupled model. In other words, the soil moisture simulated by ParFlow are passed into CLM and then CLM simulates infiltration, evaporation and root uptake fluxes and passes these fluxes back to ParFlow. ParFlow treats CLM fluxes as water fluxes into or out of the model at every time step. Mathematically, Equation 2.25 in ParFlow replaces Equation 2.28 in CLM, and the root zone transpiration fluxes are still preserved and calculated by CLM and are treated as a general source/sink term in ParFlow.

2.4.4 Shallow Overland Flow

Previous studies that have focused on the coupling of the surface and saturated groundwater flow were based on flux exchanges using a conductance concept. This assumes an interface connecting the surface and saturated domains. This interface is commonly characterized by a proportionality constant representing connectivity between the surface and subsurface. These proportionality constants generally involve the ratio of interface hydraulic conductivity and effective thickness (Figure 2.8; left). However, this approach generally challenges numerical stability as overland flow time scales may often be much smaller than groundwater flow time scales. Therefore, a fully integrated approach to solve the system of shallow overland and groundwater flow equations simultaneously has been implemented in ParFlow. Details of the coupling procedures are presented in Kollet and Maxwell (2006), however a summary is presented below.

The continuity equation of overland flow in two dimensions is given as:

$$\frac{\partial \psi_s}{\partial t} = \nabla \vec{v} \psi_s + q_r\left(x\right) + q_e\left(x\right) \tag{2.31}$$

where ψ_s is the surface ponding depth (L), t is time (T), $\vec{v}$ is the average velocity vector (LT^{-1}), $q_r\left(x\right)$ is the rainfall rate (LT^{-1}) and $q_e\left(x\right)$ is the exchange rate with the subsurface (LT^{-1}). The exchange rate in Equation 2.31 is the component of the overland flow equation which is coupled with the groundwater model and given as a boundary condition (q_{bc}) to the coupled model. The velocity in the equation above can be determined following the well known Manning's depth-discharge equation.

As reported in Kollet and Maxwell (2006), the conductance concept that was used to couple the groundwater and surface water in the past is shown in Figure 2.8 (left),

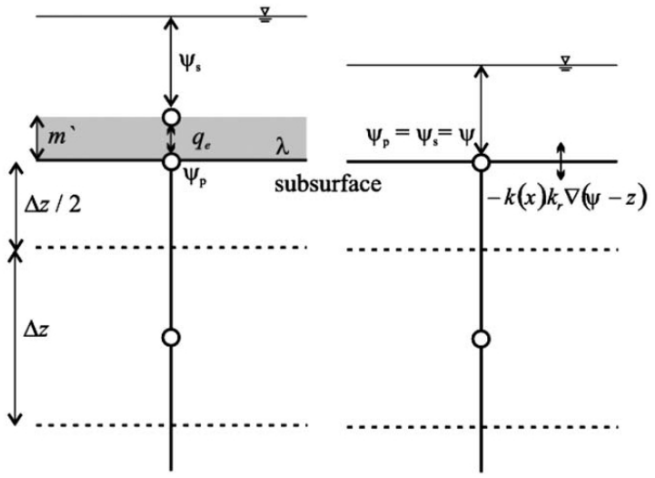

Figure 2.8: Schematic of the conductance concept (left) with an interface of thickness m' , which is represented by the conductance coefficient λ in theoretical models. The more general overland flow boundary is shown on the right side (After Kollet and Maxwell, 2006).

and expressed in Equation 2.32.

$$q_e(x) = \lambda(x)(\psi_s - \psi_p) \tag{2.32}$$

The exchange rate was based on the gradient across an arbitrary interface and the proportionality constant $\lambda(x)$ (T^{-1}) was a measure of the hydraulic connectivity between the two domains. However, this concept was replaced in ParFlow where the overland flow equation was implemented with Richard's equation at the upper boundary under saturated conditions. Using conditions of pressure and flux continuity $(\psi_s = \psi_p = \psi)$ and flux $(q_{bc} = q_e = -k(x)k_r\nabla(\psi - z))$ at the ground surface (Figure 2.8, right), Equation 2.31 can be solved for q_e as:

$$q_e(x) = \frac{\partial \|\psi, 0\|}{\partial t} - \nabla\vec{v}\|\psi, 0\| - q_r(x) \tag{2.33}$$

where $\|\psi, 0\|$ indicates the greater of ψ and 0. Equation 2.33 is substituted into Equation 2.25 as a boundary condition at the land surface so that the pressures of the surface and subsurface domains are continuous at the land surface. This head-dependent boundary condition accounts for the movement of the free surface of ponded water at the ground surface in ParFlow and, as a result, a fully coupled groundwater, LSM and overland flow can be evaluated simultaneously.

This coupled model can be used to evaluate the effect of groundwater on land surface processes such as surface soil temperature, evapotranspiration and shallow soil moisture storage (Kollet and Maxwell, 2008). Moreover, it will help to investigate the land surface processes during drought, which in turn may be used to compare the model results with the ongoing development efforts that incorporates groundwater simulation within atmospheric modeling as part of the Drought Research Initiative (DRI) (Loukili et al., 2007).

2.4.5 The Assiniboine Delta Aquifer (ADA) of Manitoba

In order to assess the applicability of the GRACE total water storage for coupled groundwater and surface water model calibration, a test will be applied to the Assiniboine Delta Aquifer (ADA) region of Manitoba. The focus of this modeling effort is to examine the groundwater distribution and the groundwater storage in the basin using the downscaled GRACE-based groundwater storage estimate as a tool for model calibration. The study area is a portion of the Assiniboine River Basin, centered on the community of Carberry. Figure 2.9 shows the mapped location of the ADA superimposed on the major drainage basins contributing to Manitoba. A detail

map of the ADA including all river tributaries within the aquifer is shown in Figure 2.10.

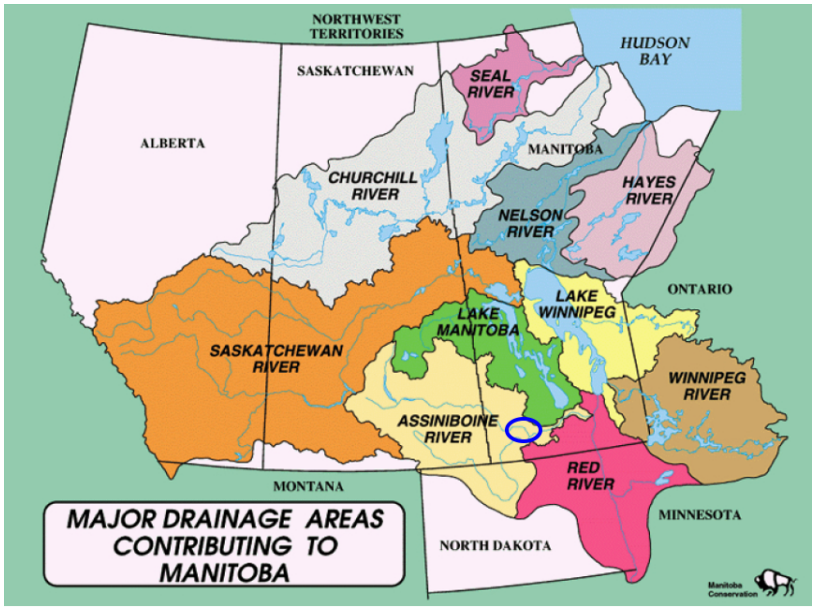

Figure 2.9: Approximate location of the Assiniboine Delta Aquifer (ADA) indicated by the circle (Source: Manitoba Conservation)

The ADA is an unconfined sand and gravel deposit that extends approximately 4,000 km^2. The aquifer serves a wide range of domestic, municipal, agricultural, industrial and irrigation water uses. As cited by Frost and Render (2002), geological and hydrological investigation of the aquifer were carried out by many investigators (Johnson, 1934; Halstead, 1959; Pedersen, 1968; Render, 1987; Burton and Ryan, 2000). Their studies suggested that the thickness of the sand and gravel units varies from 1.5 to over 30 meters, the grain size varies from coarse gravel to medium sand with a mean grain diameter varying from 0.508 to 0.127 mm along the western and easter boundaries, respectively. The aquifer bottom lies on an impervious bed dominated by silt and silty clay. The hydraulic conductivity in the aquifer varies from

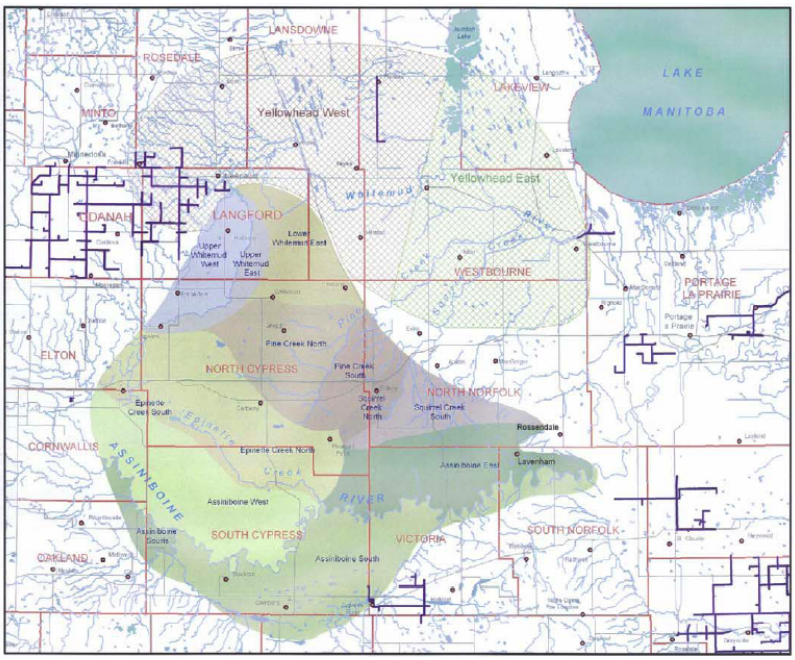

Figure 2.10: Map of the Assiniboine Delta Aquifer (ADA) (Source: http:// www.townof carberry.ca /PDFfiles/Neepawa.pdf, Accessed on June 2005)

43.5×10^{-6} to 2174×10^{-6} m/s, storage coefficient values between 0.0006 and 0.001 and specific yield values between 0.11 and 0.39. Hydrological budget studies suggest that the aquifer stores about 14.8 km^3 of water. Recharge to the aquifer is primarily from local rainfall and snowmelt. A majority of the precipitation is lost as evapotranspiration while a substantial amount of water enters the aquifer as recharge and is eventually discharges naturally as streamflow.

Hydrologically, the aquifer is divided into 13 sub-basins (Figure 2.11). Measured groundwater information is used to determine the sub-basin aquifer limits. It is believed that each sub-basin functions independently with little groundwater movement from one sub-basin to another. Several groundwater, soil moisture and rain gauge stations have been established in the area and have been collecting data on a regular

basis. The locations of these monitoring stations are shown in Figure 2.12.

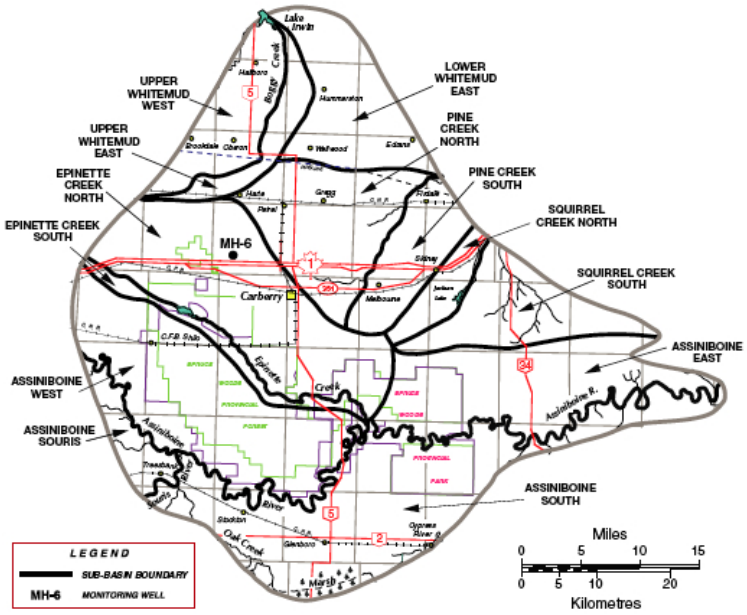

Figure 2.11: The Assiniboine Delta Aquifer Sub-basins (Source: Manitoba Conservation)

The ADA has been selected for this study because of the extensive data available for aquifer modeling. Data has been collected from the majority of the monitoring stations shown in Figure 2.12 since the early 1980s. Detailed studies and knowledge of the water resources have led to growth of the potato industry in the area. This has increased the value of aquifer water very significantly because of the industrial economic activity that has been generated. Therefore, assessing the quantity of water in the aquifer through modeling will help to better understand the sustainability of the aquifer resource including water volumes, water depth or drawdown, water quality, water temperature, reliability and whether water is accessible at the surface or underground.

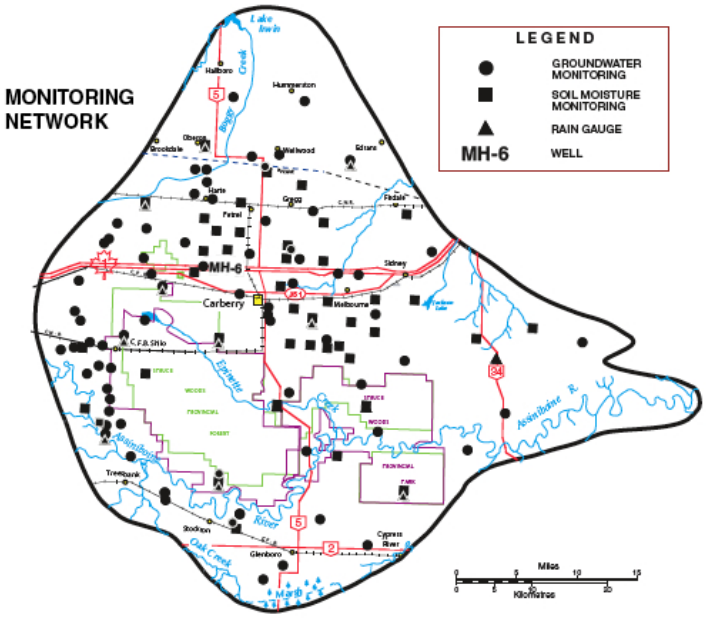

Figure 2.12: Assiniboine Delta Aquifer Monitoring Stations (Source: Manitoba Conservation)

In May 2005, after a careful investigation of previous studies and reports, updated technical information, key aquifer issues, management options and public input, the ADA Round Table group recommended the development of a sound management plan for the groundwater resources to ensure its long-term sustainability. They made a commitment to develop an aquifer management plan through a policy of continual monitoring and data analysis. This will aid the development of simulation models to demonstrate our understanding of the ADA, its sustainable yield and allocation limits for future water use. Therefore, in addition to the objectives of this study, which are mentioned in the previous chapter, modeling the aquifer will help to better understand long term sustainability of the aquifer and assess climatic variability that can influence or alter these attributes.

Chapter 3

Assessment of the WATCLASS Hydrological Model Result of the Mackenzie River Basin Using the GRACE Satellite Total Water Storage Measurement

Abstract

[1]Earlier efforts have been geared towards modeling the hydrological water balance of the Mackenzie River basin and its sub-basins using a coupled land surface and hydrological model known as WATCLASS. The goal of this study is to intercompare

[1]This chapter is a reprint from a paper published in Hydrological Processes (Yirdaw et al., 2009) with minor typographical corrections.

the total water storage anomalies estimated from the Gravity Recovery And Climate Experiment (GRACE) satellite with those estimated from the atmospheric-based water balance approach and the model output from WATCLASS over the $1.8 \times 10^6 km^2$ Mackenzie River Basin in Canada. Since the success of the parameter estimation stage of the coupled land surface and hydrological model, WATCLASS over this large catchment was entirely based on goodness of fit between the simulated and observed flows, it is desirable to assess the reliability of the generated state variables against other measured data. A major challenge lies in finding suitable datasets with which this comparison can be made to further assess the ability of the model to reproduce mass fluxes. The outcome of this inter-comparison reveals the potential application of the GRACE-based approach for the closure of the hydrological water balance of the Mackenzie River Basin as well as serving as a source of data for the calibration of traditional hydrological models.

3.1 Introduction

Modeling of the Mackenzie River Basin hydrologic processes is a difficult task owing to the complexity of the terrain and the lack of available data for hydrological model calibration and validation. Prior to the Mackenzie Global Energy and Water Cycle Experiment Studies (MAGS), a project designed to increase the understanding of the interaction between the moisture and energy fluxes over this basin, many attempts had been made to study this watershed in support of navigation, hydropower and pipeline construction (Solomon et al., 1977; Soulis and Vincent, 1977; Fassnacht, 1997). Efforts have recently been made to characterize the Mackenzie sub-basin's

hydrological processes by drawing upon the skills and lessons learnt from modeling the whole region and to continue in the development of a hydrological model which will facilitate future prediction of streamflow and state variables at any designated outlet within this basin.

The goal of this new effort is to assess the physics of the watershed model, especially those related to cold processes, in order to close the water and energy budgets throughout the Mackenzie basin. It is anticipated that this will provide greater confidence in cold soil algorithms suitable for use in atmospheric models. Calibration of WATCLASS was achieved through the comparison of the model's simulated streamflow with the available streamflow record (Souils and Seglenieks, 2007). However, assessing the performance and reliability of any hydrological model solely on a visual match and statistical measures of goodness of fit between observed and simulated streamflow may lead to flawed conclusions. Streamflow comparisons are very important and desirable part of a hydrological model performance assessment. However, streamflow is the aggregation of many different hydrological processes. In certain instances, it is possible to incorrectly simulate internal state variables that could cancel out and yet result in correct streamflow simulations. For example, an incorrect hydrological model simulation that overestimates snowmelt runoff could be compensated for by an overestimation of evapotranspiration resulting in accurate streamflow simulations, but for the incorrect reasons.

If internal variables simulated from this hydrological model can be shown to compare well with other measured data over long simulation periods bracketing hydrologic extremes, then greater confidence in the generated streamflow will result. Recently,

there has been a number of model intercomparison studies (Nijssen et al., 2003). While these are useful, the search for and use of measured data remains paramount. In light of this, this chapter will undertake an assessment of the performance of the coupled land surface and hydrological model WATCLASS (Snelgrove, 2002), by comparing its output with the total water storage anomalies obtained from GRACE (Gravity Recovery And Climate Experiment Mission: Tapley et al., 2004) and that estimated from the atmospheric-based water balance over the Mackenzie River Basin.

A number of studies currently exist which detail the origin and numerous applications in which the Gravity Recovery and Climate Experiment (GRACE) satellite remote sensing mission had been employed (Rodell et al., 2002; Swenson et al., 2003; Rodell et al., 2004; Tapley et al., 2004; Yeh et al., 2006; Syed et al., 2005 & 2007; Yirdaw et al., 2008). This remote sensing satellite has provided estimates of the changes in the terrestrial water storage in relatively large watersheds since its launch in March, 2002. A demonstration of the potential utility of the gravity measurements obtained from GRACE satellite for hydrological applications within the domain of large watersheds ($> 150,000\ km^2$) is documented in the work of Rodell and Famiglietti (1999). This study demonstrates the robustness of the data retrieved from GRACE in constraining water storage estimates from numerical land surface models. In addition, GRACE was used to detect variations in groundwater levels and intermediate zone moisture storage. The usefulness of the data measured from the GRACE-based technique in catchments larger than 400,000 km^2 was the focus of the study by Swenson et al. (2003). Accuracies of approximately 1 cm of water depth were reported in the estimates of monthly changes in total moisture storage. In light of these earlier

successful applications, there is a reasonable basis to expect that this study would benefit from the use of the GRACE total water storage estimation.

The coupled hydrologic and land surface model, WATCLASS employs the vertical process mechanisms contained in the Canadian Land Surface model (CLASS) (Verseghy, 1991) which is suited for studying cold region hydrologic processes. Lateral flows and routing are performed in a coupled fashion with the hydrological model, WATFLOOD (Kouwen et al., 1993). In order to assess the reliability of the GRACE-retrieved data for use in assessing WATCLASS performance, the atmospheric-based water balance estimation was employed in the validation of the GRACE-based computed terrestrial water storage anomalies. As noted in Oki et al. (1995), estimation of water balance components from atmospheric data has become easier than ever owing to the increasing availability of high-resolution atmospheric data at various temporal scales. These datasets are of paramount importance to the hydrologic community in terms of the evaluation of atmospheric and hydrologic water budgets. Kite et al. (1994) showed the utility of atmospheric data by using climate model outputs (precipitation, temperature and evaporation) retrieved from the General Circulation Model (GCM) as forcing variables for the hydrological model, SLURP. This model was then used to generate streamflow hydrographs for the Mackenzie River Basin which were subsequently used to assess the performance of the feedbacks from the GCM. Additionally, Kite and Haberlandt (1999) compared the outputs from a hydrological model employing a number of atmospheric data sources such as those from the GCM and Numerical Weather Prediction models (NWP) over a number of river basins to evaluate their quality. Furthermore, a comparison of the land surface water

budget to that of the atmospheric water budget was the focus of the work of Strong et al. (2002) wherein it was concluded that the observed discharge from the land surface budget suffered from errors attributed to the undetected diurnal signals.

The underlying approach in this study involves the determination of the precipitation less evaporation from the atmospheric-based water balance method and then factoring in the measured streamflow from sub-basin outlets to estimate the corresponding individual basin total water storage anomalies. Thereafter, comprehensive comparison of atmospheric-based total water storage anomalies for Mackenzie sub-basins are compared with those obtained from GRACE. These are then inter-compared with the total water storage simulated from the hydrological model WATCLASS over the same sub-basins.

3.2 Methodology

Three methods have been used to estimate the total water storage anomalies over the Mackenzie River Basin and these are the focus of discussion in this sub-section. The total water storage anomalies retrieved from the GRACE-based technique were validated with those estimated from the atmospheric-based water balance approach. Subsequently, an inter-comparison was done with the water storage anomalies simulated from the coupled land surface and hydrologic model WATCLASS. The underlying mathematical and physical principles involved in each of these methods are summarized in the following sub-sections.

3.2.1 Site Descriptions

The Mackenzie River originates from Great Slave Lake in the Northwest Territories. Great Slave Lake is the fourth largest fresh water lake on the North American continent and contributes runoff to the Mackenzie River, which flows to the Arctic Ocean. The Mackenzie River is the longest in Canada with an approximate length of 4,240 km. Its basin gross drainage area at its outlet at the Arctic Red River encompasses an area of approximately 1.8×10^6 km^2, constituting approximately 20 % of the landmass of Canada. Geographically, the basin spans from approximately 52^oN to 70^oN latitudinally and 102^oW to 140^oW longitudinally (from the Rocky Mountains on the western flank to the Canadian Shield on the east). The Mackenzie River Basin is further divided into six sub-basins; Athabasca, Bear, Liard, Peace, Peel and Slave with the gross drainage area and the location of each sub basins as shown in Table 3.1 and Figure 3.1, respectively.

Table 3.1: Sub basins gross drainage area of the Mackenzie River Basin as reported by Mackenzie River Basin Board (MRBB)

Sub Basins	Area (km^2)
Athabasca	268624
Bear	475146
Liard	274794
Peace	323017
Peel	74271
Slave	379159

Owing principally to its unique climatic conditions, the basin has received considerable attention as a result of efforts from the Global Energy and Water Balance Experiment (GEWEX). GEWEX activities are an offshoot from the World Climate

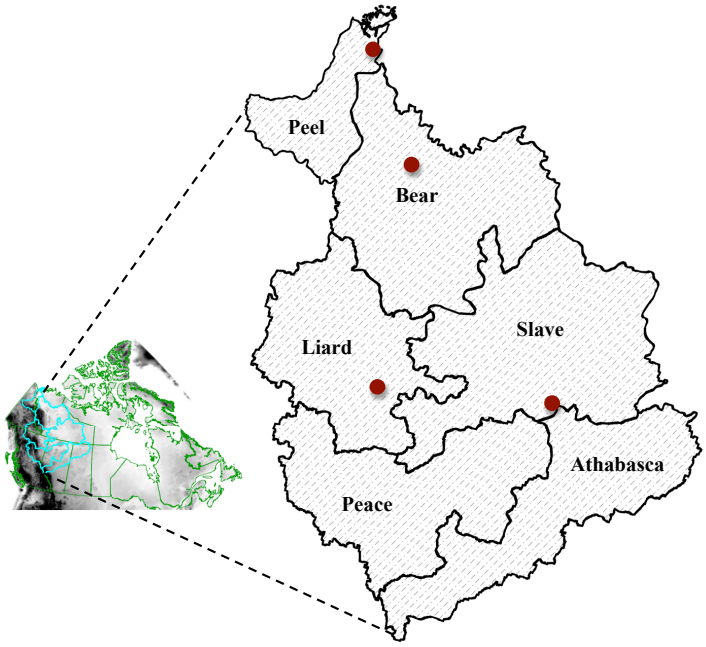

Figure 3.1: Location of the study area (Mackenzie River Basin and its sub basins) with locations of upper air stations (circle)

Research Program (WCRP). The Mackenzie GEWEX Study (MAGS) had as one of its objectives the need to understand and model the high latitude water and energy cycles and to improve the ability to assess the changes to Canada's water resources (Ronald, 2002). The basin receives an average annual precipitation of 426 mm with an average annual evapotranspiration and runoff estimated as 185 and 241 mm, respectively (Snelgrove et al., 2005).

3.2.2 GRACE-Based Moisture Storage

The geopotential spherical harmonic coefficients (level 2 dataset) are developed from the raw data retrieved from the GRACE satellite by the Centre of Space Research at the University of Texas, the National Aeronautics and Space Administration

(NASA) as well as the Deutsches Zentrum fur Luft und Raumfahrt (DLR) in Germany. This level 2 dataset is subsequently distributed freely to GRACE data users worldwide and has been employed in various hydrological applications and related research areas. In accordance with methods discussed in Chen et al. (2005a), atmospheric and oceanic anomalies together with the solid earth tides (non-hydrological gravitational components) are removed from the level 2 products. This is achieved by utilizing atmospheric mass re-analysis data and oceanic tide model data to correct for the atmospheric and oceanic contributions to the terrestrial water storage estimate from the GRACE remote sensing satellite. Consequently, as would be expected, the uncertainties in these models could lead to significant errors in the GRACE estimated total water storage anomalies. In essence, the preliminary step involved in the study of the monthly changes in temporary variations in the water storage requires the extraction of these monthly variations. Here, it is assumed that all remaining variability can be attributed to changes in land surface moisture.

Gravity field estimates comprising sequences of 46 monthly variations were extracted from the GRACE level 2 data (CSR RL01) retrieved from April 2002 to May 2006 with the exclusion of the May, June, July 2002 and June 2003. Owing to the high non-physical variability in GRACE data, an exclusion of the C_{20} geopotential spherical harmonic coefficient from these computations was necessary. Since harmonic degrees greater than 15 are dominated by non-gravitational errors described in Wahr et al. (2004), only the first fifteen spherical harmonic coefficients were utilized for this study. Successful retrieval of average terrestrial water storages from gravity measurements entails an initial step of transforming the GRACE geopotential spher-

ical harmonic coefficients (SHCs) into a spatially time-varying series of geopotential heights. These heights were then converted into water equivalent amounts (storages). The average terrestrial moisture storage estimated from GRACE was determined in accordance with the approach outlined in Heiskanen and Moritz (1967), Wahr et al. (1998) and Ramillien et al. (2004). Subsequently, an 800 km Gaussian smoothing radius was employed to further process the GRACE-based terrestrial water storage yielding a minimum RMS (Root Mean Square) residual over the land surface (Chen et al, 2005b). These storages were then validated using storage estimates computed from the atmospheric-based water balance approach in conjunction with the measured streamflow for the Mackenzie River Basin and its sub-basins adopting a technique similar to that of Rodell et al. (2004), Hirsch et al. (2006) and Yirdaw et al. (2008).

3.2.3 Atmospheric-based Water Balance

Description

Atmospheric-based water budget studies by Strong et al., (2002), and Walsh et al., (1994), attempted to calculate evaporation $[E]$ (m/s) less precipitation $[P]$ (m/s) based on the net advection of atmospheric moisture through a closed atmospheric volume. From an atmospheric perspective, this is expressed as:

$$\frac{\partial W}{\partial t} + \nabla \cdot Q = E - P \tag{3.1}$$

where W (m) is the water content in an atmospheric column, $\nabla \cdot Q$ is the divergence or net outflow of water vapour across the side of an atmospheric column, and Q (m/s) is the vertically integrated moisture flux vector derived from wind and relative

humidity measurements. The divergence measures the difference between the inflow and outflow to a specific region, in other words, it measures the rate at which fluid is being transported into or out of the region at any given location. A positive divergence means that outflow is greater than inflow, conversely, a negative divergence (or convergence) indicates that inflow is greater than outflow. The land surface water balance can be compared with the atmospheric water balance by formulating a similar equation. From the land surface perspective, the water balance can be expressed as:

$$\frac{\partial S}{\partial t} + \nabla \cdot F = P - E \tag{3.2}$$

S (m) is the total water storage in the basin, $\nabla \cdot F$ (m/s) represents the lateral transport of water with E and P representing evaporation and precipitations respectively. If a watershed is assumed to be a closed system, which means that there is no watershed boundary leakage, then the only lateral flow across the boundary of the watershed is the runoff, R (m/s), at the outlet of the basin. Therefore, this provides a means of estimating the value of $P - E$ for a specific basin. The usual approach adopted by most hydrologists is to deal with these components of the water budget in terms of their time dependencies, which is expressed mathematically as;

$$\frac{\Delta S}{\Delta t} + R = P - E \tag{3.3}$$

Combining Equations 3.1 and 3.3 yields:

$$-\left(\frac{\partial W}{\partial t} + \nabla \cdot Q\right) = \left(\frac{\Delta S}{\Delta t} + R\right) = (P - E)$$

$$\frac{\Delta S}{\Delta t} = -\left(\frac{\partial W}{\partial t} + \nabla \cdot Q\right) - R \tag{3.4}$$

Therefore, the negative divergence combined with the precipitable atmospheric water and the runoff, at the outlet of the basin, yields an estimate of the change in the water storage in the basin. The distinction between continuous time derivatives and delta-based time in Equation 3.4 is due to the time steps used in the estimation of S and W. The precipitable atmospheric water content (W) was derived at six hourly time step where as the total water storage (S) was estimated at a monthly time step. The precipitable atmospheric water content is computed as:

$$W = \frac{1}{\rho g} \int_{p_s}^{p_t} q dp \tag{3.5}$$

where q is the specific humidity (kg/kg), p is the atmospheric pressure ($kg/m/s^2$) and g is the gravitational constant (9.81 m/s^2). The limits of integration are the surface pressure (p_s) and the pressure at the top of the atmosphere (p_t). The divergence in spherical coordinates is computed as:

$$\nabla \cdot Q = \frac{1}{R_e \cos\phi} \left(\frac{\partial Q_\lambda}{\partial \lambda} + \frac{\partial (Q_\phi \cos\phi)}{\partial \phi} \right) \tag{3.6}$$

The vertically integrated vapour fluxes Q_λ and Q_ϕ are estimated according to Equations 3.7 and 3.8.

$$Q_\lambda = -\frac{1}{\rho g} \int_{p_s}^{p_t} q u dp \tag{3.7}$$

$$Q_\phi = -\frac{1}{\rho g} \int_{p_s}^{p_t} q v dp \tag{3.8}$$

Q_λ and Q_ϕ are the east-west and north-south components of vapour flux in (m^2/s), respectively, whilst ρ is the density of water (1000 kg/m^3). R_e is the mean Earth

radius taken as $6.3712 \times 10^6\ m$, and λ and ϕ are respectively, the longitude and latitude in radians. The negative sign arises from the fact that a hydrostatic assumption was used when converting from elevation to pressure.

Finally, the total water storage anomaly in a hydrologic reservoir can be computed as:

$$S_n = S_{n-1} + \left(\frac{\Delta S}{\Delta t}\right)_n \tag{3.9}$$

where S_n is the storage anomaly for the current month, S_{n-1} is the storage anomaly for the previous month and $\frac{\Delta S}{\Delta t}$ is the average change in monthly storage for the current month obtained from Equation 3.4. These storage anomalies are equivalent to storage anomalies from GRACE which are averaged over an approximate one-month period and used for comparison with storages estimated from the other two methods (GRACE- and atmospheric-based computations). In determining the initial value of total water storage anomaly, i.e. when $n = 1$ in Equation 3.9 above, the estimated terrestrial moisture storage anomaly from GRACE for the first month (April, 2002) was utilized.

Dataset for Atmospheric Water Balance Computation

The water content in the atmospheric column and the average divergence, or net out flow of water vapour across the boundaries of the atmospheric column in Equation 3.8, were computed using the North American domain of the global analysis developed by CMC (Canadian Meteorological Center). The analysis variables employed within this study include the dew point depression, temperature, and east-west and

north-south wind speeds at 16 upper-air pressure levels in addition to the surface pressure. The CMC analysis is produced using a data assimilation technique. This technique is used to estimate the state of the upper atmosphere using all available information including both measurements at upper air stations (Mackenzie stations shown in Figure 3.1) and the latest forecast from the Numerical Weather Prediction (NWP) model. As described in Talagrand (1997), the grid points of the forecast model are interpolated onto the observation locations, and the differences between the observations and the interpolated forecast values are interpolated back onto the model grid-points in order to define corrections to be applied to the model first-guess. This first-guess is then used as the initial condition of the next numerical weather forecast. The analysis data, however, could potentially contain error due to low station densities that exist in Northern Canada and errors from within the NWP model. As shown in Figure 3.1, only four upper air observation stations are located within the Mackenzie River Basin. As a result, the analysis data in this area would certainly have a lower quality than data from Europe or the continental United States where station densities are much higher.

No quantitative assessment of analysis data quality has been performed as part of this thesis. While grid point errors at individual time steps may well be large, it is expected that the large integrations in time (one-month) and space (the Mackenzie Basin) preformed here would reduce this error to acceptable values. On a long-term average basis, the runoff at the mouth of the Mackenzie River should equal average basin atmospheric divergence. For the 4-year (April 2002 to May 2006) of data available from this study, the average Mackenzie River Basin runoff is 14.6 mm/yr

while the average atmospheric divergence for the same period is 18.0 mm/yr. This discrepancy of 3.4 mm/yr or 19% represents a potential source of validation error that should be investigated further. When the 4-year average basin total water storage from the GRACE measurements, which is 10.4 mm or 2.6 mm/yr, is added to the measured runoff as it is counted for in the divergence calculation but remains in the basin and not detected by the runoff measurement, the average Mackenzie River Basin runoff with the basin water storage become 17.2 mm/yr. This resulted a reduction in discrepancy from 3.4 mm/yr to 0.8 mm/yr or from 19% to 5%.

The provided dataset spans the North American continent at a spatial resolution of 1^o by 1^o and a temporal resolution of 6 hours commencing April 2002 to May 2006. The vapor pressure and saturated vapor pressure were calculated from the dew point temperature (^oC), T_d and the actual temperature, respectively. The specific humidity, q, which is the concentration of water vapor expressed as the mass of water vapor per unit mass of air, is calculated by:

$$q = \frac{\rho_v}{\rho_a} = \frac{0.622 \times e}{P} \tag{3.10}$$

where P is the pressure at different pressure levels in $millibar$ and e is the vapor pressure.

The average monthly streamflow data are continuously being recorded for the Mackenzie River Basin by the Water Survey of Canada (WSC) at the Arctic Red River outlet and for other sub basins depicted in Figure 3.1. The gross drainage areas bordering these sub basins are given in Table 3.1.

3.2.4 Numerical Simulation from WATCLASS

WATCLASS

WATCLASS, the model used for the estimation of the water and energy budget components for the Mackenzie River Basin is an offspring arising from the coupling of the Canadian Land Surface Scheme, CLASS (Verseghy, 1991) and a physically based semi-distributed hydrological model developed originally at the University of Waterloo in Canada called WATFLOOD (Kouwen et al., 1993). These models employ land cover distributions as a basis sub-grid process modeling. The CLASS approach is designed using a properties-summed-by-area approach to define a single equivalent landscape unit. Conversely, the WATFLOOD approach is based on the use of a fluxes-summed-by-area multiple hydrologic units generally referred to as the Group Response Unit (GRU) (Kouwen et al., 1993). The strength of the CLASS model lies in its detailed representation of the lower atmosphere and land surface processes required for the computation of the energy fluxes (radiative and turbulent) with state variables including soil moisture. The emphasis of WATFLOOD rests in its representation of the horizontal runoff generation processes within a hydrologic system and hence, on the grid cell runoff routing required to simulate streamflow. WATFLOOD, however, does possess a rudimentary yet robust treatment of the energy based processes and all other state variables.

Vertical hydrologic process represented in WATCLASS remain the same as those of the parent CLASS model but with enhancements made to the treatment of the soil column, which in the coupled model is represented as a sloping soil layer. Additionally, it employs a set of generic grouped response units that are more detailed than

those implemented in the WATFLOOD model. These grouped response units are capable of representing any land surface cover. For example, it is possible to generate the hydrological response of a peat plateau or glaciers, however, the most common representation remains that of the classical hillslope terrain. The approach adopted in this representation entails an assignment of local slopes to various landscape units irrespective of their types to make provision for a gradient necessary for the lateral flow transport. In essence, this can be viewed as modeling using "Aggregated Sloped Tiles" which possess better parameterizations as opposed to that employed in the parent model, WATFLOOD. The works of Snelgrove (2002) as well as that of Soulis and Seglenieks (2007) contain comprehensive discussion of the processes implemented in the coupled model, WATCLASS.

Dataset for Numerical Simulation

The slopes of the stream network in the basin, which serve as one of the inputs into the model, are extracted from the GTOPO-30 digital elevation dataset for the Mackenzie River Basin. This is followed by an aggregation of the initial 31 land cover classes represented in the original Canadian CCRS-II classification (Cihlar and Beaubien, 1998) to seven distinct classes, viz water, wetland, agricultural, tundra, coniferous forest, mixed forest, and glacier, which are depicted in Figure 3.2. Incidentally, the forcing datasets required to drive WATCLASS were made available from the earlier MAGS project. These datasets were derived from the Regional Finite Element (RFE) Environment Canada operational weather forecasting model and later substituted with the output from the Global Environmental Model (GEM) (Cote et

al., 1998).

The precipitation data retrieved from the RFE and GEM models contain known biases, which is not uncommon with this kind of Numerical Weather Predictions (NWP) precipitation retrievals. In order to compensate for the shortcoming inherent in this dataset, there was a need to make adjustments to the RFE/GEM precipitation data utilizing a set of measured monthly precipitation data (Louie et al., 2002) that spans the period 1994 to 2000. Extensive discussion of the calibration and validation of the WATCLASS model are discussed in the work of Soulis and Seglenieks (2007) and readers are referred to this paper for discussion of the procedures involved.

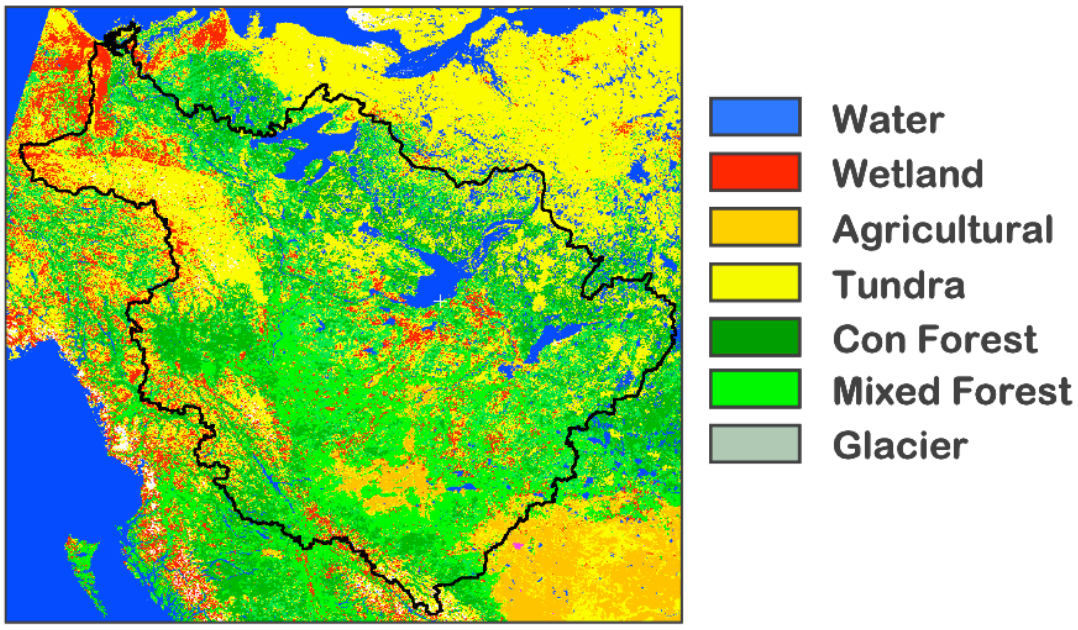

Figure 3.2: Land cover from the CCRS-II classification (After Soulis and Seglenieks, 2007)

In order to estimate the total water storage anomalies from WATCLASS, the simulated runoff (R), simulated evaporation (E), and measured precipitation (P)

were used as inputs into Equations 3.3 and 3.9 for each GRU. This total water storage anomaly was then averaged over each of the sub-basins of the Mackenzie River Basin. Similar to the total water storage anomalies computed from the atmospheric-based water balance technique discussed earlier, these results were compared to the total water storage anomalies from GRACE.

3.3 Results and Discussions

Computation and analyses of the GRACE-derived gravity measurements over the continental scale reveal spatial variability in moisture storage distribution globally. These were transformed into terrestrial water storage anomalies in units of centimetres of water equivalent thickness in relation to the mean computed storage as depicted in Figure 3.3. The upper and lower plots are the mean monthly terrestrial moisture storage anomalies for the months of March and October 2004 obtained at a spatial resolution of 1^o by 1^o, derived from the estimated time series of the average value retrieved from the GRACE-based total water storage.

In assessing the reliability of the estimated GRACE-based terrestrial moisture storage for subsequent inter-comparison with the soil moisture from the coupled hydrologic-land surface model, WATCLASS, it was necessary to undertake a prior validation of these computed total storages with those obtained from the atmospheric-based water balance. A good qualitatitive visual match or high statistical correlation coefficient between these different total storage estimates means that the GRACE-derived total water storage anomalies are sufficiently reliable for use in comparison with the total water storage anomalies simulated from WATCLASS over the

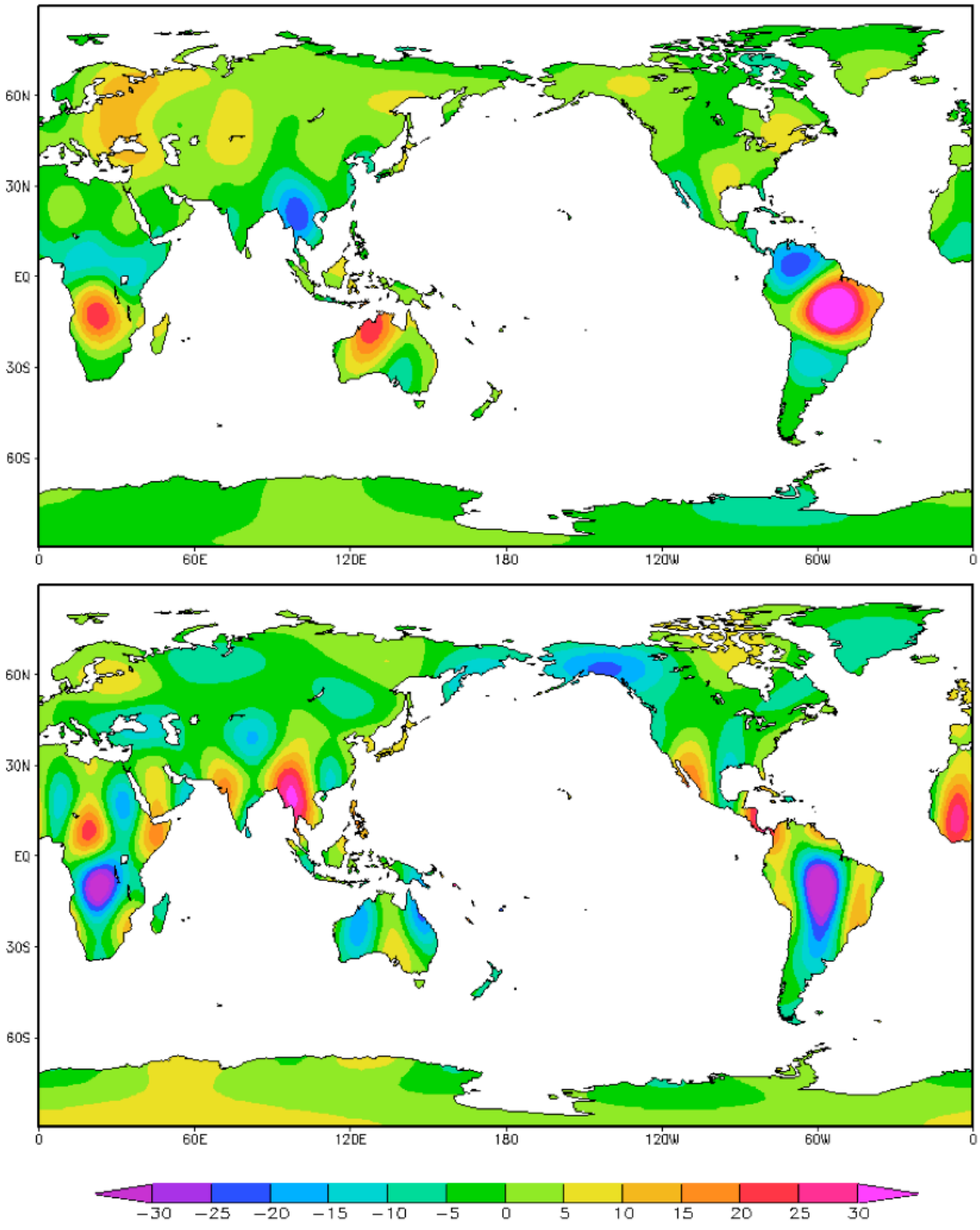

Figure 3.3: Terrestrial water storage anomalies in cm of water equivalent thickness relative to the mean storage for March 2004 (top) and October 2004 (bottom)

Mackenzie River Basin and its constituent sub-catchments. Time series plots of the spatially-varying storage estimates from the three approaches employed in computing the terrestrial water storage anomalies are as depicted in Figures 3.4 and 3.5.

The approach employed in the estimation of the GRACE-based terrestrial water storages is tailored after the relevant expressions developed in Section 3.2.3 with Equation 3.9 being the mathematical expression for the computation of the total water storage anomalies at monthly time steps. Successful closure of the water balance for the Mackenzie River Basin and its corresponding sub-basins entails the utilization of the simulated streamflow in Equation 3.3 for the coupled land surface-hydrologic model, WATCLASS, whilst the measured streamflow at the designated outlets over the basins was used in closing the water budget for the atmospherically-derived water balance over the basin. As stated earlier, the estimation of the total water storage anomalies over the basin in WATCLASS relies on the use of the simulated runoff and evaporation from this model in conjunction with the precipitation used in forcing it.

As illustrated in Figure 3.4, the patterns in the time series plots of the GRACE-based and atmospherically-derived total water storage anomalies over the Mackenzie River Basin appeared to agree qualitatively with each other, suggesting that the two techniques do seem to capture the dynamics of the relevant moisture storage processes. The seasonal amplitudes in the time series of the estimated total water storage anomalies from these techniques appeared to peak at a water equivalent thickness amount of about 10 *cm*. Corresponding minimum values in the estimated terrestrial water storage anomalies fluctuate between values of -8 and -10 *cm* water equivalent thickness which occurred in the months of July, August and September for

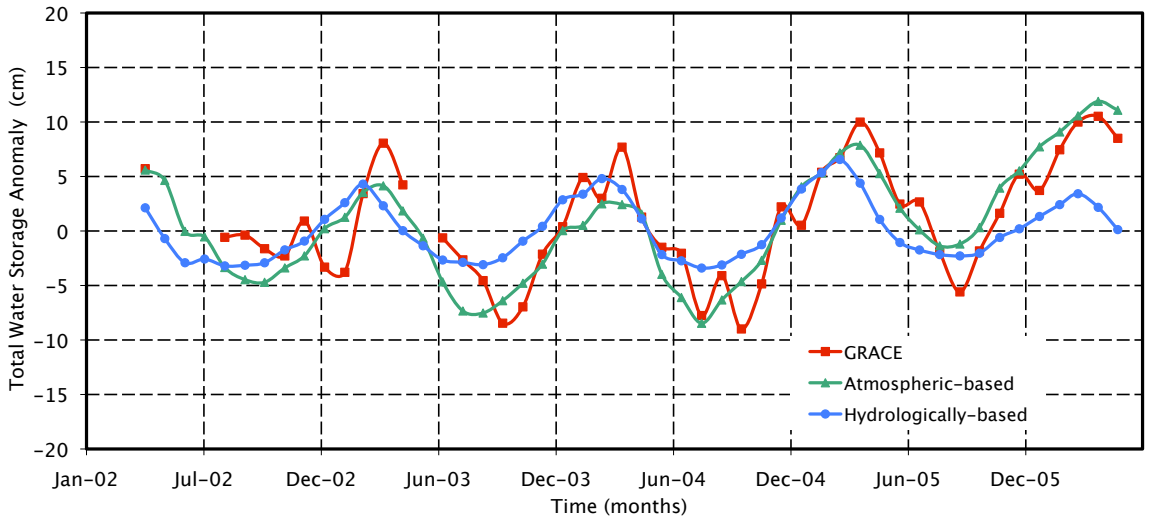

Figure 3.4: Total water storage anomalies derived from GRACE, atmospheric-based water balance technique and WATCLASS for the Mackenzie River Basin

the 4-year period of analyses (i.e. April 2002 to May 2006). Conversely, the maximum computed terrestrial moisture storage anomalies are observable in the months of January, February and March with values ranging from about 8 to 10 *cm* of water equivalent thickness. Incidentally, these peaks in total water storage anomalies correspond to the period of maximum snow accumulation at the end of the winter season over this basin. The spring season is characterized by the melting of the snow accumulated and redistributed over the basin, hence, this melting process contributes to the obvious loss of moisture which is seen in Figure 3.4 and is well captured by the two techniques.

Furthermore, an assessment of Figure 3.4 reveals a similar pattern of the temporal variability in the computed total water storage anomalies over the Mackenzie River Basin from the coupled land surface-hydrologic model, WATCLASS. As depicted in these time series plots, there is a good visual agreement in the seasonal cycles of the

computed terrestrial moisture anomalies from the coupled model with those derived from the GRACE- and the atmospherically-based techniques. Interestingly, WATCLASS performed acceptably in its estimation of the maximum terrestrial moisture storage anomalies in about all the seasonal cycles except for the year 2006 where the WATCLASS estimates are much lower than that of the GRACE and atmospherically-based estimates. Unlike with the GRACE- and atmospheric-based techniques, it did not quite capture the representation of the hydrologic processes responsible for the minimum values of the seasonal cycles in the terrestrial moisture storage anomalies over the basin. These minimum values in the estimated terrestrial water storage anomalies fluctuate between values of -2 and - 3 cm water equivalent thickness which occurred in the months of July, August and September for the 4-year period of analysis.

Table 3.2 below is a tabulation of the computed correlation coefficient estimated for the three techniques in use for this study. Apparently, the correlation coefficient between the terrestrial water storage anomalies from WATCLASS and those from the other two techniques are significant (0.68 for WATCLASS versus GRACE and 0.72 for WATCLASS versus atmospheric). There is a substantial reduction in these computed correlation coefficient values vis-a-vis a correlation coefficient of 0.86 that was obtained between the GRACE- and atmospheric-based techniques.

The total water storage estimated from the three techniques was further assessed using parametric statistical tests. The sample means and variances were tested to determine if there are evidence of differences in the population means and variances. The two tests considered were the two-sample t-test and F-test for the equality of two

population means and variances, respectively. The results of the two-sample t-test and F-test on the three datasets (i.e. GRACE-, Atmospheric- and WATCLASS-based total water storage) are presented in Tables 3.3 and 3.4, respectively. The values in these tables represent p-values. In terms of hypothesis testing, p-value has the following interpretation (Montgomery and Runger, 2002): The p-value is the smallest level of significance that would lead to rejection of the null hypothesis with the given data. Thus, the p-value measures the strength of evidence against the null hypothesis. The most commonly used level of significance (α) is 0.05 (5 %). When the significance level is set at 0.05, any test resulting in a p-value under 0.05 would be significant, therefore, the null hypothesis, which is assumed that the two datasets have equal mean and variance, would be rejected.

The p-values shown in Table 3.3 are all greater than the threshold (α; 5 %) value for the Mackenzie River Basin, suggesting that the means of the total water storage estimates between the three techniques are statistically equal. In the case of variance, however, the p-values between the GRACE and WATCLASS total water storage estimates and the atmospheric- and WATCLASS-based total water storage estimates are below the threshold value (Table 3.4). This indicates that the variance of WATCLASS total water storage estimate is statistically different from that of the GRACE- and atmospheric-based estimates. In essence, this would lead to a recommendation for the recalibration of WATCLASS with feedback from GRACE, by utilizing the total water storage anomalies estimate as an additional calibration dataset. This would enhance the performance of WATCLASS over the basin rather than simply relying on the traditional historical streamflow data as the only source

of calibration dataset for this coupled model.

Table 3.2: The correlation (R) of the total water storage estimates between the GRACE (G) and the Atmospheric-based water balance computation (A), the GRACE and the WATCLASS (H: hydrologic model) and the WATCLASS and the Atmospheric-based water balance computation

	Mackenzie	Peel	Bear	Slave	Liard	Peace	Athabasca
G Vs. A	0.86	0.46	0.66	0.77	0.70	0.75	0.81
G Vs. H	0.68	0.46	0.65	0.64	0.66	0.36	0.27
A Vs. H	0.72	0.59	0.83	0.61	0.74	0.40	0.42

Total water storage anomaly estimates from the three techniques being used for this study as obtained from the Mackenzie's six sub-catchments are the focus of this sub-section. The time series plots of Figure 3.5 with the computed correlation coefficients (Table 3.2) for the Peel, Bear, Slave, Liard, Peace and Athabasca indicate positive relationship in the temporal variability of the estimated terrestrial water storage anomalies resulting from the GRACE- and atmospheric-based techniques over these sub-catchments. However, the Peel sub-basin appeared to be an oddity to this general high positive correlation coefficient values obtained for the other five sub-basins. This might be attributable to its relatively small drainage area resulting in a low correlation coefficient value of 0.46 and a significantly different mean and variance (p-values are less than the threshold α-value; Tables 3.3 and3.4). GRACE spatial resolution is very coarse and applying it over very small catchments poses some issues. The lowest computed correlation coefficient value in the GRACE- and atmospheric-based terrestrial moisture storage anomalies in the remaining basins is 0.66 occurring at the Bear sub-catchment whilst the Athabasca basin yielded the highest correlation coefficient value of 0.81. The Athabasca River Basin, on the other

hand, resulted a statistically significant mean between the GRACE- and atmospheric-based total water storage estimates.

Table 3.3: Statistical test results (p-values) for the difference of means of the GRACE (G) and the Atmospheric-based water balance computation (A), the GRACE and the WATCLASS (H: hydrologic model) and the WATCLASS and the Atmospheric-based water balance computation

	Mackenzie	Peel	Bear	Slave	Liard	Peace	Athabasca
G Vs. A	0.783	0.002	0.812	0.105	0.000	0.001	0.000
G Vs. H	0.225	0.214	0.916	0.019	0.987	0.184	0.005
A Vs. H	0.358	0.000	0.852	0.758	0.000	0.000	0.004

Table 3.4: Statistical test results (p-values) for the equality of variances of the GRACE (G) and the Atmospheric-based water balance computation (A), the GRACE and the WATCLASS (H: hydrologic model) and the WATCLASS and the Atmospheric-based water balance computation

	Mackenzie	Peel	Bear	Slave	Liard	Peace	Athabasca
G Vs. A	0.479	0.000	0.009	0.425	0.284	0.446	0.096
G Vs. H	0.000	0.074	0.000	0.000	0.000	0.000	0.000
A Vs. H	0.000	0.000	0.170	0.000	0.000	0.000	0.000

Figure 3.5 presents the time series of the simulated total water storage anomalies from the coupled hydrologic-land surface model WATCLASS over the Mackenzie River sub-catchments. Different vertical scales are used in each plot in order to show the patterns in the total water storage anomalies for each sub-basin. From these plots, there appears to be an agreement in the pattern of the signature captured by both the GRACE-based technique and the hydrological model, WATCLASS. It is evident that there are significant discrepancies in the magnitudes of the estimated total moisture storages through the seasonal cycles which might be explained by the quality of available data for the calibration of the WATCLASS model. Low quantity and

quality of measured data of the huge expanse of the Mackenzie basin could partially explain the failure to adequately capture snowmelt processes and computed soil water equivalent. Additionally, these discrepancies might also stem from errors associated with the issue of the uncertainty in the GRACE dataset as detailed in Rodell et al. (2004), Wahr et al. (2004) and Andersen et al. (2005a). Expectedly, the values of the computed correlation coefficients between GRACE and WATCLASS were also reduced and the Peel, Peace and Athabasca exhibiting very low positive correlations. An alternate source of error that may be responsible for the observed discrepancies between the two techniques is the spatial scales associated with the output from the hydrological model WATCLASS and the remote sensing system, GRACE. Hydrologic output from the WATCLASS model are simulated at a spatial resolution of 20×20 km whilst the total water storage estimates from GRACE are from a coarser scale of approximately 100×100 km. The scaling effects from the two sources could significantly reduce the correlation in the estimated total water storage anomalies given that there is a significant loss of energy at the edges of the basins as well as possible energy leakages from the surrounding sub-basins.

In light of this, the usefulness of GRACE derived terrestrial moisture storage as a validation data source for constraining the simulation output over a basin from a hydrological model becomes apparent. Successful modeling of streamflow over a number of the catchments especially in northern Canada is an enormous challenge. In essence, a difficult question that has to be answered by the modeler developing a hydrological model for or deploying one over such basins is the spatial extent of the basin actually contributing flow to a specific outlet at a particular point in time.

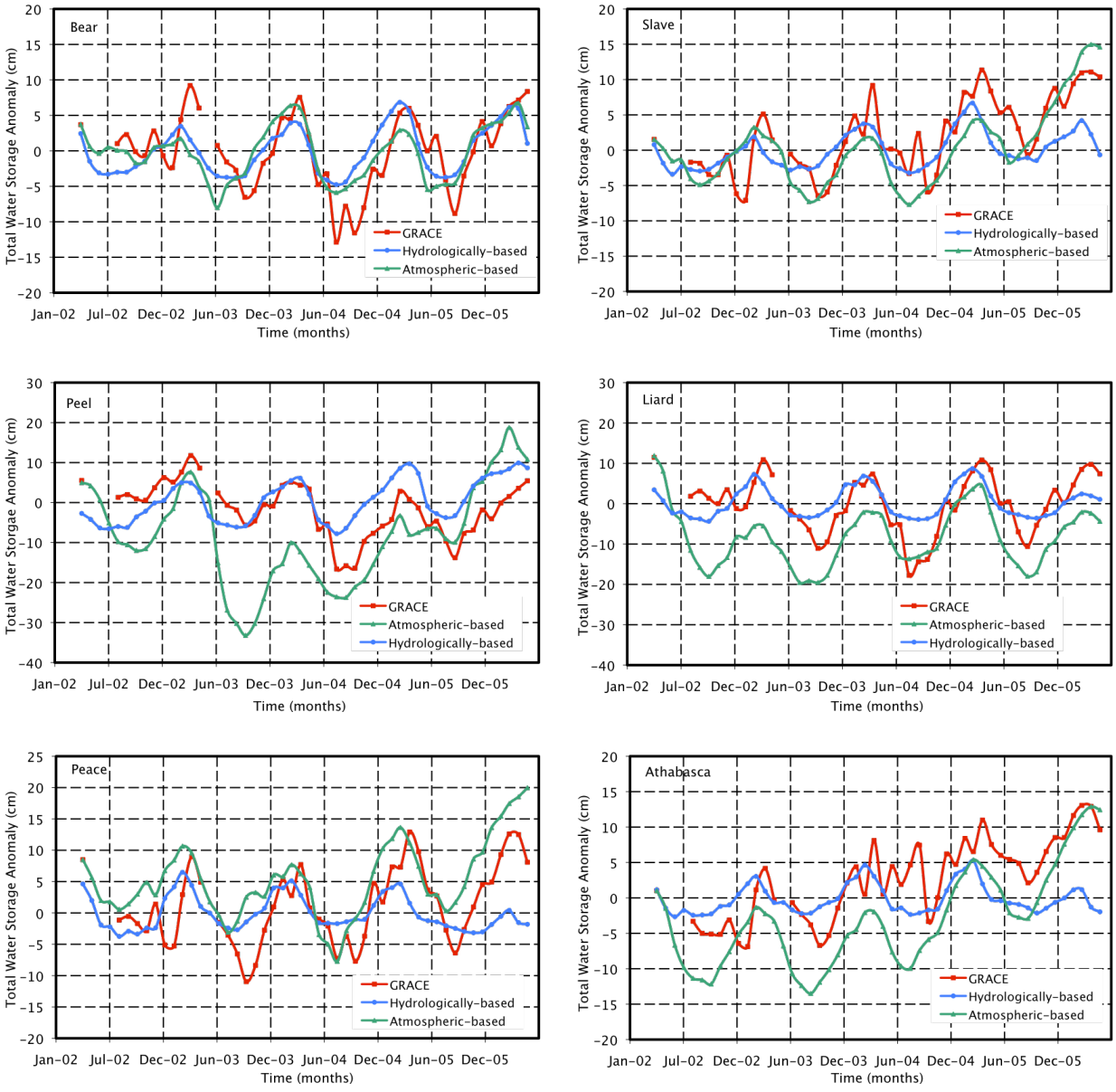

Figure 3.5: Total water storage anomalies derived from GRACE, atmospheric-based water balance techniques and WATCLASS for the different Mackenzie River sub basins

Owing to the inexactness in the determination of the area of a catchment contributing to streamflow at a chosen outlet, this constitutes an added source of uncertainty in the accuracy of the model-simulated streamflow. Consequently, the applicability and relevance of GRACE-derived terrestrial moisture storage for constraining and assessing the performance of any hydrological model deployed over regions such as this is of paramount importance.

Furthermore, the GRACE derived total water storage dataset in conjunction with the $P-E$ from the atmospheric-based water balance technique would be of great use in the derivation of streamflow information in basins that lack streamflow data. This lack of data might result from the economic situation in developing countries and the difficulty associated with the inaccessibility of the terrain or from harsh climatic conditions making it impossible to site streamflow gauges along the desired points on a river reach. Future research on the reconstruction of streamflow based storage measurement from GRACE would be a useful exercise.

3.4 Conclusions

The potential use of the GRACE-derived total water storage as a validation data source for land surface/hydrological models is explored in this study. The traditional approach of assessing the performance of a hydrological model based solely on the goodness of fit between the simulated and observed streamflow results may lead to inconclusive hydrologic model performance assessment. Hence, as emphasized in this study, alternative models state variables or derivatives of these should ideally be inter-compared with reliable data sources before any conclusion can be drawn as to the

reliability of the model's outputs or on its overall performance. The estimation of the terrestrial water storages from GRACE, atmospheric $P - E$ water balance and the coupled land surface-hydrologic model WATCLASS over the Mackenzie River Basin and its six sub-catchments was the focus of this study. Prior to employing the GRACE-derived total water storage in assessing the performance of the hydrologic model, WATCLASS over these basins, it was necessary to ascertain the reliability of the estimated total water storage from GRACE through validation by an independently computed terrestrial water storage from the atmospheric $P - E$ water balance technique over these basins. A high value of the computed correlation coefficient (R) between the GRACE-derived and the atmospherically-derived total water storage suggests a good linear agreement between these techniques. Given that the GRACE estimate of the terrestrial water storage over the basins is well validated by the atmospherically- derived estimates of the total water storage, this therefore serves as a premise upon which the GRACE-derived total water storage can be employed in constraining and assessing the quality of the total water storage estimated from the coupled land surface-hydrologic model in the different sub-basins. Moreover, this study has shown the potential of GRACE to assess water storage that will be used to examine the Canadian prairie basins.

Inter-comparsion of total water storages from GRACE and WATCLASS yielded high correlation coefficient values (greater than $R = 0.8$) in some of the sub-catchments, however, low positive correlation values were obtained for the Peel, Peace and Athabasca sub-basins. The reasons behind the low correlation values estimated for these sub-catchments has not been fully investigated. However, they may be attributed to issues

related to parameter estimation in the model as well as on the quality of the input data used in forcing the hydrological model. Furthermore, the difference in scales between the outputs retrieved from the two approaches could also explain the lower correlation coefficients. Finally, future modeling in the basin would benefit from the use of GRACE and atmospheric water balance storage estimates as a data source for model recalibration.

Chapter 4

GRACE Satellite Observations of Terrestrial Moisture Changes for Drought Characterization in the Canadian Prairies

Abstract

[1]The purpose of this paper is to undertake an investigation of the recent Canadian Prairie drought by employing total water storage anomalies obtained from GRACE (Gravity Recovery and Climate Experiment) remote sensing satellite mission. In order to successfully retrieve average terrestrial water storages from gravity measurements, it is necessary to first transform GRACE geopotential spherical harmonic coefficients

[1]This chapter is a reprint from a paper published in Journal of Hydrology (Yirdaw et al., 2008) with minor typographical corrections.

into a spatially varying time series of geopotential heights to determine water equivalent amounts. These GRACE-based total water storages are then validated using storages estimated from an atmospheric-based water balance $P - E$ computation in conjunction with the measured streamflow records for the Saskatchewan River Basin at its Grand Rapids outlet in Manitoba, Canada. Interestingly, the results from this study corroborate the potential of GRACE-based techniques as a tool for the characterization of the 2002/2003 Canadian Prairie droughts. Especially, this approach would prove useful for other regions globally where soil moisture availability is sparse.

4.1 Introduction

Understanding the physical characteristics and processes responsible for the initiation, sustenance and cessation of the past Canadian Prairie droughts are the primary goals of the Canada Drought Research Initiative (DRI) network. One of the agreements reached by the collaborating scientists in this network was that a system of sustained research is desirable in order to contribute to improved prediction of future droughts on the Prairie through effective watershed modeling.

In British Colombia, the year 2003 was marked as the driest year on record with rainfall so low and infrequent that all small rivers dried up, medium-sized rivers lacked sufficient flows to support even the smallest of fish whilst lake levels dropped at an alarming rate with a corresponding drastic drop in groundwater levels (Wheaton et al., 2005). According to Filmon (2004), this period was marked as the hottest and driest summer on record in the southern flank of the country leaving forests tinder-dry and vulnerable to 2500 wildfires that charred 2650 square kilometres of forested land. Sim-

ilarly, on the Canadian Prairie (Alberta, Saskatchewan and Manitoba provinces), the summer of 2003 saw above normal temperature and below normal observed precipitation. These in conjunction with searing heat and moisture-absorbing winds nullified any earlier moisture gains within this region. Expectedly, these abnormal climatic conditions that led to the acute Prairie drought between 2001 and 2003 caused huge economic and environmental losses that were felt nationwide. To adequately quantify the magnitude of the drought, a monitoring network of soil moisture would normally be required. Since such a network is not available within the Canadian Prairie, the need for a satellite-based total water storage anomalies determination becomes imperative and these constitute the underlying motivation for this investigation.

Characterization of drought is possible if available stored moisture in the soil can be measured or estimated. Unfortunately, the estimation of moisture storage via watershed modeling can be challenging and sometimes yield incorrect estimates since these models typically transfer moisture and energy between model stores, using physically-based transfer laws and conservation equations to produce streamflow hydrographs. Judging by the problem of non-uniqueness in the generation of model hydrographs, it has become increasingly important to ensure the representativeness of model results. Therefore, direct measurement of integrated watershed storage via satellite, such as GRACE, could serve as a surrogate for the deficiencies arising from the determination of moisture storage from traditional watershed modeling methods. Subsequently, storage in different reservoirs (snow depth, soil moisture, groundwater levels and lake storage) can be used to characterize droughts that affect water availability required to support agricultural, urban, human as well as environmental water

needs.

A number of studies detailing the origin and application of the Gravity Recovery and Climate Experiment (GRACE) satellite remote sensing mission exist (Rodell et al., 2002; Swenson et al., 2003; Rodell et al., 2004; Tapley et al., 2004; Yeh et al., 2006; Boronina and Ramillien, 2007; Syed et al., 2005 and 2007). Since its launch in March 2002, this satellite remote sensing mission has provided highly accurate estimates of the temporary changes in terrestrial water storage in relatively large watersheds. Its primary objective has been to accurately map the Earth's gravity field and to ascertain how this field changes as mass distributions shift. In essence, these measurements yield a time series of mass changes occurring in the earth-atmosphere system which, when integrated over an extended period, yield a detailed picture of the earth's gravity. However, from a hydrologic perspective, the interest is in capturing the monthly changes in mass, which serves as an index of the integrated value of the watershed storage.

Rodell and Famiglietti (1999) have demonstrated the potential utility of the gravity data obtained from the GRACE satellite for hydrologic applications in large watersheds ($\geq$ 150,000 km^2). They further discussed the robustness of GRACE data for constraining estimated water storage in land surface models when combined with surface soil moisture storage, groundwater as well as in intermediate zone storages. Similarly, Swenson et al. (2003) had demonstrated in their study the application of GRACE data for estimation of monthly variations in water storage with accuracies of approximately 1 cm of water thickness for catchments larger than 400,000 km^2. In order to successfully retrieve average terrestrial water storages from grav-

ity measurements, a necessary procedure was to first undertake a transformation of the GRACE geopotential spherical harmonic coefficients into a spatially varying time series of geopotential heights, which were subsequently converted into water equivalent amounts. These storage measurements were thereafter validated using storage estimates from an atmospheric-based water balance $P - E$ computation combined with measured streamflow for the Saskatchewan River Basin in Canada. Hirsch et al. (2006) have employed a similar approach for the estimation of terrestrial water storage from ECMWF operational forecast analysis.

The underlying hypothesis here is that gravity measurements obtained from GRACE are useful for the characterization of droughts as evident in the application for the Canadian Prairie. In their study of the massive heat wave that affected a large part of the European continent between 2002 and 2003, Andersen et al. (2005b) had demonstrated the application of GRACE-derived terrestrial water storage for capturing a negative trend in regional water storage in Central Europe. In light of this, the objectives of this paper are to undertake an inter-comparison of GRACE-based total water storage in relation with hydrologically derived storages and to present a detailed case study of the application of these moisture storages for drought characterization in the Canadian Prairie. To accomplish these defined objectives, this paper is ordered as follows: the next section (Section 4.2) delves into the description of the methods and the corresponding datasets used. Section 4.3 is dedicated to the presentation and analyses of results obtained and a subsequent comparative analysis of the two alternate storage assessment mentioned earlier. Additionally, the characterization of the Prairie drought employing the Total Storage Deficit Index (TSDI) as a tool is

presented. Finally, the fourth section will recap this study and present conclusions reached.

4.2 Methods and Datasets

4.2.1 GRACE-Based Terrestrial Water Storage

Raw data retrieved from GRACE satellite remote sensing mission are being transformed to time series of geopotential spherical harmonic coefficients (level 2 data) by a number of groups including the Center for Space Research (CSR) at the University of Texas, the National Aeronautics and Space Administration (NASA) and the Deutsches Zentrum fur Luft und Raumfahrt (DLR) in Germany. Level 2 data is then distributed freely up to an accuracy of 120 degrees and orders to the GRACE user community globally for a number of applications including hydrology. Essentially, the non-hydrological gravitational contributions, such as atmospheric and oceanic contributions plus solid earth tides, are removed from the level 2 products (Chen et al., 2005a). Thus, the initial step for studying the monthly variation of temporary change in total water storage entails extracting monthly variations of these storages within hydrological reservoirs.

Sequences of 46 monthly variations of gravity field estimates were extracted from GRACE level 2 data (CSR RL01) collected between April 2002 and May 2006 (with the exception of missing data for May, June, July 2002 and June 2003). Due to large non-physical variability in GRACE data, the C_{20} geopotential spherical harmonic coefficient was excluded in these computations. Moreover, only the first fifteen spherical

harmonic coefficients were utilized since spherical harmonic degrees greater than 15 are presently dominated by noise (Wahr et al., 2004). The change in average terrestrial water storage resulting from GRACE was determined according to the approach of Heiskanen and Moritz (1967), Wahr et al. (1998) and Ramillien et al. (2004). Following frequency to spatial space expansion, an 800 km Gaussian smoothing radius was employed to derive GRACE-based terrestrial water storage as this smoothing produces minimum RMS (Root Mean Square) residuals over the land surface (Chen et al., 2005b).

4.2.2 Hydrological Storage

The components of the hydrological budgets, namely precipitation (P), evaporation (E), runoff (R) and total water storage (S), vary significantly owing to the dynamic geophysical and climatic processes. These components can be determined via atmospheric measurement or from the more traditional hydrologic water balance techniques. The computed $P - E$ from either techniques can then be coupled with the measured or modeled R at the outlet of the basin to determine the total change in water storage (S) for the basin. Figure 4.1 is a schematic diagram of the various components of the hydrological and atmospheric water budgets. These two budget equations interchange the $P-E$ values on the land surface as illustrated in this figure.

The precipitation (P) (m/s) less the evaporation (E) (m/s) was computed based on the net advection of atmospheric moisture through a closed atmospheric volume in accordance with Walsh et al. (1994) and Strong et al. (2002). From an atmospheric

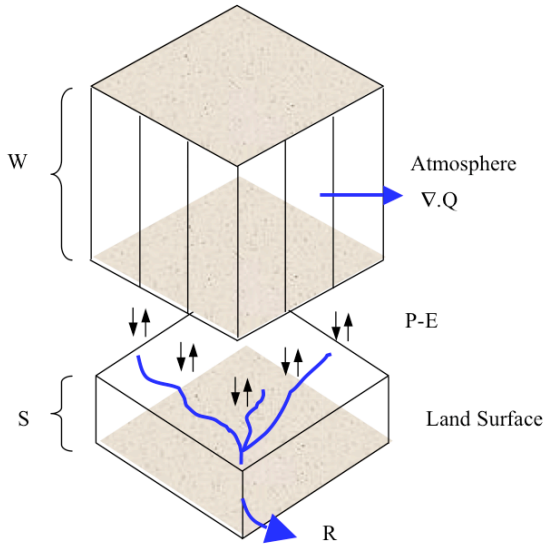

Figure 4.1: Schematic diagram of the hydrologic and atmospheric water budget.

water balance perspective, this can be expressed as:

$$\frac{\partial W}{\partial t} + \nabla \cdot Q = -(P - E) \tag{4.1}$$

where W (m) is the water content in an atmospheric column, t (s) is the time, $\nabla \cdot Q$ (m/s) is the divergence or net outflow of water vapour across the side of the atmospheric column, and Q is the vertically integrated flux of specific humidity derived from wind and humidity measurements. The divergence in spherical coordinates can be calculated as:

$$\nabla \cdot Q = \frac{1}{R_e \cos\phi} \left(\frac{\partial Q_\lambda}{\partial \lambda} + \frac{\partial (Q_\phi \cos\phi)}{\partial \phi} \right) \tag{4.2}$$

The vertically integrated vapour fluxes Q_λ and Q_ϕ are estimated according to the following equations:

$$Q_\lambda = -\frac{1}{\rho g}\int_{p_s}^{p_t} qudp \tag{4.3}$$

$$Q_\phi = -\frac{1}{\rho g}\int_{p_s}^{p_t} qvdp \tag{4.4}$$

Q_λ and Q_ϕ are the east-west and north-south components of vapour flux in (m^2/s) respectively, whilst q is the specific humidity (kg/kg), u and v are the zonal and meridian components of wind velocity (m/s), p is the pressure $(kg \times m/(s^2 m^2))$, g is the gravitational constant $(9.81\ m/s^2)$ and ρ is the density of water $(1000\ kg/m^3)$. R_e is the mean Earth radius taken as $6.3712 \times 10^6\ m$, λ and ϕ are respectively the longitude and latitude in radians. The negative sign arises due to the fact that a hydrostatic assumption was used when converting from elevation to pressure. The limits of integration are the surface pressure (p_s) and the pressure at the top of the atmosphere (p_t).

The water content in the atmosphere, W (m) is computed using

$$W = \frac{1}{\rho g}\int_{p_s}^{p_t} qdp \tag{4.5}$$

From a land surface perspective, the term $P - E$ can be expressed in a similar fashion as:

$$P - E = \frac{\partial S}{\partial t} + \nabla \cdot F \tag{4.6}$$

where S (m) represents the total water content of a land surface column, and $\nabla \cdot F$ (m/s) signifies the lateral transport of water. If one considers a watershed as a closed system, i.e. there is no watershed boundary leakage, then the only lateral flow across

the boundary of the watershed is runoff (R) at the outlet of the basin. This provides a means of estimating the value of $P - E$ for a specific basin. The usual approach adopted by most hydrologists is to deal with these components of the water budget in terms of their time dependencies, which is given mathematically as

$$\frac{\Delta S}{\Delta t} = P - E - R \tag{4.7}$$

where ΔS is the change in total water storage over a given time interval. The runoff R (m/s) incorporates the surface as well as the baseflow components. Equations 4.1 and 4.7 can be combined effectively to estimate the change in total basin water storage from the atmospheric-based water balance technique resulting in

$$\frac{\Delta S}{\Delta t} = -\left(\frac{\partial W}{\partial t} + \nabla \cdot Q\right) - R \tag{4.8}$$

Average monthly streamflow records (R) measured at the outlet of the basin, depicted in Figure 4.2, are required in Equation 4.8. It is worthwhile emphasizing at this point that $\frac{\Delta S}{\Delta t}$ which is the quantity of most interest to hydrologists is not directly measured by GRACE, but rather instantaneous storage anomalies that require further differentiation in time to develop the desired output. Hence, the total water storage anomaly in a hydrologic reservoir can be computed as

$$S_n = S_{n-1} + \left(\frac{\triangle S}{\triangle t}\right)_n \tag{4.9}$$

where S_n is the total water storage anomaly for the current month, S_{n-1} is the total water storage anomaly for the previous month and $\frac{\Delta S}{\Delta t}$ is the average monthly change in storage for the current month obtained from Equation 4.8. These anomalies are

equivalent to from those GRACE measurements, which are averaged over approximately a one month period and used for comparison with storages estimated from the two methods mentioned previously (GRACE- and atmospheric-based computed storages). In determining the initial value of the total water storage anomaly, i.e. when $n = 1$ in Equation 4.9 above, the estimated terrestrial moisture storage anomaly from GRACE for the first month (April, 2002) was utilized.

4.2.3 Dataset

The water content in the atmospheric column and the average divergence or net outflow of water vapour across the side of the atmospheric column in Equation 4.8 are computed using the data from the global analysis product retrieved from the CMC (Canadian Meteorological Center). The analysis variables employed for this study are the dew point depression, surface pressure, temperature, east-west wind speed and north-south wind for 16 pressure levels [1000 925 850 700 500 400 300 250 200 150 100 70 50 30 20 10]. The CMC dataset domain spans the North American continent at a spatial resolution of 1^0 by 1^0 and a temporal resolution of 6 hours starting from April 2002 to May 2006. The specific humidity was calculated from temperature and dew point depression dataset. Additionally, the average monthly streamflow data are recorded for the Saskatchewan River Basin by the Water Survey of Canada (WSC) at the Grand Rapids outlet depicted in Figure 4.2. The gross drainage area of this river basin with its outlet at Grand Rapids is approximately $406,000\ km^2$.

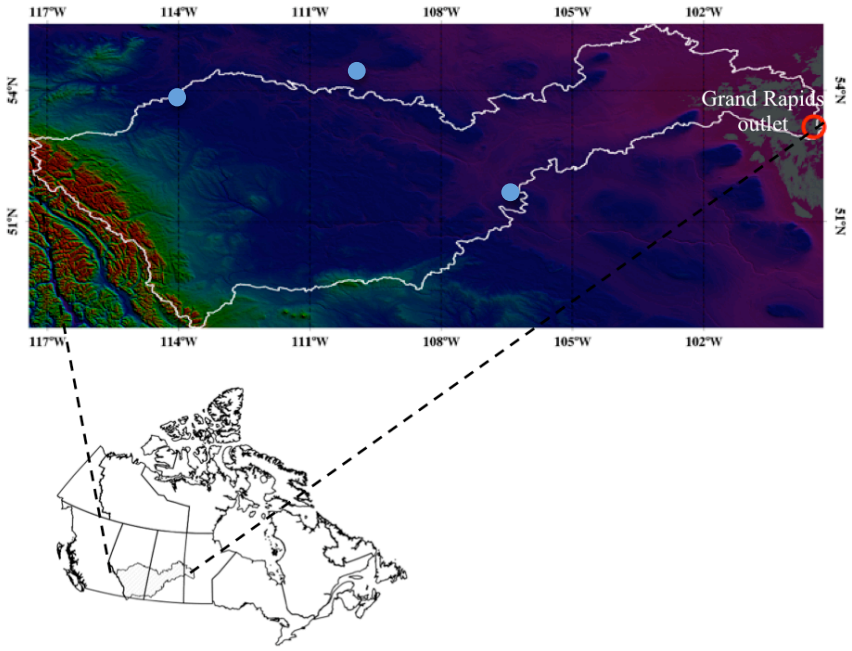

Figure 4.2: Saskatchewan River Basin showing the Grand Rapids outlet and locations of upper air stations (circle).

4.3 Results and Discussion

The initiation of the last Prairie drought occurred sometimes in 1999 and continued until 2004/2005 (Wilson et al., 2002; Wheaton et al., 2005). Since GRACE data are not available prior to April 2002, the focus of this study will surround the 2002-2003 drought event. The plots shown in Figure 4.3 reveal the spatial variability in terrestrial water storage over all Western Canada where the impacts of the last drought was most severe. The mean monthly terrestrial moisture storage anomalies (deviations from the time series (April 2002 to May 2006) of the average value obtained from GRACE-based total water storage) for October and November 2003 are depicted in these plots with a spatial resolution of 1^0 by 1^0. These months were

selected from the total analysis period (46 months) for discussion since these months fell within the most crucial period during the last Canadian Prairie drought episode. Interestingly, these plots reveal that the monthly total water storage anomalies in most parts of the drought-affected areas are well below the mean storage values. This is a clear indication of the relevance and applicability of the GRACE-based terrestrial water storage estimation technique for this region.

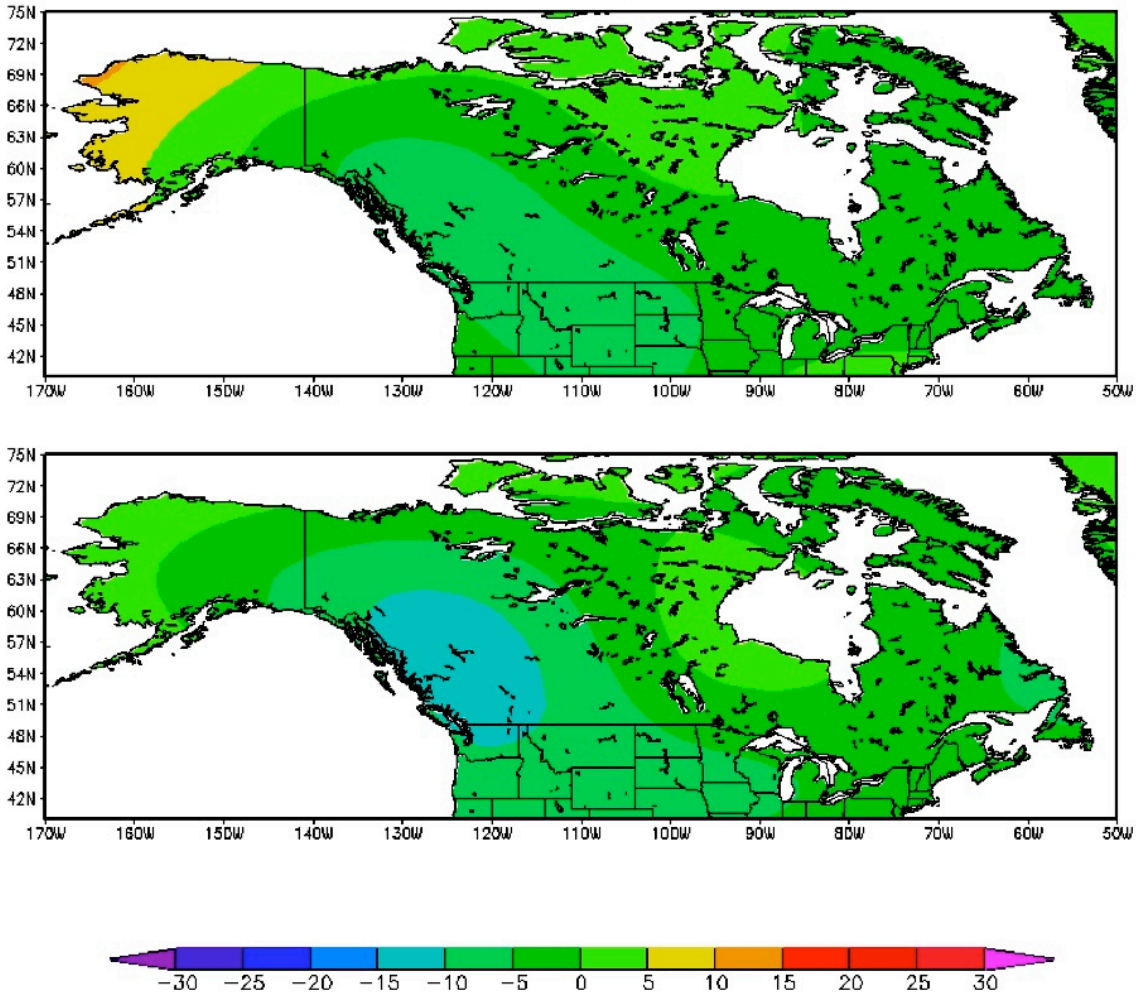

Figure 4.3: Terrestrial water storage anomalies in cm of water equivalent thickness relative to the mean storage for October 2003 (top) and November 2003 (bottom).

An important step to be undertaken prior to employing the GRACE technique for this study is to first determine the reliability of GRACE-based terrestrial water storage measurement, which is achieved by validating these computations with the total water storage estimated from Equation 4.9 for the Saskatchewan River Basin. For this task, a time series plot of GRACE-based terrestrial water storage anomalies are compared with those of the hydrologically-derived terrestrial water storage anomalies for the Saskatchewan River Basin as illustrated in Figure 4.4a. As can be seen in these time series plots, there is a good correlation in the pattern of the average basin storage distribution for the study area. However, there appears to be slight discrepancies for certain months and this is not unexpected, as it has often been observed that these simulations do generally yield under-or over-prediction of terrestrial water storage.

These discrepancies are associated with errors from either limited spatial or temporal resolutions or limited data accuracy in the analysis data (CMC dataset) used for the $P - E$ computations. An additional source of uncertainty revolves round the GRACE dataset in accordance with Rodell et al. (2004), Wahr et al. (2004) and Andersen et al. (2005a) where the accuracies were equally reduced. Interestingly, the range of discrepancies in the time series plots falls within 4 cm of water thickness with a RMSE of residuals of 2.13 cm. This agrees quite well with the average RMSE of the predicted residuals from the NASA-based GLDAS (Global Land Data Assimilation System) and GRACE-based terrestrial water storage developed by Chen et al. (2005a) for six different river basins. The basins studied by Chen et al. (2005a) were the Mississippi, Amazon, Ganges, Ob, Zambezi and Victoria River where minimum

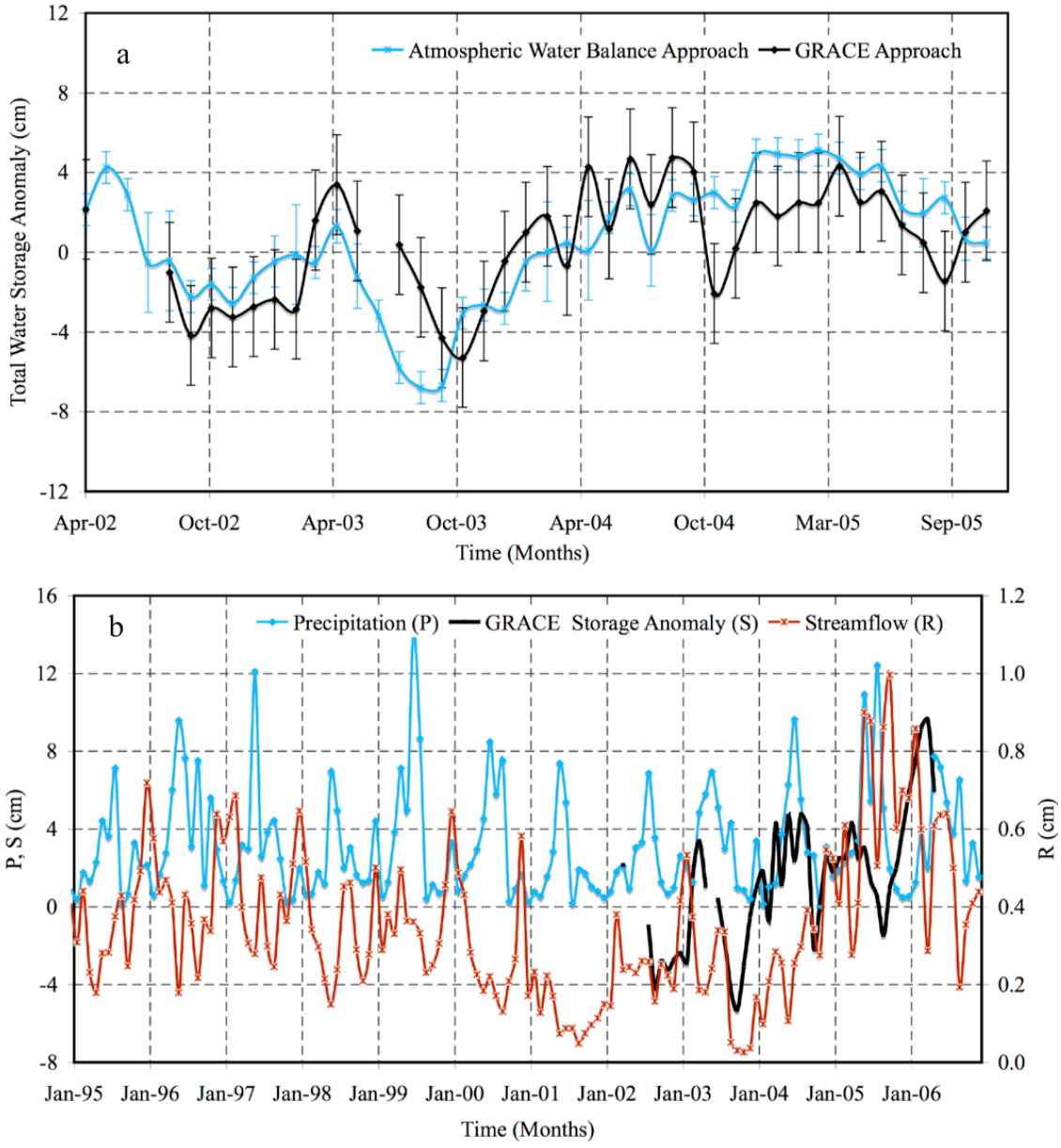

Figure 4.4: (a) Total water storage anomalies derived from GRACE and the atmospheric-based water balance techniques with the corresponding estimated relative uncertainties in the two methods for the Saskatchewan River Basin. (b) Trends in measured monthly average precipitation and streamflow at the Grand Rapids outlet for the Saskatchewan River Basin in conjunction with the monthly computed GRACE total water storage anomalies.

and maximum RMSEs of 1.55 *cm* and 3.1 *cm*, respectively, were found. Seo et al (2006) obtained RMSEs values in the range of 1 to 7 *cm* of water equivalent over twelve river basins of various sizes located in a number of different climatic zones. Moreover, statistical tests confirm that the mean and variance of the total water storage anomalies estimated from the two techniques are statistically equal at 95% confidence interval (p-values of 0.20 and 0.12 for mean and variance, respectively). Based on these findings, there seems to be a reliable basis for the use of the GRACE analysis technique to meet the objectives of this study.

Similar to the works of Rodell et al. (2004) and Syed et al. (2005), relative uncertainties in the computed atmospheric-based water balance approach and the GRACE-based terrestrial water storage anomalies were estimated at the 95% confidence limit. Wahr et al. (2004) estimated a total error value of 1.8 *cm* in monthly GRACE-based total water storage using a 750 *km* averaging radius filter. Since an 800 *km* radius filter was used for this study, an absolute error value of 2.5 *cm* was utilized in accordance with Rodell et al. (2005) which results from the multiplication of the total error value for the 750 *km* radius filter with a value of $\sqrt{2}$ in order to account for the monthly variation in mass. Furthermore, 10% relative uncertainties in $\frac{\partial W}{\partial t}$ and $\bigtriangledown.Q$ terms with a corresponding 15% relative uncertainty in observed streamflow were assumed in accordance with Syed et al. (2005) in the quantification of the relative errors in the atmospheric water balance. The relative uncertainty in the monthly total water storage (v_S) is computed as:

$$v_S = \frac{\sqrt{-v^2_{\frac{\partial w}{\partial t}} \left(\frac{\partial w}{\partial t}\right)^2 - v^2_{\nabla \cdot Q} \left(\nabla \cdot Q\right)^2 - v^2_R \left(R\right)^2}}{-\frac{\partial w}{\partial t} - \nabla \cdot Q - R} \tag{4.10}$$

where $v_{\frac{\partial w}{\partial t}}$, $v_{\nabla.Q}$ and v_R are the relative uncertainties in the monthly precipitable water storage change, net divergence term and observed streamflow, respectively. Finally, the 95% confidence limits on the estimated total water storage anomaly (S) can thus be expressed as $S \pm v_S S$. Figure 4.4a depicts the uncertainties in the computed atmospheric-based water balance approach and the GRACE-based terrestrial water storage anomalies for the Saskatchewan River Basin.

In Figure 4.4a, the seasonal amplitudes of terrestrial water storage anomalies in the basin are also illustrated and these vary approximately from 7 to 10 cm for the two methods used. As evident in this plot, the minimum terrestrial water storage anomalies from the two techniques lie in the neighbourhood of -5 to -7 cm, which occurred in October 2003 for the GRACE-based approach and between September and October of 2003 for the hydrologically-based approach within the 4-year period of analysis (April 2002 to May 2006). With the exception of the positive anomalies observed from April to June 2003, the remainders of the months are clearly marked by negative average terrestrial water storage anomalies over the entire Saskatchewan River Basin commencing August 2002 to December 2003 with respect to the GRACE-based approach. These negative anomalous storages represent the drought period that occurred in this basin and are well captured by the GRACE-based technique.

Trends in two water balance components (measured monthly average precipitation and streamflow at the chosen outlet) for the Saskatchewan River Basin in conjunction with the monthly computed GRACE total water storage anomalies are depicted in Figure 4.4b. As evident in this plot, the average measured precipitation and streamflow for the greater number of the months from 2001 to 2004 are below the 12 years

computed monthly average for the basin, which are approximately 3.20 *cm* and 0.35 *cm*, respectively. Owing to the effects of snow redistribution, accumulation and melting within the millions of sloughs and wetlands in this basin, a bit of difficulty is posed attempting to draw any striking correlation between the measured precipitation that falls on the entire Saskatchewan River Basin and the measured runoff at the designated outlet. Incidentally, GRACE-based terrestrial water storage results are insufficient to characterize this drought in terms of its severity and the overall effects of dryness and wetness within the basin; hence, the need to integrate this technique with an appropriate soil moisture index becomes imperative.

Similar in meaning to the Soil Moisture Deficit Index ($SMDI$) developed by Narasimhan and Srinivasan (2005), a related index termed the Total Storage Deficit Index ($TSDI$) was employed in the characterization of the 2002/2003 drought episode to generate a pictorial representation of long-term dryness and wetness within this basin. When dryness persists for an extended period of time, this leads to the initiation of a drought event. It has to be stressed at this point that this is not in anyway the evolution of a new index but a renaming of Narasimhan and Srinivasan (2005) original index to better cater to the variables being dealt with in the subsequent paragraphs. This new term seemed more relevant for the characterization of the Prairie drought since what is derived from GRACE satellite observation is the terrestrial or total water storage which differs from the soil moisture storage that is utilized in Narasimhan and Srinivasans (2005) original deficit index.

As with the $SMDI$, the $TSDI$ utilises hydrological and meteorological variables for monitoring and characterizing droughts and it has considerable application in the

determination of total storage deficit (TSD) in a basin. This index parallels the more popular drought assessment tool known as the $PDSI$ -Palmer Drought Severity Index (Palmer, 1965). The monthly total water storage anomalies earlier computed from the GRACE-based method serve as input for estimating the TSD which is expressed as:

$$TSD_{i,j} = \frac{TSA_{i,j} - MTSA_j}{MaxTSA_j - MinTSA_j} \times 100 \tag{4.11}$$

where $TSD_{i,j}$ is the total storage deficit (%), $TSA_{i,j}$, the monthly total storage anomaly as obtained from the GRACE-based technique (cm), $MTSA_j$, $MaxTSA_j$, and $MinTSA_j$ are respectively, the long-term mean, maximum and minimum total storage anomaly of the month (cm) (with i = April 2002 to May 2006 and j= 1-12 months).

As Palmer (1965) noted, the $TSDI$ can be calculated from the previous drought index and the current total storage deficit as

$$TSDI_i = p \times TSDI_{i-1} + q \times TSD_i \tag{4.12}$$

The determination of the parameters p and q is based on the cumulative TSD as illustrated in Figure 4.5 in conjunction with Equation 4.13 below with the drought severity and its duration estimated by making an incremental plot of the TSD.

$$\begin{aligned} p &= 1 - \frac{m}{m+b} \\ q &= \frac{C}{m+b} \end{aligned} \tag{4.13}$$

where C is the $TSDI$ value obtained from the best-fit line (drought monograph) for the period of dryness and m is the slope whilst b is the intercept of the cumulative TSD curve. A plot of historical dryness and wetness for this basin is shown in Figure 4.5 below and as can be seen, the Prairie drought terminated in the month of May 2004 and this maybe attributed to the effects of heavy spring rainfall and winter snowmelt.

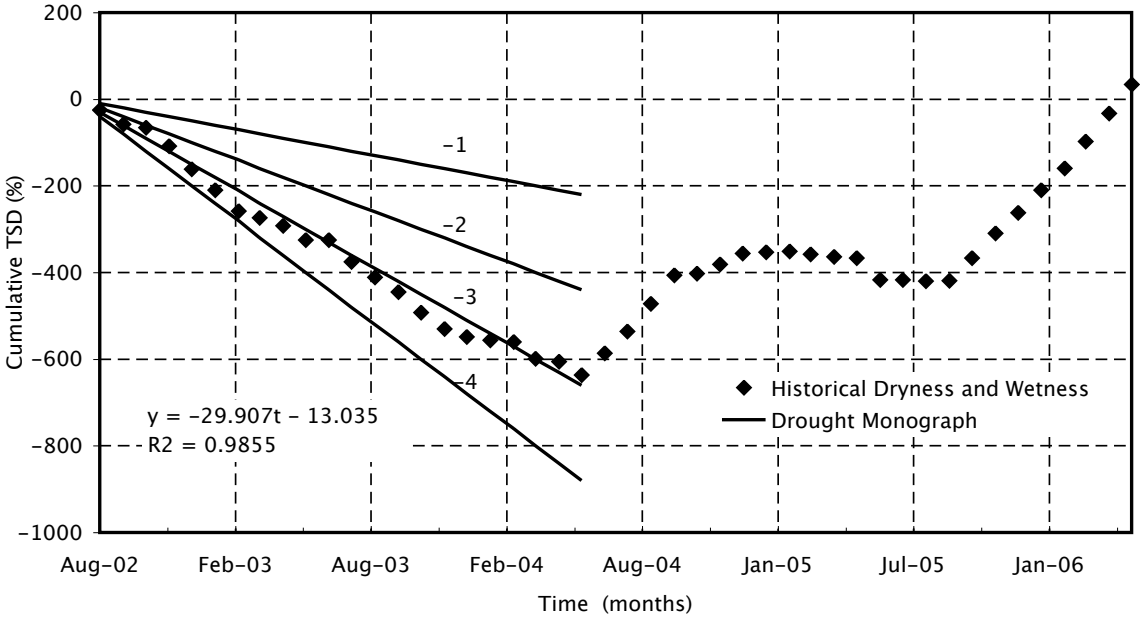

Figure 4.5: Cumulative Total Storage Deficit (TSD) for the Saskatchewan River Basin derived from GRACE-based total water storage.

Evidently, the best-fit line for this plot correlates with the $TSDI$ value of -3 (which corresponds to the C parameter), this in conjunction with the estimated slope, m = -29.907 and the y-intercept, b = -13.035 were then used to determine the duration factors, p and q according to Equation 4.13, yielding values of 0.304 and 0.070 respectively. Substituting the above values in Equation 4.12 results in Equation 4.14 which

enables a computation of the total storage deficit index for a particular month. The starting value of $TSDI_{i-1}$ for the case when $i = 1$ in Equation 4.14 was estimated by multiplying the TSD for the first month by a value of 2 % in accordance with Narasimhan and Srinivasan (2005).

$$TSDI_i = 0.304 \times TSDI_{i-1} + \frac{TSD_i}{14.30} \tag{4.14}$$

Similarly, a plot of the total storage deficit index ($TSDI$) is shown in Figure 4.6 for the 46 months period being analysed and it can be seen that negative $TSDI$ values were obtained for the period spanning from mid-2002 to mid-2004. Despite the fact that there were occurrences of positive total storage anomalies as observed in Figure 4.4a from April to June 2003, the contributions of these did not cause a cessation in the drought episode which persisted until the subsequent year. Additionally, in terms of the slope of the cumulative TSDI values as a means of drought characterization, Figure 4.7 below depicts a best-fit line with a slope of -3 which is an indication that the last Canadian Prairie drought falls under the severe drought classification in accordance with Palmer (1965).

4.4 Conclusions

The usefulness of the GRACE-based total water storage estimation has been explored in this study. The GRACE satellite remote sensing mission has proven pertinent as an alternate means for studying Prairie hydrology especially from the perspective of a scenario of insufficient data on water storage variations. This study has successfully compared two different techniques for the estimation of total water stor-

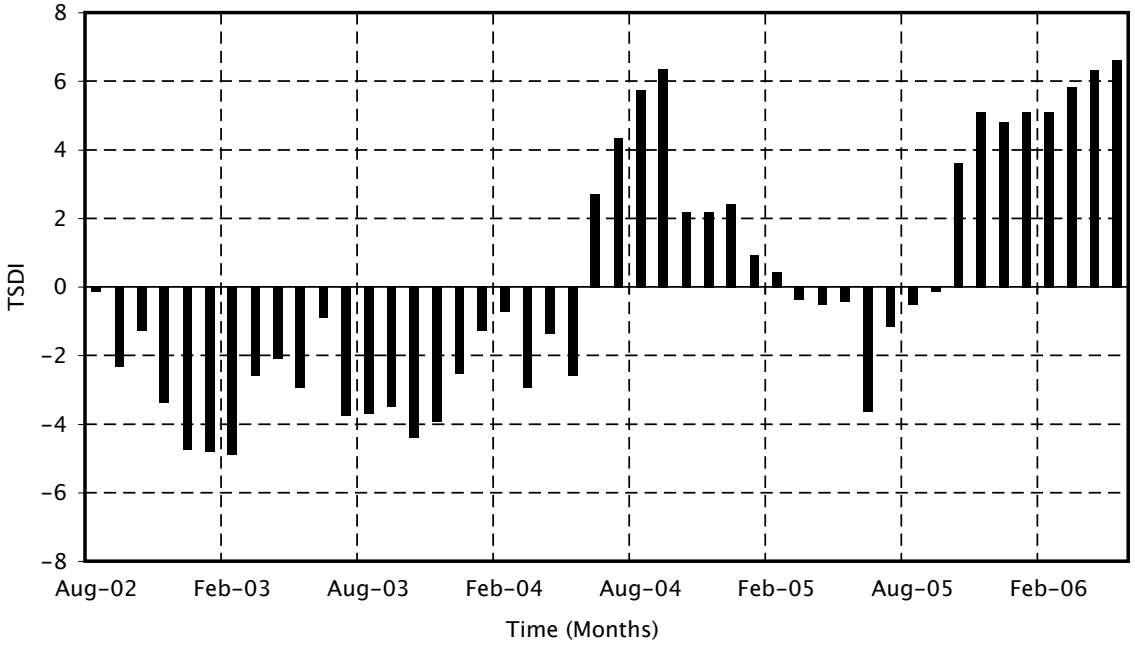

Figure 4.6: Total Storage Deficit Index (TSDI) computed from Equation 4.14.

age: the GRACE-based terrestrial water storage computation and the hydrologically-based total water storage approach for the Saskatchewan River Basin with its outlet at Grand Rapids. The hydrologic storage is derived from the atmospheric-based water balance $P - E$ whilst the measured streamflow records were obtained from the Water Survey of Canada for the chosen outlet.

The results obtained from this study clearly show a strong correlation between the GRACE-based and the hydrologically-derived total water storages. As evident in the time series plots generated, there is a good correlation in the pattern of the average basin storage distribution for the studied area. There appears to be slight discrepancies for certain months but this is not unexpected as it has often been observed that these simulations generally yield under- or over-prediction of terrestrial

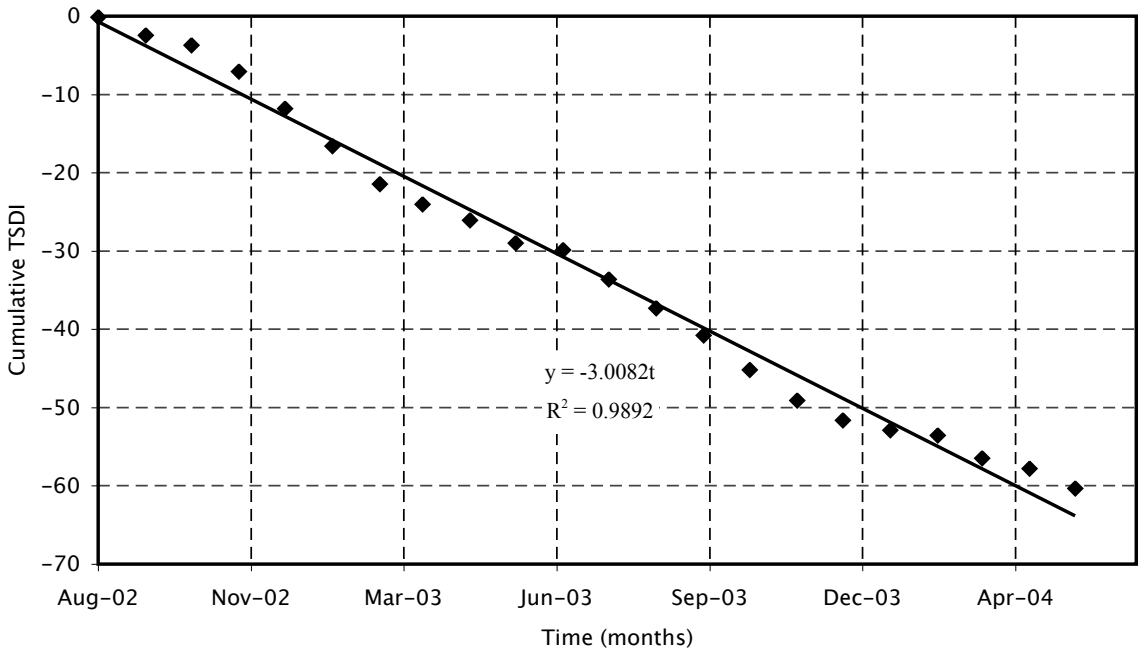

Figure 4.7: Cumulative Total Storage Deficit Index (TSDI) for the Saskatchewan River Basin.

water storage as earlier stated. These discrepancies are associated with errors or limitations emanating from either limited spatial or temporal resolutions or limited data accuracy in the analysis data (CMC dataset) used for the $P - E$ computations. An additional source of uncertainty revolves round the GRACE dataset which could yield RMSE of 2.13 *cm* over the Saskatchewan River Basin.

Using the $TSDI$, it was possible to characterize the 2002/2003 drought episode in order to generate a pictorial representation of the long-term dryness and wetness within this basin. From the $TSDI$ plot, it can be seen that this drought terminated in May 2004 which is attributable to the effects of heavy spring rainfall and an associated winter snowmelt. Additionally, the slope of the best-fit line to the cumulative $TSDI$ plot was estimated as -3 which classifies this drought as severe on the basis of Palmer's

drought severity classification scheme. The outcome of this study therefore supports the pertinence and robustness of GRACE satellite remote sensing data as a means of estimating basin total water storage necessary for drought studies.

Chapter 5

Regional Groundwater Storage from GRACE Over the Assiniboine Delta Aquifer (ADA)

Abstract

[1]Total water storage, which includes groundwater, surface water and snow storage components, plays a major role in hydrologic water balance and has many applications in hydrological modeling. High spatial resolution distributed moisture storage could be considered as a valuable information source for model parameterization and validation. However, it is well known that moisture storage is difficult to measure over the scales needed for hydrological model applications. This paper explores the feasibility of the Gravity Recovery And Climate Experiment (GRACE) gravity infor-

[1]This chapter is a reprint from a paper to be submitted to Water Resources Research (Yirdaw et al., 2010).

mation for regional hydrological model studies. The significance of the total water storage measured by the GRACE satellite is investigated through downscaling efforts using measured groundwater level data available over the Assiniboine Delta Aquifer (ADA) in Manitoba. The goal is to obtain and evaluate local groundwater storage information from coarse resolution GRACE-based total water storage. The result shows that downscaled groundwater storage estimates compares favorably with measured groundwater storage over the study area. It was found that the correlation between the measured and downscaled groundwater storage varies from 0.5 to 0.85. Moreover, the study has shown that it is possible to extract any of the sub-components of storage from the GRACE integrated total water storage on the condition that there is sufficient data to train and validate a transfer scheme.

5.1 Introduction

Moisture stored in the surface and subsurface plays a major role in the hydrologic water balance and is the basis for most hydrological models. It influences the partitioning of energy and precipitation/snow melt inputs at the land surface. As a result, total water storage is a key variable for weather and climate prediction, flood forecasting, drought studies, and the determination of groundwater recharge (Reichle et al., 2001). Therefore, spatially distributed total water storage with high spatial and temporal resolution is considered a valuable information source for model parameterization and validation. However, it is well known that hydrologic storage is difficult to measure and remains essentially unmeasured over the scales needed for hydrological model applications.

Traditionally, there are two possibilities to measure total water storage: namely in-situ measurement and through remote sensing techniques. In-situ techniques have been used to obtain total water storage information at the point scale. These techniques provide accurate total water storage estimates but hydrological models need storage data that effectively represent large spatial areas (Western et al., 1999). This requirement can be realized using remote sensing techniques. In the 1970s, scientists began to hypothesize and test the potential of aircraft and satellite based remote-sensing systems for measuring hydrologically and meteorologically significant phenomena. Since then, remote-sensing systems have contributed to the hydrological community by measuring soil moisture at various space and time scales. Remarkable efforts have been undertaken to obtain soil moisture from these techniques (Njoku and Kong, 1977; Jackson et al., 1999; Wagner et al., 1999). However, most retrieval methods remain experimental because of the strong interference of vegetation and surface roughness on measurements.

In addition to the challenges in retrieving total water storage from remote sensing measurements, the techniques only generally measure unsaturated zone moisture within the first few centimeters (5-10 *cm* in general) of the soil profile. These measurements are meant to determine the root zone soil moisture that can interact with the atmosphere on short diurnal time scales. As a result, groundwater and other surface water storages are generally unable to be retrieved by direct use of these traditional methods. In 2002, the Gravity Recovery And Climate Experiment (GRACE; Tapley et al., 2004a) satellite platform mission was launched to measure, among other things, the gravitational field of the earth. It is the first satellite remote sensing mission that

is directly applicable for the assessment of the groundwater storage under all types of terrestrial conditions. Over its life span, a pair of orbiting satellites will produce a time series of mass changes of the earth-atmosphere system. When integrated over a number of years, this will yield a highly refined picture of the earth's gravity to be used in many geodetic applications. However, the month-to-month changes in gravity are an indicator of the integrated value of watershed moisture storage. Determining these changes requires the expansion of the GRACE geopotential spherical harmonic coefficients into a spatial time series. These spatial estimates are then converted to water equivalent amounts and compared to those monthly estimates of the basin moisture storage derived from more traditional measurements and models.

The GRACE system proved its capability in capturing the changes in terrestrial water storage in large watersheds such as the Mackenzie and Saskatchewan River Basins in Canada (Snelgrove et al., 2004; Yirdaw et al., 2006, 2008 & 2009) and large river basins globally (Rodell et al., 2002; Swenson et al., 2003; Rodell et al., 2004; Tapley et al., 2004; Yeh et al., 2006; Syed et al., 2005 & 2007). Because of the coarse resolution inherent in the GRACE system, its application for regional hydrological studies is still a challenge. Therefore this section of the thesis will infer the GRACE total water storage estimate for small-scale hydrological modeling over the Assiniboine Delta Aquifer (ADA) in Manitoba where a detailed case study has been conducted. The focus will be on downscaling GRACE-based total water storage into finer scale groundwater storage using measured groundwater storage for transfer scheme training, validation and testing. The validation and testing of the downscaled results are required to evaluate the performance of the downscaling scheme.

The process of downscaling refers to a reconstruction of the variation of a value at a specific scale under the assumption that the values recorded at the larger scale are the average of the values at the finer scale (Becker and Braun, 1999). There are many varieties of downscaling techniques that can be used, but in practice, two primary methods can be identified, namely deterministic and statistical downscaling. Deterministic procedures are based on the distribution of spatial patterns, while statistical procedures use stochastic distribution functions based on empirical relationships of features between two scales (Hay and Clark, 2003).

Traditionally, downscaling methods have been used in the field of climatology and meteorology to obtain regional meteorological or climatological information (precipitation, temperature, etc.) from remotely sensed data and coarse resolution climate model output. So far, only a few studies such as Reichle et al. (2001), Kim and Barros (2002), Pellenq et al. (2003) and Lavado et al. (2006) have dealt with the feasibility of disaggregating low resolution soil moisture to a finer scale. For successful application of a downscaling method, it is necessary to determine the relationship between the large-scale and local-scale characteristics. For example, Reichle et al. (2001) investigated the possibility of achieving fine resolution soil moisture from lower resolution passive microwave measurements using data assimilation techniques for interpolation and extrapolation of remotely sensed data. The downscaling method showed that soil moisture can be reasonably estimated at scales finer than the resolution of the passive microwave images, provided that micrometeorological, soil texture, and land cover inputs are available at finer scales.

Other studies such as Kim and Barros (2002) examined the downscaling potential of large scale, remotely sensed soil moisture data in order to determine the temporal and spatial variability of soil moisture. Their study demonstrated that the applied downscaling method captured all the basic statistical and scaling behavior of soil moisture at the higher resolution for a wide range of environmental conditions (wet and dry soils). Pellenq et al. (2003) also applied a similar method to disaggregate soil moisture data. Their downscaling algorithm took topography and soil depth into account. An alternate approach of downscaling near surface soil moisture was carried out using digital terrain modeling and artificial neural networks (Lavado et al., 2006). The Lavado et al. (2006) study used digital models of topographic and land cover variables as inputs and a series of soil moisture measurements as training datasets. Results suggested that artificial neural network techniques provide an efficient analytical data procedure to determine the spatial pattern of non-linear processes such as those related with the near-surface soil moisture. In general, the above noted studies suggest that a finer scale moisture storage can be estimated from low resolution measurements or remotely sensed soil moisture data. In addition, because of the ability of artificial neural network to resolve non-linear processes, it is proposed to use this technique to downscale the GRACE moisture storage into regional groundwater storage over the ADA.

5.2 Methodology

To accomplish the objective of this study, suitable methodologies must be investigated. The following headings explain detailed methodologies that will be used to

accomplish the objective outlined in the previous section. In addition, a brief descriptions of the GRACE-based terrestrial moisture system and descriptions of the study area will be presented.

5.2.1 Site Descriptions

The Assiniboine Delta Aquifer (ADA), located in Manitoba, Canada, is centered on the community of Carberry. The area is dominated by an unconfined sand and gravel deposit that extends approximately 4,000 km^2 (Figure 5.1). The aquifer serves a wide range of domestic, municipal, agricultural, industrial and irrigation water uses. As Frost and Render (2002) cited, many geological and hydrological investigations (Johnson, 1934; Halstead, 1959; Pedersen, 1968; Render, 1987; Burton and Ryan, 2000) have been carried out over the ADA. Their studies suggested that *i*) the thickness of the sand and gravel units vary from 1.5 to over 30 m, *ii*) soil texture varies from coarse gravel to medium sand with a mean grain diameter ranging from 0.508 to 0.127 mm along the western and eastern boundaries respectively, *iii*) an impervious aquifer bottom exists, composed of silt and silty clay. The hydraulic conductivity of the aquifer varies from 4.35×10^{-5} to 2.17×10^{-3} m/s, storage coefficient values are between 0.0006 and 0.001, and specific yield values between 0.11 and 0.39. Hydrologic budget studies suggest that the aquifer stores about 14.80 km^3 of water with recharge to the aquifer being primarily from local rainfall and snowmelt.

The aquifer has been divided into 13 sub-basins based on hydrological divides (Figure 5.1). Measured groundwater information has been used to divide the aquifer hydrologically. It is believed that each sub-basin functions independently and ground-

water does not move from one sub-basin to another. Several groundwater, rain gauge and soil moisture monitoring stations exist in the study area and these monitoring stations are used to collect groundwater level data on a regular basis (Figure 5.1).

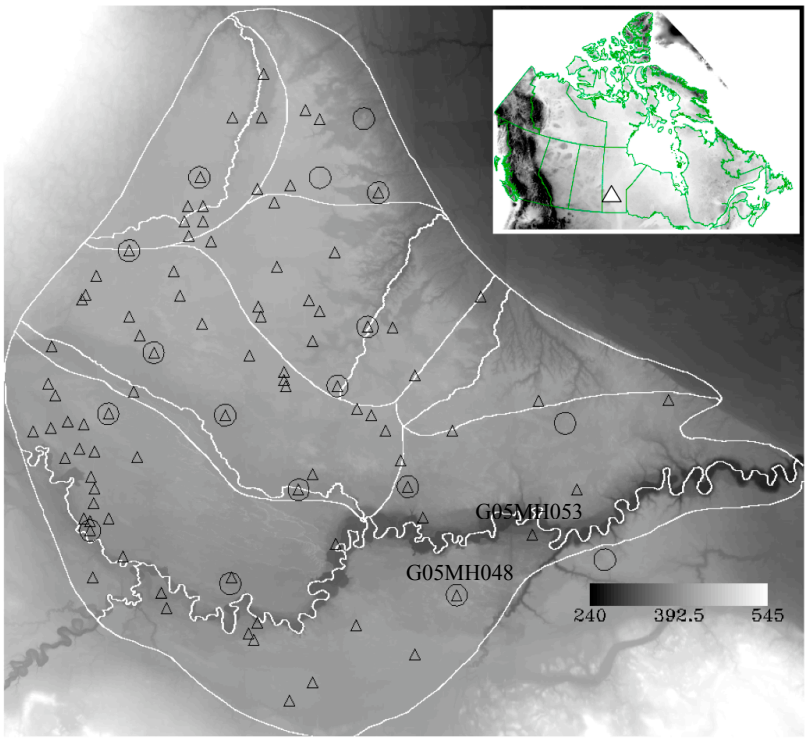

Figure 5.1: Location of the study area (ADA) along with the sub-basins of the aquifer and the location of the observation wells (triangle) and rain gauges (circle) superimposed over the DEM (elevation units of meters)

5.2.2 Measured Groundwater Storage

Extensive groundwater head records required to characterize the region are available at more than 100 monitoring wells distributed across the ADA (Figure 5.1). Daily data were collected at monitoring stations since the early 1980s. These datasets are available and provided by Manitoba Conservation. Each well has been determined

to be open to an unconfined aquifer and representative of the local water table. An example of the groundwater head distribution across the region for December 2006 is shown in Figure 5.2. The monthly spatial groundwater heads are obtained by averaging the daily groundwater head from all piezometers into monthly groundwater head and then interpolating spatially. Subsequently, the monthly groundwater head anomalies are calculated by subtracting the mean groundwater head of each well from the monthly values. An average specific yield value of 0.25 is used to compute water storage anomalies from the groundwater head anomalies. These anomalies are then used as an input to the Artificial Neural Network (ANN) model to downscale the GRACE total water storage anomalies into groundwater storage anomalies during model training, validation and testing. This is described in Section 5.2.4.

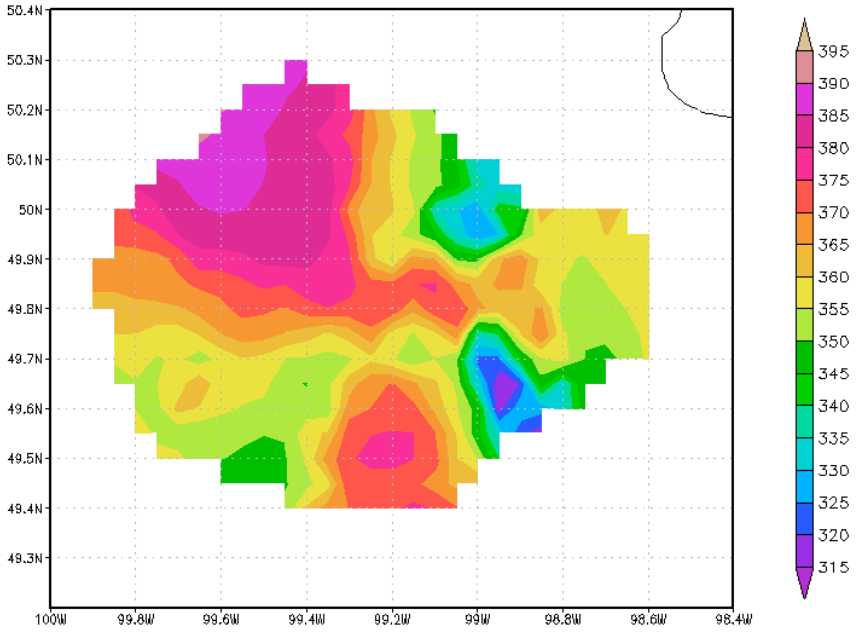

Figure 5.2: The average groundwater head (meter) distribution interpolated from the measured pizometric head for December of 2006.

5.2.3 GRACE-based Moisture Storage

As described in previous chapters, the preliminary dataset retrieved from the GRACE satellite remote sensing mission are transformed to time series of geopotential spherical harmonic coefficients (level 2 dataset, release CSR-RL01) by research groups at the Centre for Space Research (CSR) at the University of Texas, the National Aeronautics and Space Administration (NASA) and the Deutsches Zentrum fur Luft und Raumfahrt (DLR) in Germany. These level 2 data are then distributed freely to the GRACE data user community for hydrological and sundry applications. Essentially, the non-hydrological gravitational contributions, such as atmospheric and oceanic contributions plus solid earth tides, are removed in the level 2 product (Chen et al., 2005a). Thus, the initial step for studying the monthly variation of temporary change in water storage entails extracting monthly variations of these storages from hydrological reservoirs.

Sequences of 46 monthly variations of gravity field estimates were extracted from GRACE data collected between April 2002 and May 2006 (with the exception of missing data for May, June, July 2002 and June 2003). Due to large non-physical variability in GRACE data, the C_{20} geopotential spherical harmonic coefficient was excluded in these computations. Moreover, only the first fifteen spherical harmonic coefficients were used since spherical harmonic degrees greater than 15 are presently dominated by errors (Wahr et al., 2004). The change in average moisture storage resulting from GRACE was determined according to the approach of Heiskanen and Moritz (1967), Wahr et al. (1998) and Ramillien et al. (2004). Thereafter, an 800 km Gaussian smoothing radius was employed to derive GRACE-based terrestrial water

storage as this produces minimum RMS (Root Mean Square) residuals over the land surface areas (Chen et al., 2005b).

5.2.4 Artificial Neural Network (ANN) Model Training

As it was mentioned in Section 5.2.2 above, the general approach is to train the ANN model using the GRACE total water storage estimates as an input and the measured groundwater storage as an output. In so doing, the model learns a mapping from low resolution GRACE moisture storage into point (measured) groundwater storage and seeks to replicate the measured patterns of the groundwater storage. Among the 104 piezometric groundwater level locations, only those measurements that have continuous records of groundwater level data from April 2002 to December 2006 were used for downscaling the GRACE terrestrial moisture storage anomalies. A total of 59 piezometers are identified and used for this purpose. Those piezometers that contain missing data during the simulation periods are not included for downscaling of the GRACE total water storage estimates. The GRACE total water storage anomalies are then downscaled to the piezometric groundwater storage anomalies and finally interpolated spatially. GRACE measurements, on the other hand, have missing data during the months of May, June, July 2002 and June 2003 (as mentioned in Section 5.2.3), and as a result, the measured groundwater storage data during these months are not considered for training or validation of the downscaled GRACE-based groundwater storage anomalies which resulted in a total of 46 month simulation periods. The first 30 months of measured groundwater storages are used for model training, the following 8 months are used for model validation and the remaining 8 months are

used for model testing.

5.3 Result and Discussion

The spatial variability of total water storage anomaly derived from GRACE-based gravity measurements for April and May 2006 are shown in Figure 5.3. The anomalies are calculated by subtracting the long-term mean gravity measurements (mean of the 46 months) from each monthly result and converting these into equivalent water thickness of the total water storage. The spatial resolution of these plots is 1^o by 1^o. These months were selected from the total analysis period to show how the GRACE gravity harmonic coefficients were converted to the spatial varying total water storage. These monthly storage anomaly values were used to drive the regional groundwater storage over the Assiniboine Delta Aquifer using the statistical downscaling technique described in the previous section. Details of the downscaled GRACE groundwater storage anomalies at selected locations over the ADA are presented below.

Figures 5.4, 5.5 and 5.6 show the monthly time series of GRACE-based total water storage, measured groundwater storage and downscaled groundwater storage anomalies at two observation well locations (specifically, well numbers G05MH048 and G05MH053 whose locations are shown in Figure 5.1). Also shown are the averaged groundwater storage anomalies over the study area (average of the 59 pizometric groundwater storages). The time series spans from April 2002 to May 2006, with the exception of May, June, July 2002 and June 2003 where GRACE measurements are unavailable. Data from these plots serve as input and output total water storage and groundwater storage during model training, validation and testing. As shown

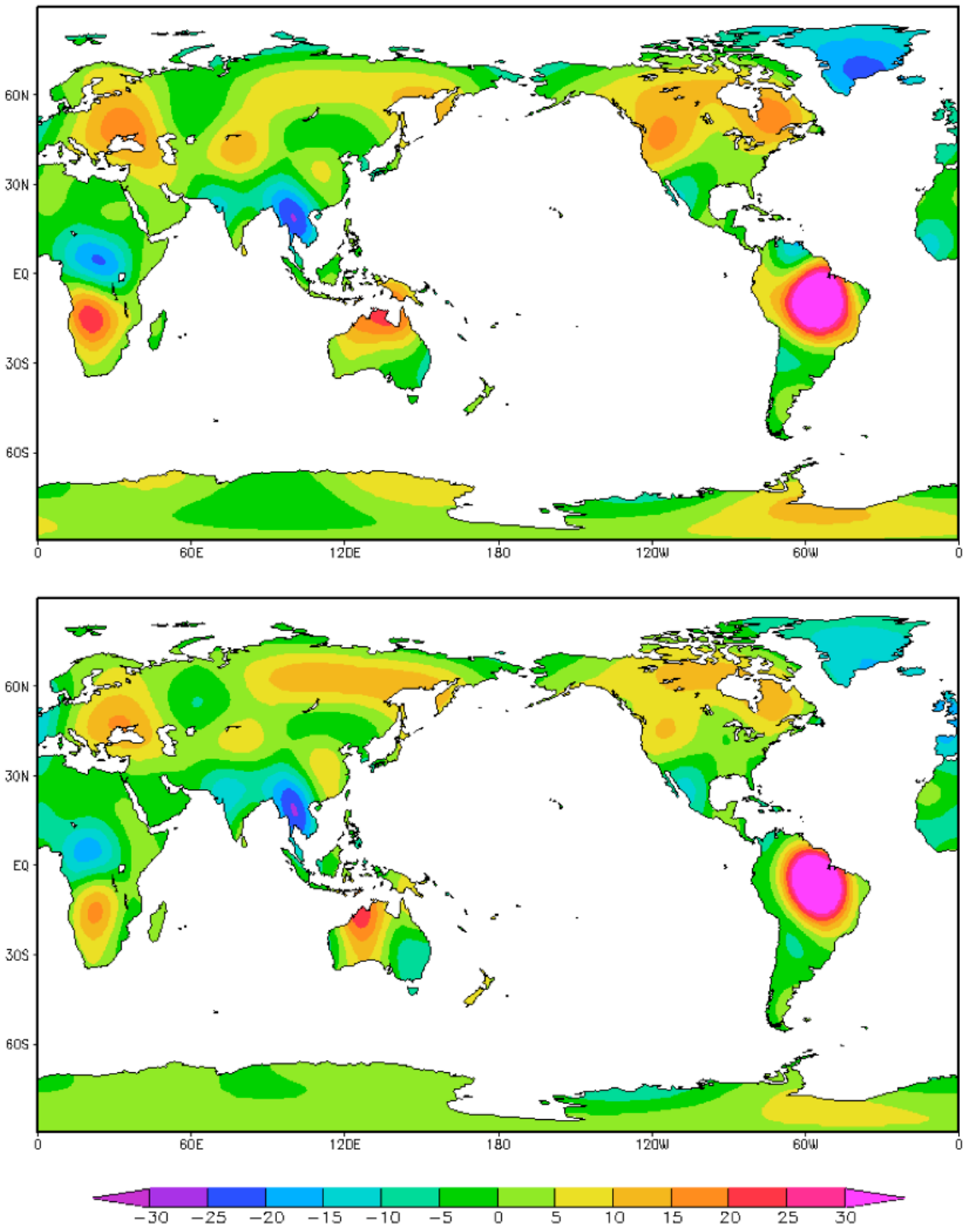

Figure 5.3: Terrestrial water storage anomalies in cm of water equivalent thickness relative to the mean storage for April 2006 (top) and May 2006 (bottom)

in these figures, significant correlation exists between the downscaled and measured groundwater storage anomalies. Correlation (R) value ranges from 0.5 to 0.85 (not shown on these figures) have been calculated. In most pizometric location, such as G05MH048 (Figure 5.4), where the correlation between the downscaled and measured groundwater storage anomalies are as close as 0.85, the time series of groundwater storage anomalies of these two methods are in good agreement during model training, validation and testing. A statistical test further confirms that the mean of the measured and downscaled groundwater storage anomalies are statistically equivalent at 5% significant level (p-value = 0.852). The variances of the two anomalies were, however, statistically significant with a p-value of 0.014. Moreover, the downscaled result is able to capture the measured groundwater storage anomalies in terms of both the amplitude and time series variation through most of the simulation period. This suggests that the ANN methods are useful in retrieving the groundwater storage component from the GRACE total water storage anomalies for regional hydrological studies.

On the other hand, in some locations, such as G05MH053 (Figure 5.5), where the correlation values are as low as 0.5, one can observe discrepancies between the downscaled and measured groundwater storage anomalies. Even though there exist a high correlation between the two and statistically equal mean at 5% significant level (p value = 0.889), the month-to-month groundwater storage anomalies tend to have a significant variation with variances of the measured and downscaled groundwater storage anomalies become statistically significant with a p-value of 0.003. For example, in Figure 5.5, clear discrepancies between the measured and downscaled

groundwater storage anomalies from June 2004 to October 2004 are shown. This may be due to the fact that during the months from July to October 2004, Yeh et al. (2006) reported that the GRACE data are problematic. Among other uncertainties in the input data, problems existing in the GRACE data during these months could be partially responsible for the discrepancies.

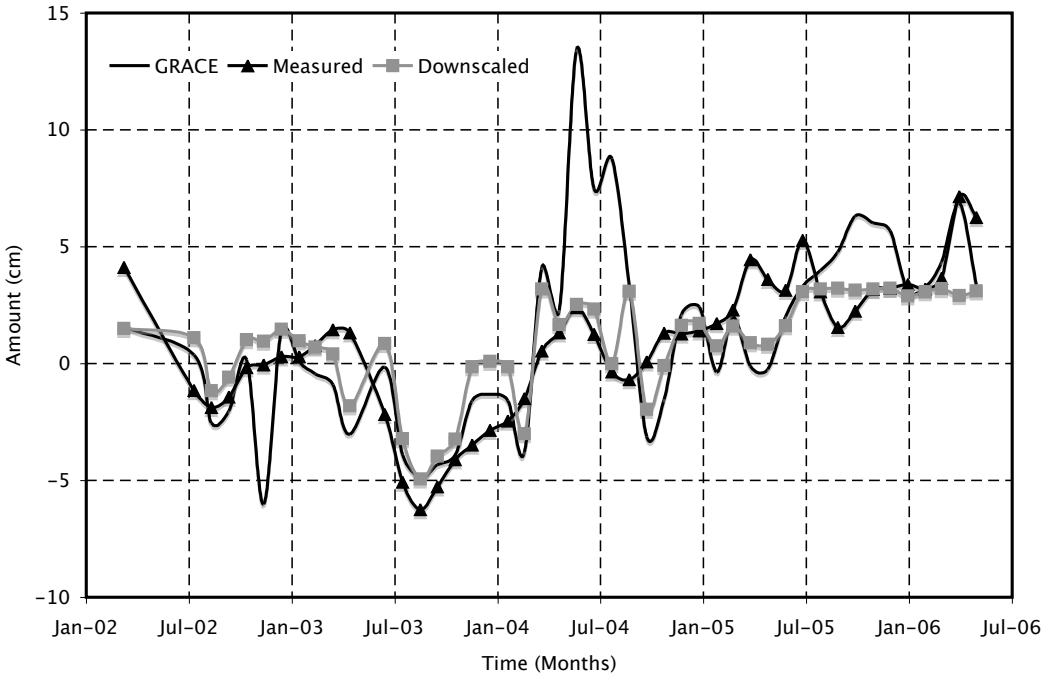

Figure 5.4: Comparison between GRACE total water storage anomalies and measured and downscaled groundwater storage anomalies at pizometric location of G05MH048

Figure 5.6 plots the same as Figures 5.4 and 5.5 but it is spatially averaged over the ADA. This figure shows that the average measured and downscaled groundwater storage anomalies are also generally in good agreement with a statistically equal mean at 95% confidence interval (p-value = 0.879). The variances of the two anomalies (measured and downscaled) were, however, resulted a statistically significant differences with a p-value of 0.017. The time series result further explains that the GRACE

total water storage anomalies are well correlated with the measured and downscaled groundwater storage at the scale of the Assiniboine Delta Aquifer for this area with the exception of those months where GRACE data experiences some problem, and during the winter season when snow accumulations are reflected in GRACE total water storages estimates but not in the groundwater measurement. It should be noted that the GRACE total water storage anomalies and the groundwater storage anomalies cannot be compared directly since GRACE measures the vertically integrated total water storages which includes saturated groundwater, unsaturated soil moisture, surface water storages and snow accumulations. This is in contrast to groundwater storage plotted in Figures 5.4, 5.5 and 5.6 that is only one component of the GRACE total water storage anomaly.

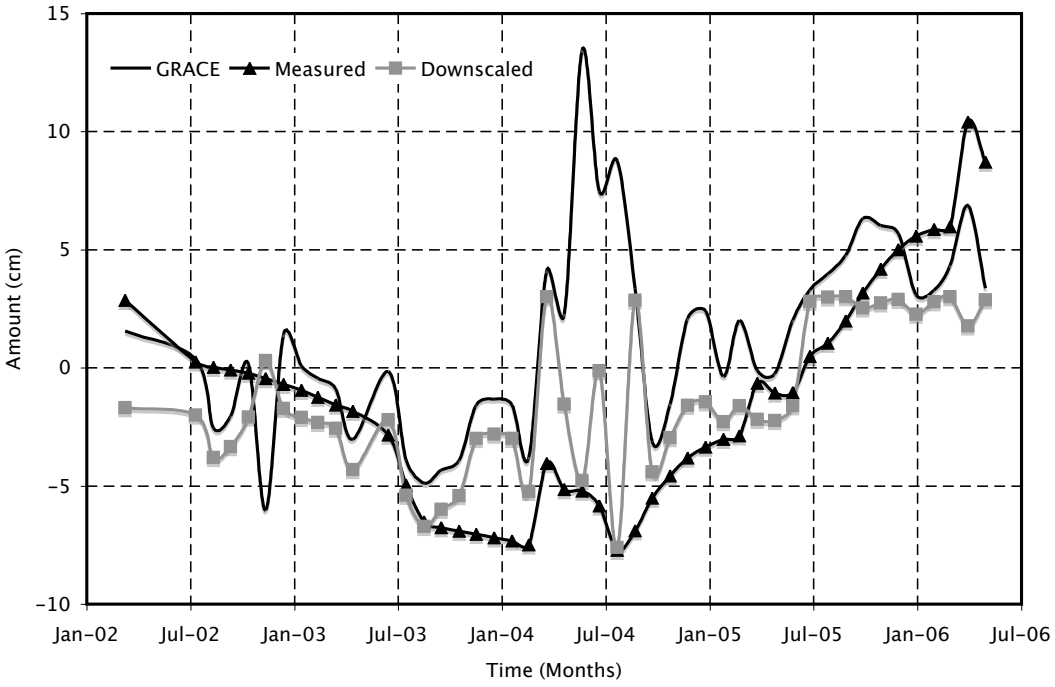

Figure 5.5: Comparison between GRACE total water storage anomalies and measured and downscaled groundwater storage anomalies at pizometric location of G05MH053

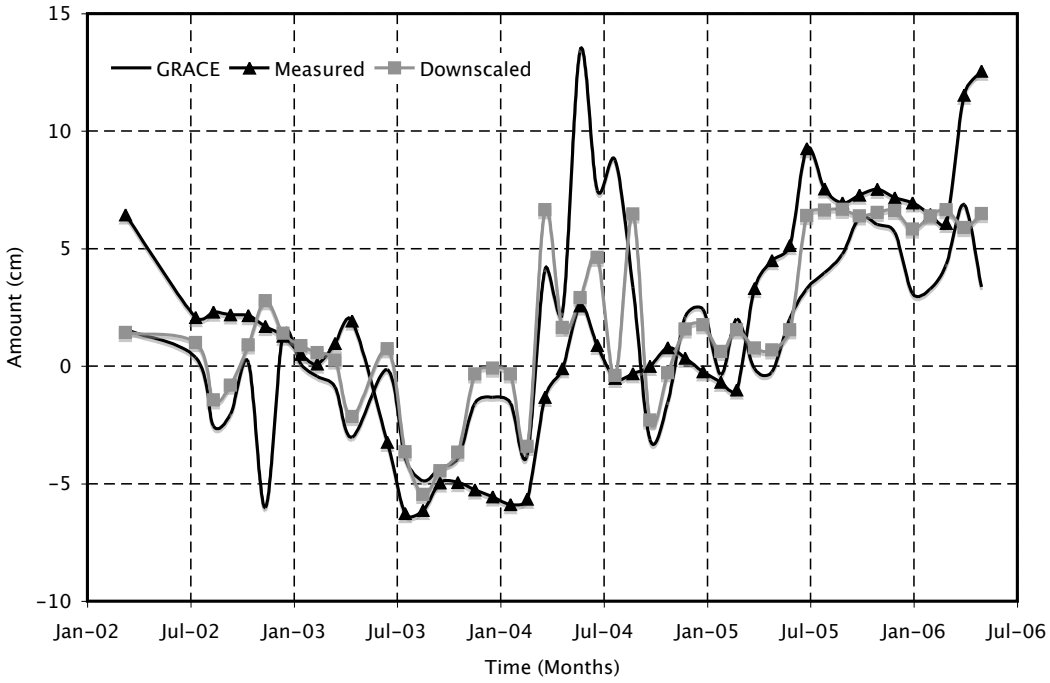

Figure 5.6: Comparison between GRACE total water storage anomalies and measured and downscaled groundwater storage anomalies averaged over the ADA

The figure further depicts that the GRACE signal is highly dominated by the groundwater storage over the ADA except during winter periods. This reinforces previous water balance studies over the aquifer which stated that the groundwater storage in the aquifer is the dominant water balance component (Frost and Render, 2002). Since aquifer hydraulic conductivity values are relatively high (ranging from 10 m/day to 180 m/day) and dominated by flow in sand deposits, the unsaturated soil moisture storage becomes less significant than the groundwater storage in areas with greater surface water dominated processes. Precipitation and snow melt inputs primarily recharge the aquifer and become groundwater storage. This is well reflected in Figure 5.6. Moreover, the ADA is part of the Canadian Prairie, which suffered from drought that started in 1999 and terminated in 2004. The measured and downscaled

groundwater storage as well as the GRACE total water storage anomalies during the years 2002 and 2003 are below the normal, which signals GRACE's ability in recording drought at this regional level. GRACE has been used for such studies at larger watershed scales (Yirdaw et al., 2008) and this study highlights the usefulness of the GRACE gravity measurements for similar studies at a regional level.

In addition to the groundwater storage time series comparison, the spatially distributed measured and downscaled groundwater storages are compared in this part of the study. Figure 5.7 illustrates the average monthly measured and downscaled groundwater storages anomalies over the ADA. Multi-color scale bars are used for each plot in order to depict spatial variation in the downscaled and measured groundwater storage anomalies for the various months. This plot is spatially interpolated at a resolution of 2.5×2.5 km of the 59-pizometric groundwater storage anomalies. Three months (April 2003, September 2005 and March 2006) have been chosen for model training, validation and testing periods, respectively. The figure shows how the techniques applied in this study may be useful for regional hydrological studies by retrieving the groundwater storage component. All three monthly results shown in Figure 5.7 agreed that the downscaled technique captures the peak and low groundwater storage anomalies in the region during model training, validation and testing.

Despite observing good spatial agreements of the measured and downscaled groundwater storage anomalies in most parts of the study area, there exist discrepancies in some locations, mostly along the north-eastern boundary of the aquifer. This may be due to the fact that few piezometers have continuous records of groundwater head in this region, resulting in unsmooth interpolation.

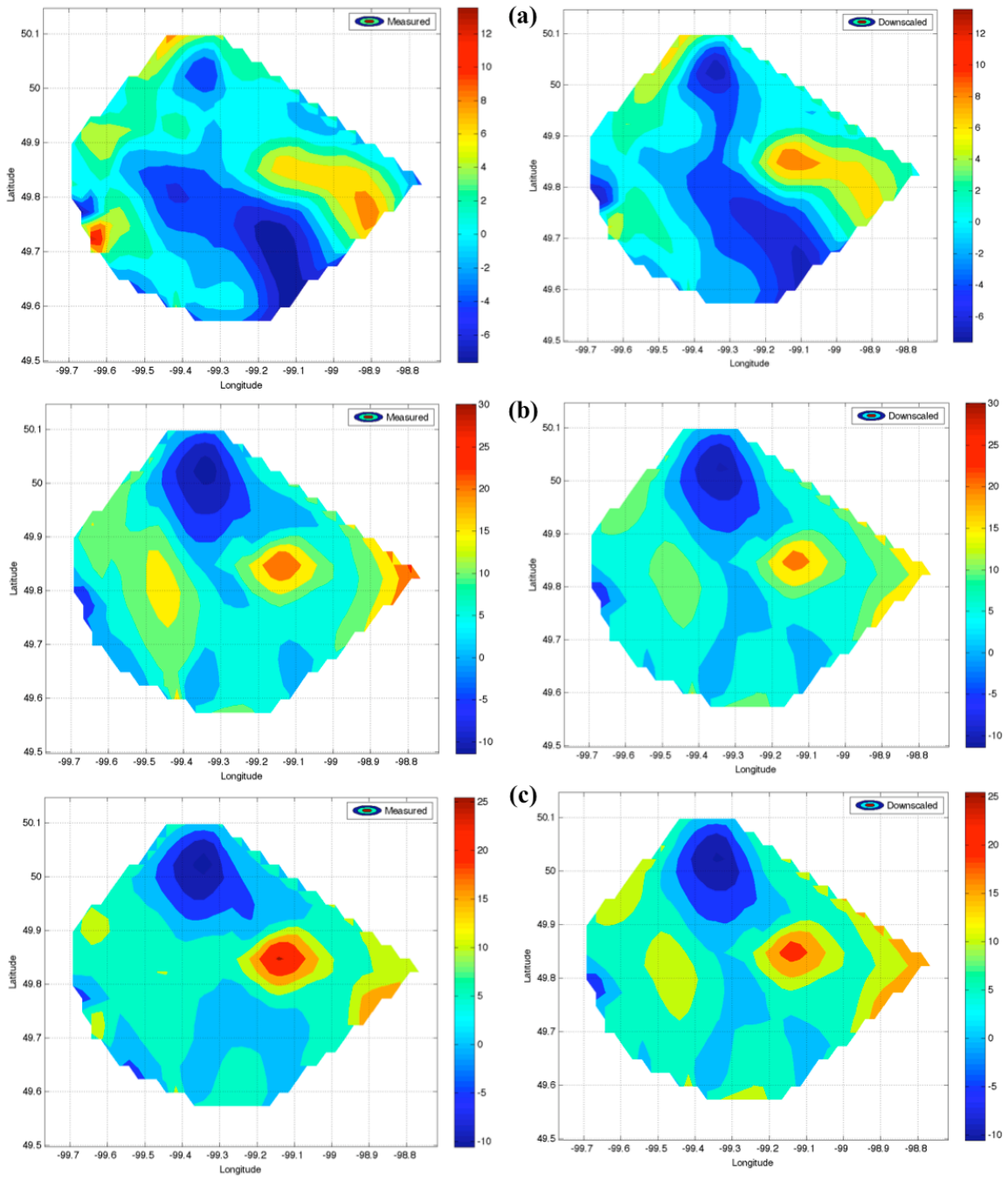

Figure 5.7: Average monthly measured and downscaled groundwater storage anomalies for the months of (a) April 2003, (b) September 2005 and (c) March 2006 over the ADA

This study suggested that the GRACE total water storages can be separated into its components (groundwater, unsaturated soil moisture, surface water and snow) if the techniques applied in this study are used. Here, groundwater storage is retrieved from the total water storage obtained from GRACE and the outputs presented above indicates a satisfactory result. Alternatively, if the goal of the study is the unsaturated soil moisture, surface water or snow storages, it may be possible to use similar techniques to separate the respective storages from GRACE total water storages if sufficient data to train, validate and test the transfer scheme is available over the given area.

5.4 Conclusions

This study has demonstrated a downscaling technique to retrieve regional ground water storage in the Assiniboine Delta Aquifer from the GRACE-based total water storage estimate. The study has focused on downscaling of the GRACE total water storage estimate into regional groundwater storage and has compared downscaled and measured groundwater storages from point scale to regional scales (approximately 4,000 km^2). These comprehensive comparisons suggest that the results from this approach are very promising for the hydrological community. The time series of measured and downscaled groundwater storage from this approach in most of the locations are in good agreement, with correlation values ranging from 0.5 to 0.85. Furthermore, the aquifer average groundwater storages (measured and downscaled) are well correlated with the GRACE total water storage estimates which indicates that among the different water storage components, groundwater storage is the most

dominant storage over the ADA.

Finally, the result may have important implications for disaggregating GRACE total water storages into the different components of water storages. This may be potentially useful in other hydrological studies. Additionally, it can be mentioned that both statistical or dynamic downscaling approaches can be used to separate the components of the GRACE total water storages into the respective storages for use in different hydrological modeling applications. However, such studies need sufficient data that can be used to train, validate and test the model.

Chapter 6

Modeling of the Assiniboine Delta Aquifer of Manitoba

6.1 Introduction

As was briefly mentioned in Chapter 2, the Assiniboine Delta Aquifer (ADA) is located in south central Manitoba centered on the community of Carberry. The aquifer contains an unconfined sand and gravel deposit covering an area of approximately 4,000 km^2. The aquifer serves as a potable water supply for domestic use and as a source for other municipal, agricultural, industrial and irrigation purposes. Frost and Render (2002) reported that the aquifer had been used primarily for small town, domestic and farm water supplies until the mid 1970's. However, water withdrawals from the aquifer have increased dramatically during the 1980's primarily due to increased irrigation demand. As a result, hydrological investigations of the aquifer have intensified as part of a federal-provincial water supply evaluation agreement. Since

then, detailed hydrological data have been collected and made available for this study through Manitoba Conservation. These data are sufficient to support the development of a groundwater model over the area. Therefore, in addition to one of the objectives of this thesis mentioned in Chapter 1, i.e. model parameterization using the downscaled GRACE groundwater storage, the development of a computer model would help as a benchmark for future groundwater modeling that would be used to manage the sustainability of the aquifer water for domestic, municipal, agricultural, industrial and irrigation uses. Furthermore, it would help to better monitor the allocation limits for future water use particularly in the development of climate change scenarios.

In order to achieve the objectives set out above, this chapter is organized as follows: Sections 6.1 and 6.2 provide a detailed description of background information of the area and the input data used to model the aquifer. Section 6.3 presents coupled surface water-groundwater results along with comparisons of the measured well data and the GRACE satellite result. Finally, Section 6.4 offers summaries of the findings from the study.

6.1.1 Geology

The ADA is dominated by the sand and gravel deposits throughout most of the aquifer. Small proportions of clay and marshland are present in the western and central parts of the aquifer. Other non-dominant land forms include alluvial sand in the southwest, silt, alluvial silty clay and coarse sand in the north and fine sand in the east. Figure 6.1 presents a 3D representation of the distribution of the surficial

deposits over the aquifer. As can be seen, the bottom boundary of the ADA is composed of glacial till overlying a shale bedrock layer that extends from the east to the west edge of the area.

As reported in Frost and Render (2002), the formation of the aquifer is a result of sediment deposits from a very large glacial river within a depression that existed in the glacial till surface in pre-historic times. Grain size distribution and deposit thickness over the ADA vary considerably due to continuing change of the pre-historic river flow and the redistribution of channels over the developing delta.

The Frost and Render (2002) report also presents information regarding the characteristics of the aquifer that have been obtained from drilling logs that are filed when municipal and private wells are completed. Depth-to-bedrock measurements range between 5 to 140 ft (1.6 to 42.5 m). Generally, sand and gravel units are thinner in the west and thicker in the north central and northeast portions of the aquifer. There is also great variation in the soil grain size distribution over the aquifer which varies from coarse gravel to medium sand (mean grain diameter of 0.50 mm) along the western portion of the aquifer to very fine sand (mean grain diameter of 0.13 mm) along the eastern boundary.

6.1.2 Topography and Surface Water Features

Surface elevations in the area range from 240 m (near Lake Manitoba) to 545 m (in the northwest corner) above sea level. As shown in the shaded relief plot of the ADA in Figure 6.2, most of the area, especially the central and northern portion is essentially flat. This shaded relief map was derived from the high resolution (90

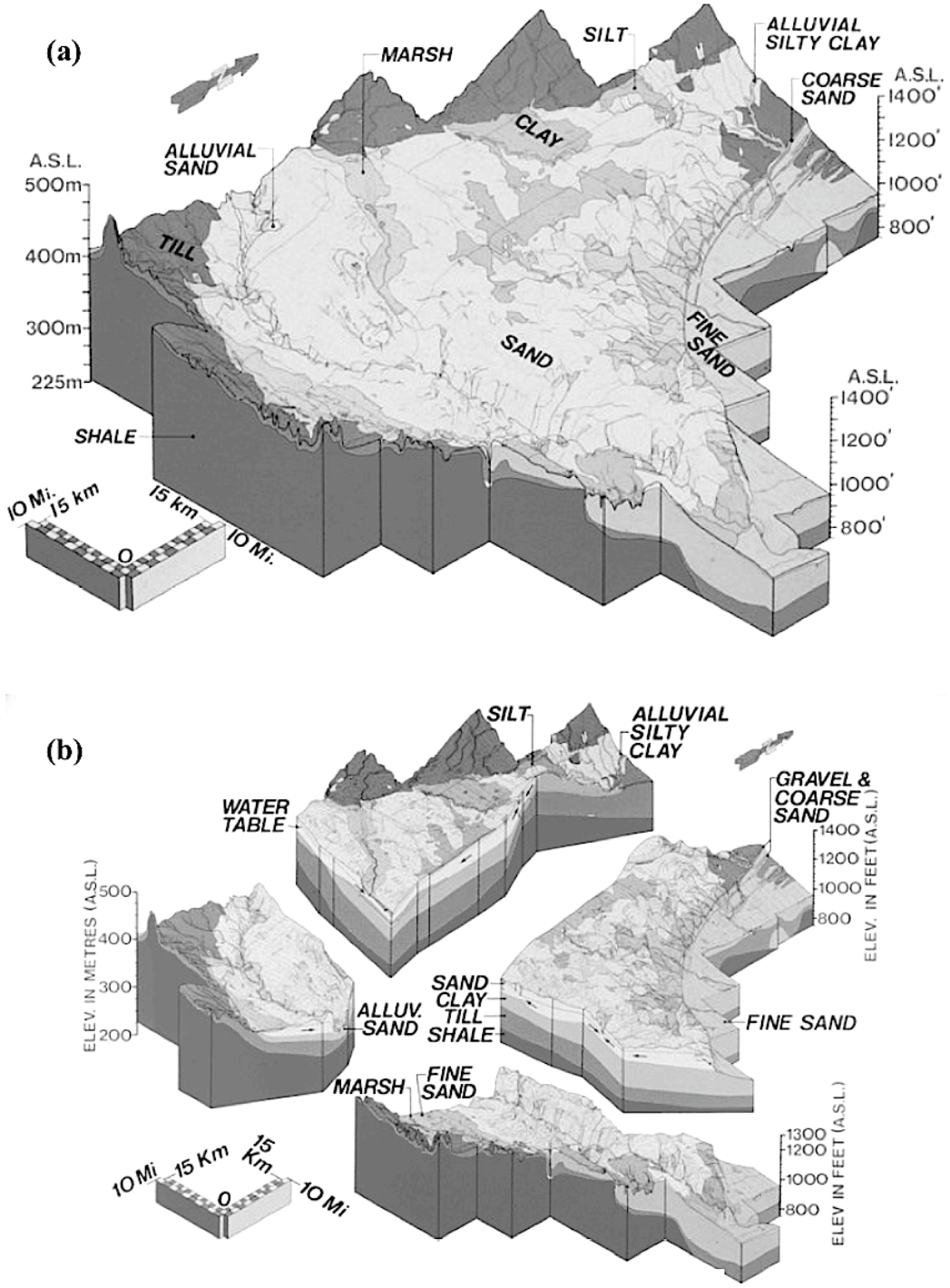

Figure 6.1: Geology of the Assiniboine Delta Aquifer: (a) Surficial Deposits of the Assiniboine Delta Aquifer, (b) the 3D plate of the geological units (After Frost and Render, 2002)

m) Shuttle Radar Topography Mission (SRTM) digital elevation model (DEM) data. This DEM data will be resampled and hydrologically modified (filling sinks) for model development later in this chapter. The aquifer is divided into thirteen sub basins (Figure 6.3) based on hydrological divides that were determined from the measured groundwater levels across the aquifer. The vector file containing these sub basin was obtained from Manitoba Conservation (personal communication). In addition, the Assiniboine River, which passes through the aquifer, serves as a hydrologic divide by separating sub basins through which it flows as shown in Figures 6.2 and 6.3.

Because the coarse textured soils allow most of the rainfall to reach the aquifer and most snow melt to infiltrate, there is little surface runoff in the study area and subsequently a poorly defined drainage network. Only small lakes and wetlands have developed. The surface drainage system over the aquifer is dominated by the deeply incised Assiniboine River channel and its tributaries. However, there are a number of smaller creeks and roadway ditches spread across the aquifer that direct water into or out of the aquifer. These small creeks include Whitemud River in the north, the Pine Creek in the north-east, the Souris River system in the west and the Oak River system in the south. A number of these smaller creeks are gauged as flow stations on or in the vicinity of the Assiniboine Delta Aquifer. However, unlike groundwater head stations, most surface water stations do not have continuous flow records. In particular records are often missing in the winter months of November to February.

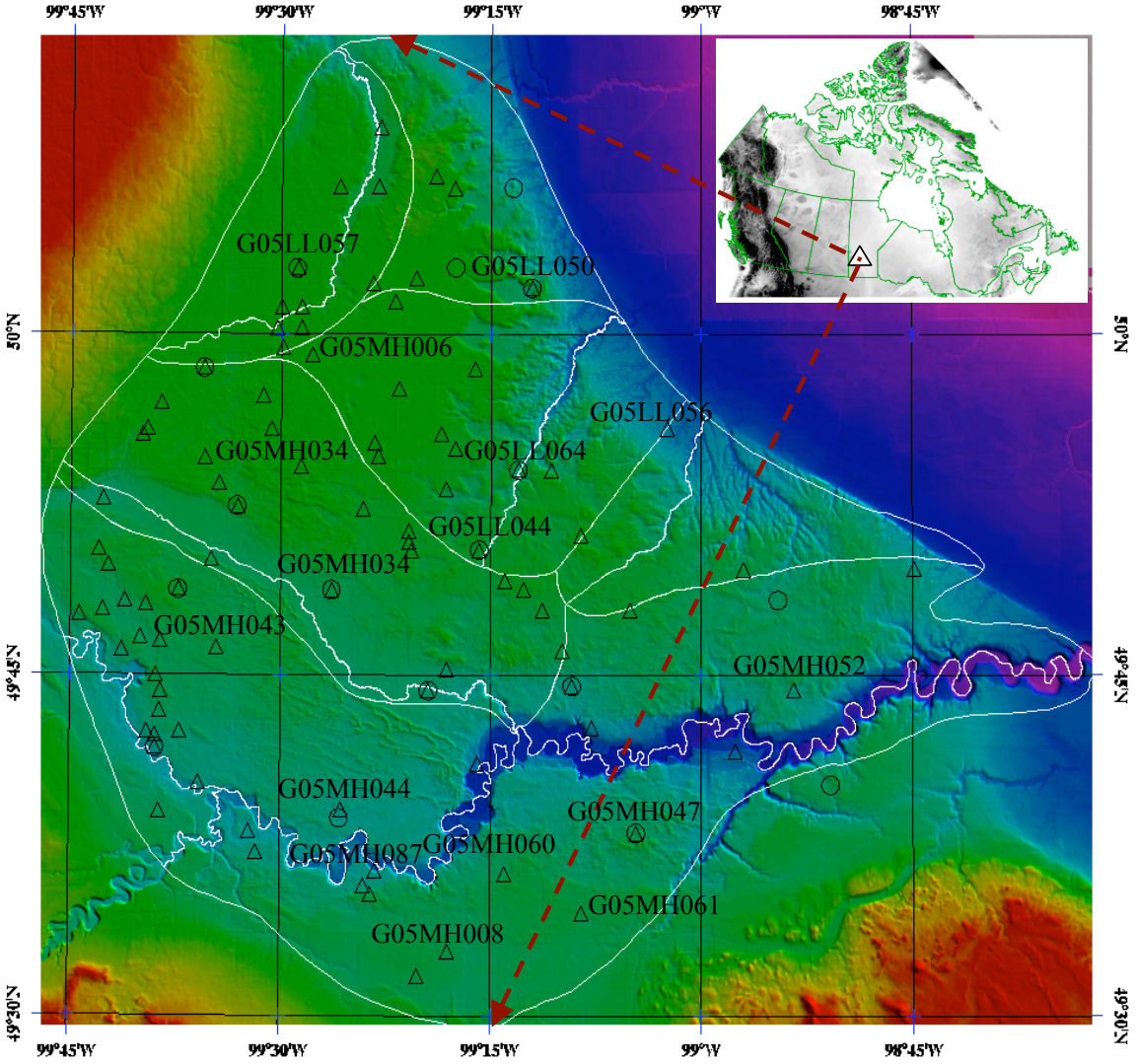

Figure 6.2: Shaded relief of the Assiniboine Delta Aquifer in conjunction with the locations of the observation wells (triangle) and the rain gauges (circle)

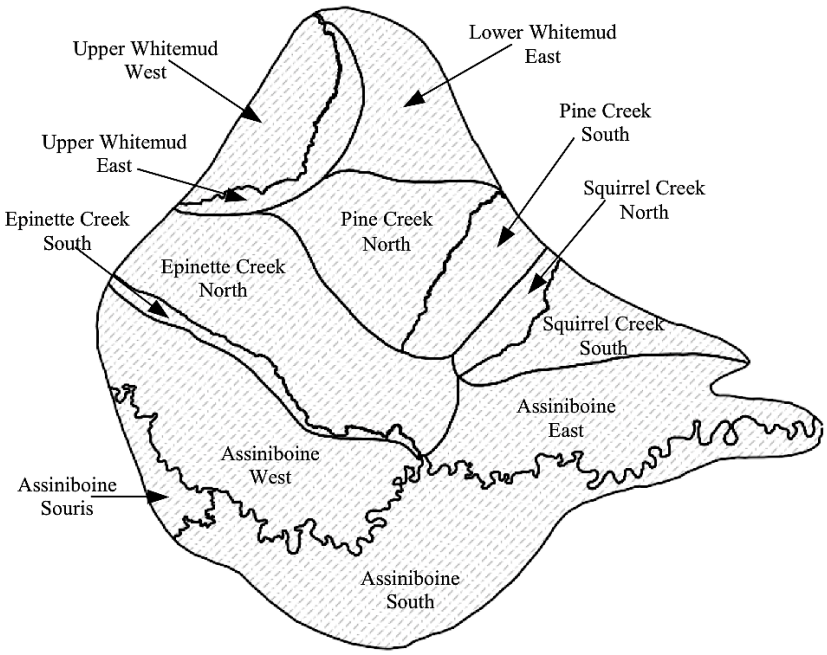

Figure 6.3: The various sub basins of the Assiniboine Delta Aquifer

6.1.3 Climate

The climate of the ADA is cool and sub-humid. The winters are cold and relatively dry while summers are hot and precipitation is dominated by summer thunder storms. The average seasonal temperatures range from -15^oC in the winter to 17^oC in the summer (based on temperature measurements near Brandon, Manitoba). Annual precipitation ranges from 260 mm to 530 mm over the period 1999 to 2006. Precipitation is the primary source of moisture into the hydrologic system, while evapotranspiration (ET) is the primary loss. It is hypothesized that vegetation type plays an important role in the area and influences the evaporative loss back to the atmosphere.

6.2 Coupled Model Setup

6.2.1 Aquifer Stratigraphy

As discussed previously, most of the ADA consists of sand interspersed with less extensive gravel deposits. It has been observed that the saturated thickness of the aquifer is thinner in the western part and thickest through the central and northeast areas. However, the observation well network is not sufficiently dense to determine variations in aquifer thickness particularly under the many large dune covered areas (Frost and Render, 2002). As a result, and for the purpose of this study, the elevation of the base of the model layer is assumed to be a constant elevation with a value of 230 $m.a.s.l.$ Therefore, the distribution of the layer thickness of the aquifer is represented by surface topography and constant elevation of the bottom boundary. More detailed mapping and stratographic exploration would be required to provide greater realism to the simulation. It is unknown whether greater realism would improve simulations. However, as will be shown, it appears that a majority of the variation in aquifer dynamics has been captured with this simplification.

6.2.2 Hydraulic Conductivity

The hydraulic conductivity of the ADA was derived from transmissivity and saturated thickness maps of the ADA developed by Manitoba Conservation. These hydraulic conductivity values were estimated from a series of detailed pumping test and soil samples that have been collected during the drilling program. For areas where no pumping tests have been conducted, hydraulic conductivity values were estimated

by empirical formulas based on soil analysis data (Frost and Render, 2002).

During the initial development of the groundwater model, average hydraulic conductivity values for each of the ADA sub-basin were estimated using average transmissivity and saturated thickness defined for each sub-basin. These values were used for the initial runs and later their values were changed through model calibration (see Section 6.3.1). Table 6.1 summarizes the estimated average hydraulic conductivity values that were used prior to model calibration. In order to calculate sub-basin average hydraulic conductivity, the average transmissivity was divided by the average saturated thickness for each sub basin. Outside the ADA domain, a very low transmissivity value (100 $USgal/ft/day$) and a minimum saturated thickness (5 ft) were assumed and the hydraulic conductivity value was calculated accordingly.

Table 6.1: Average Transmissivity (T), Saturated Thickness (S) and Hydraulic Conductivity (K) of the Assiniboine Delta Aquifer sub basins

Sub Basins	T ($USgal/ft/day$)	T (ft^2/day)	S (ft)	K (ft/day)	K (m/hr)
Lower Whitemud East	37500	5013.02	25	200.52	2.55
Upper Whitemud East	50000	6684.03	40	167.10	2.12
Upper Whitemud West	42500	5681.42	20	284.07	3.61
Pine Creek North	52500	7018.23	90	77.98	0.99
Pine Creek South	22500	3007.81	50	60.16	0.76
Epinette Creek North	70000	9357.64	70	133.68	1.70
Squirrel Creek North	17500	2339.41	50	46.79	0.59
Squirrel Creek South	5000	668.40	30	22.28	0.28
Epinette Creek South	60000	8020.83	50	160.42	2.04
Assiniboine West	60000	8020.83	50	160.42	2.04
Assiniboine East	22500	3007.81	75	40.10	0.51
Assiniboine Souris	22500	3007.81	15	200.52	2.55
Assiniboine South	22500	3007.81	50	60.16	0.76
Outside the ADA Domain	100	13.37	5	2.67	0.03

6.2.3 Storativity and Specific Yield

Storage coefficient is the volume of water released per unit area of aquifer and per unit drop in head $[m^3/(m^2 \times m)]$, while specific yield measures water drainage by gravity when the water table decreases $[m^3/m^2/m]$. Both of these non-dimensional parameters are required for groundwater modeling. In the ADA, like transmissivity, the storativity and specific yield of the aquifer were determined from the pumping tests conducted in the aquifer by Manitoba Conservation. Result from these tests indicate that the storativity and specific yield values range from 0.0006 to 0.001 and from 0.11 to 0.39, respectively (Frost and Render, 2002). Specific yield values are dependent on the grain size and the duration of the pumping test. The average values of 0.008 for the storativity and 0.25 for the specific yield were used as an input to the model.

6.2.4 Groundwater level

As shown in Figure 6.2, there exist more than 100 observation wells across the ADA. Data has been measured on daily time steps starting from the early 1970's. This data has been collected for effective groundwater management by Manitoba Conservation, Water Stewardship branch. This data is used to evaluate the quantity of the groundwater withdrawals and ensure a dependable and affordable supply of groundwater in the future. Well water is also analyzed to help protect the water quality of the aquifer to ensure that groundwater remains suitable for domestic, industrial, agricultural, and environmental uses.

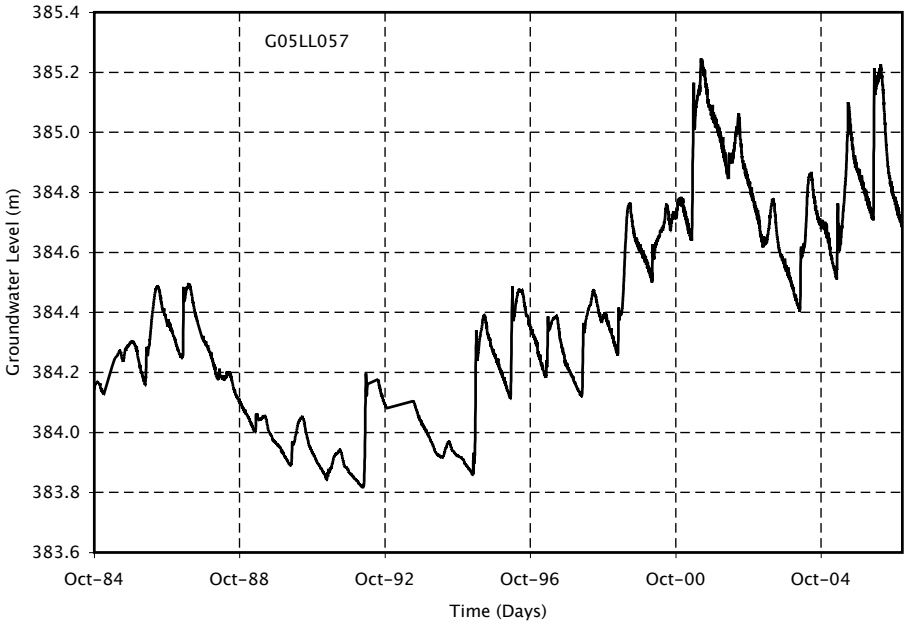

Figure 6.4: Measured groundwater head at observation well G05LL057 within the Assiniboine Delta Aquifer

Hydrographs for two of the 104 observation wells (G05LL057 and G05MH052) are shown in Figures 6.4 and 6.5, respectively. Also shown in Figure 6.6 is a map of groundwater head for the month of December 2006 that has been spatially interpolated from the 104 well records (averaged over the month). These data from across the aquifer were used to retrieve the groundwater storage from the GRACE based total water storage using the downscaled technique mentioned in Chapter 5. Here, the well data in conjunction with the downscaled GRACE total water storage will be used to compare the head distributions predicted from a coupled groundwater and surface water model to determine if the model provides reasonable matches to observations.

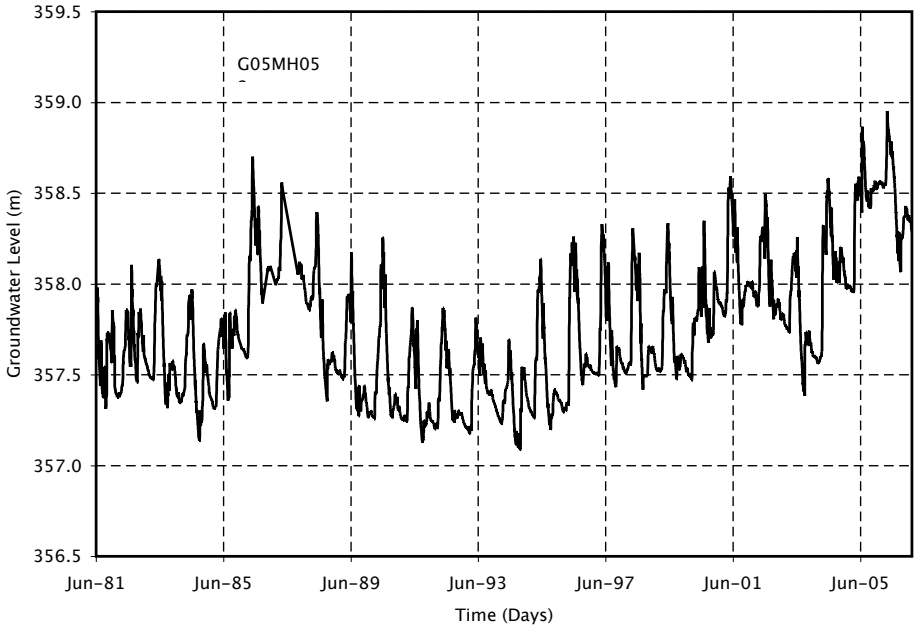

Figure 6.5: Measured groundwater head at observation well G05MH052 within the Assiniboine Delta Aquifer

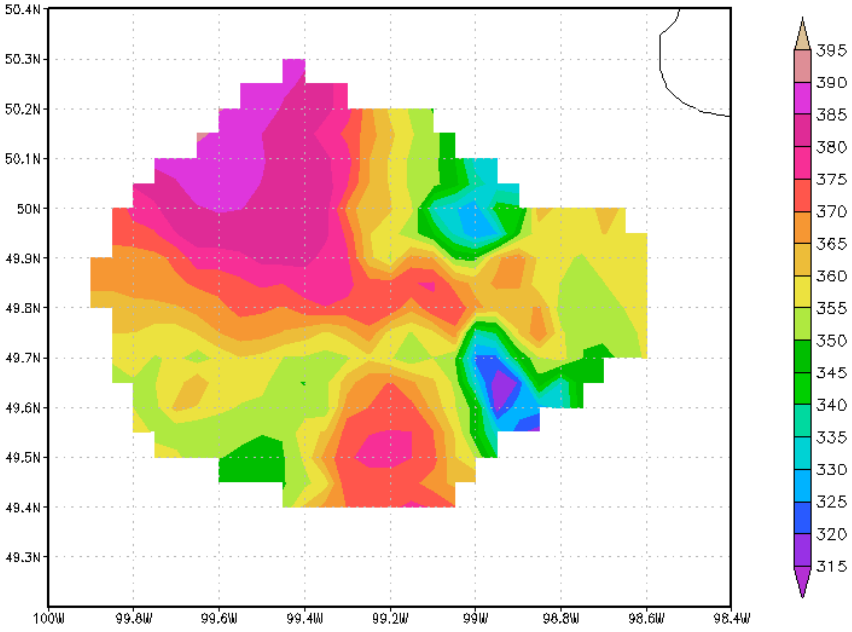

Figure 6.6: Average groundwater head (m) distribution of the Assiniboine Delta Aquifer interpolated from the measured pizometric head for December 2006

6.2.5 Land Cover

The land cover data over the ADA was determined from Landsat Thematic Mapper (TM) imagery and provided by Manitoba Conservation, Department of Remote Sensing Centre. There are sixteen land classes represented within this area, namely: agricultural crop land, forage crops, grassland, open deciduous, deciduous, coniferous, mixedwood forests, treed rock, bogs, marshes and fens, bare rock, burnt areas, forest cutovers, open water, cultural features, roads and trails. The spatial resolution of the imagery of land cover is 30 m. For the purpose of this study the sixteen classes have been amalgamated into six land use types as shown in Figure 6.7.

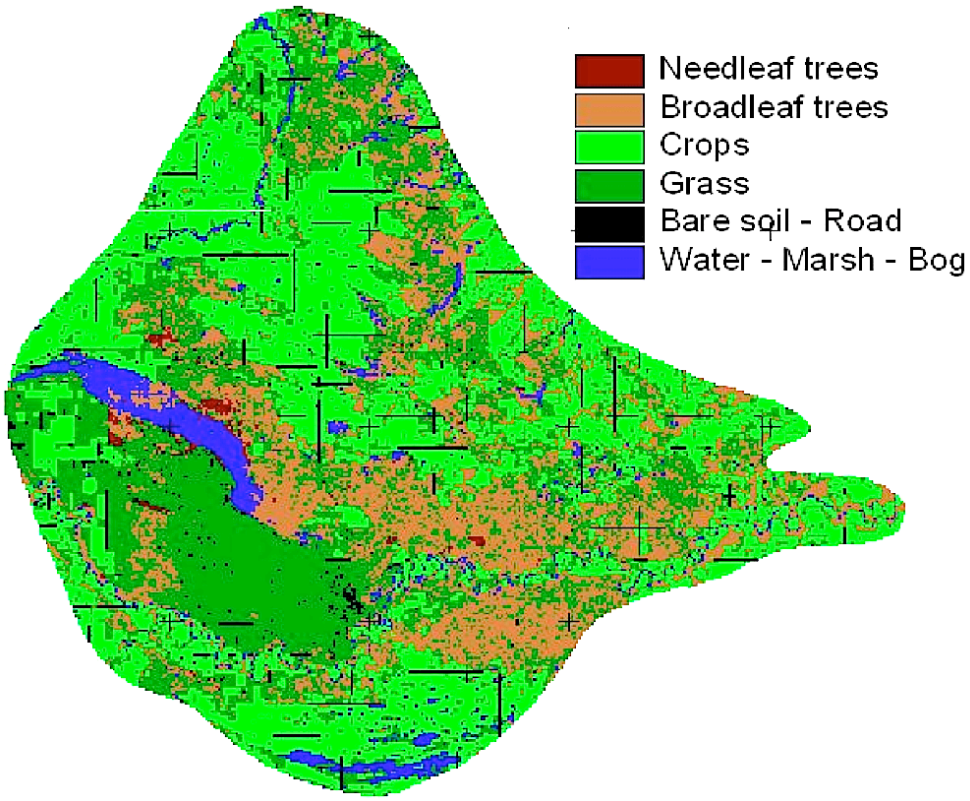

Figure 6.7: Land cover of the Assiniboine Delta Aquifer

The cool, sub-humid climate of the region provides a suitable environment for crop and grassland vegetation, and as a result, the land use of the area comprises 47 % cropland, 26 % grassland, 16 % trees, 4 % forages, 3 % wetlands, 3% urban and road area and 1% open water (2005 ADA management plan internal report). This information is used for the estimation of land surface model parameters and is provided as input for the CLM portion of the coupled groundwater and surface water model used in this study.

6.2.6 Initial and Boundary Condition

To initialize the coupled CLM-PF model, which has a spatial resolution of 5×5 km, an offline model spin-up procedure was used to generate the spatial distribution of initial soil moisture for the first ten soil layers which are considered as the unsaturated soil layers. During the spin-up period, it is assumed that mass and energy balances of the state variables are in equilibrium over a 3-year period. In reality, achieving an equilibrium condition is a challenge as it is often impossible to have identical water and energy state variables at the end of each year of simulation. As a result, threshold values indicating that equilibrium conditions have been achieved are set to allow small differences between the beginning and ending water and energy storage values. To achieve an equilibrium state, the model was repeatedly forced by atmospheric data for a three year period until differences were less than or equal to the corresponding threshold values. Atmospheric data from the water years 1999 and 2003 were used to spin-up the coupled model during model simulation and calibration periods, respectively. The source of forcing variables is from the North American Re-

gional Reanalysis (NARR) dataset, which is explained in the following section. For the deep groundwater portions of the model, the initial groundwater head is set at 4 m below the ground surface throughout the area. Following the three year spin-up period, the groundwater head simulated at the end of the water year was used as an initial condition for the groundwater model.

Like most hydrological models, the coupled CLM-PF model requires boundary conditions along all sides of the model domain for simulation of physical processes. At the land surface, an overland flow boundary condition was prescribed (Kollet and Maxwell, 2006) while along the lateral and lower boundaries of the model domain, no flow boundary condition were applied. Similar to the study of Kollet and Maxwell (2008), the model domain extended beyond the ADA boundaries; therefore it is assumed that the location of the water divide of the Assinibone Delta Aquifer will be developed naturally within the model.

6.2.7 North American Regional Reanalysis (NARR) Data

The NARR forcing data includes incoming short- and long-wave radiations, surface air temperature, precipitation, pressure, horizontal wind velocities (X and Y directions) and humidity. The spatial resolution of this dataset is 32×32 km with a temporal resolution of three hours. Four NARR grid cells represent the ADA domain, and these grid-cell metrological variables are spatially averaged and used to force the model. Detailed evaluation of the NARR dataset with physically available station dataset has not been made for each forcing variable primarily due to the unavailability of measured data for most of these variables. NARR precipitation and

temperature fields were compared prior to undertaking the modeling task over this domain to assess how well they compare with the observation. The outcome of this analysis did show that the daily NARR temperature (Figure 6.8) and cumulative monthly NARR precipitation (Figure 6.9) compare fairly well with observed measurements, however, the daily NARR precipitation underestimates the precipitation field (Figure 6.10). The five years (1999-2003) cumulative measured and adjusted precipitation at Cypress River (99.08^oW, 49.55^oN) are also compared with NARR precipitation and the result shows that both the NARR and measured precipitation fields are lower than that of the adjusted precipitation (Figure 6.11). The outcome of this preliminary evaluation agrees quite well with the works of Mesinger et al. (2006). It was concluded in their study that owing to the small numbers of gauging stations in Canada, the accuracy of the precipitation field over most Canadian catchments is poor relative to catchments in the USA. But owing to enormous data requirements needed to drive the coupled model over a relatively small basin such as the ADA, it becomes imperative to rely on the NARR dataset in order to accomplish the groundwater-modeling task over this domain. Moreover, it should be noted that the modeling result over the ADA is not to recommend the model for general use rather to assess the applicability of the downscaled GRACE-based groundwater storage in calibrating the groundwater model and to compare the modeled groundwater storage changes with that of the observed groundwater storage changes in the ADA.

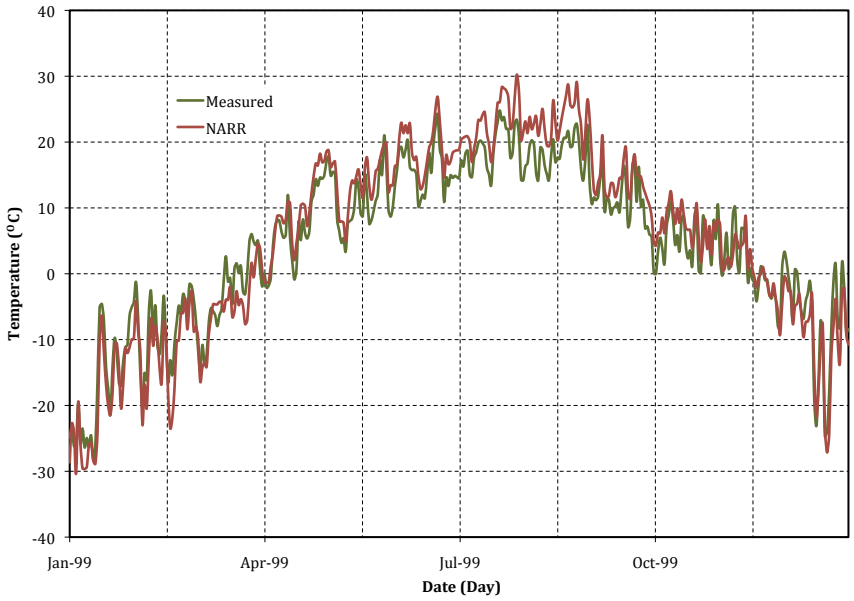

Figure 6.8: Measured and NARR Temperature within the Assiniboine Delta Aquifer for the year 1999

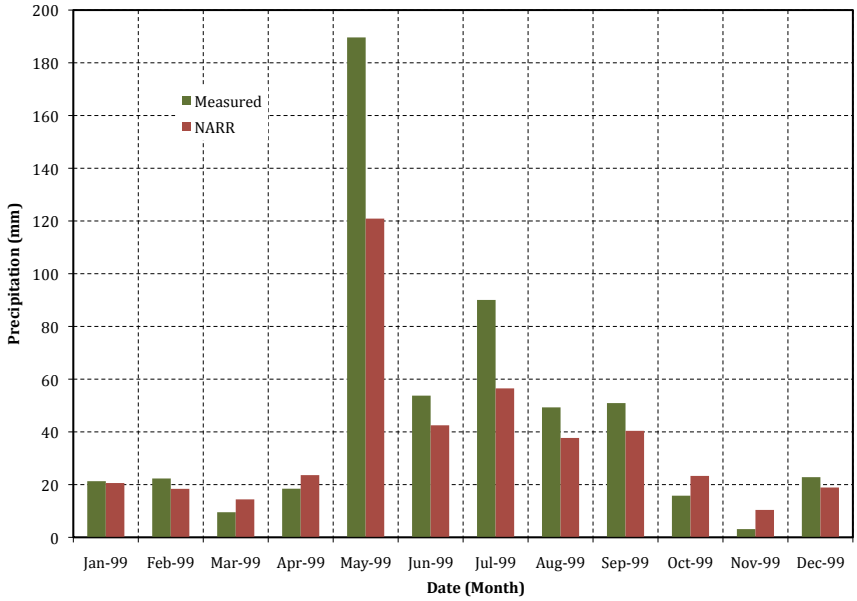

Figure 6.9: Monthly Measured and NARR Precipitation within the Assiniboine Delta Aquifer for the year 1999

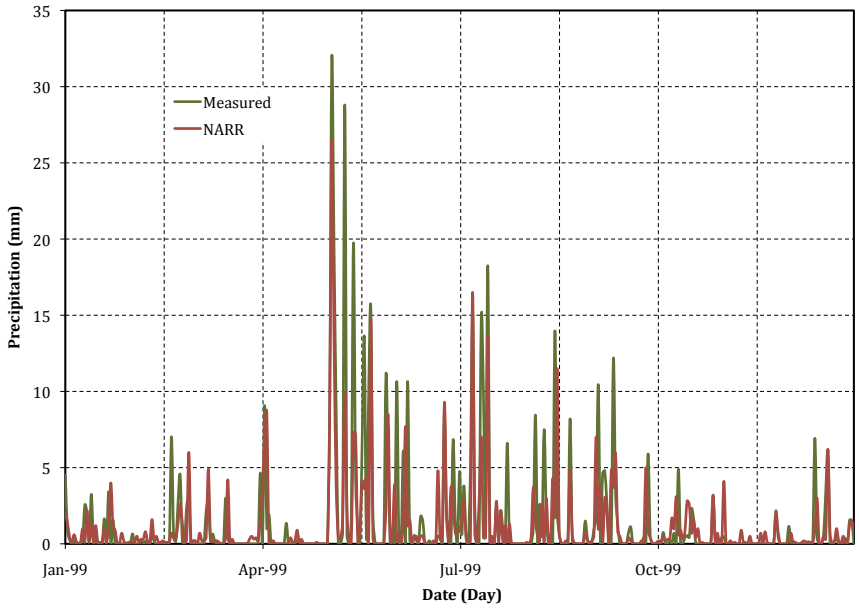

Figure 6.10: Daily Measured and NARR Precipitation within the Assiniboine Delta Aquifer for the year 1999

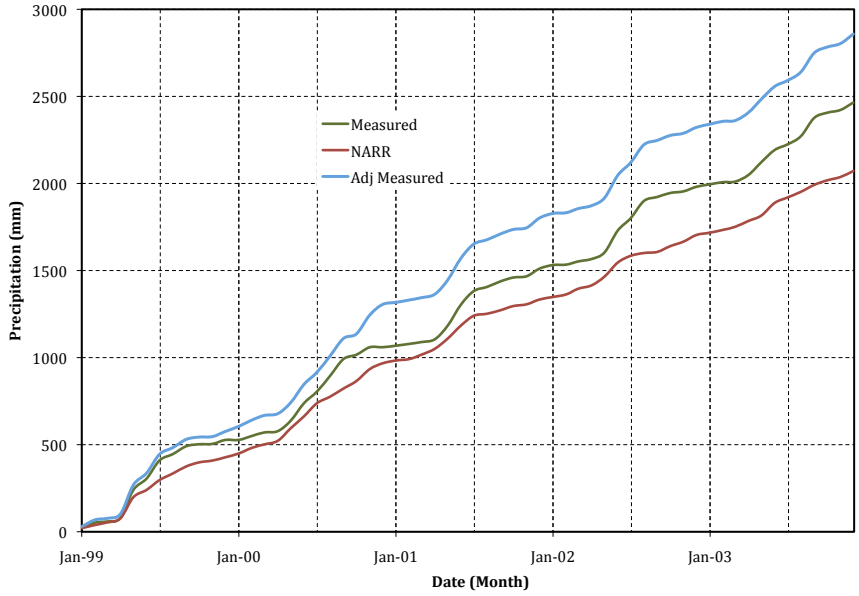

Figure 6.11: Cumulative Measured, Adjusted and NARR Precipitation within the Assiniboine Delta Aquifer

6.3 Results and Discussions

6.3.1 Calibration

In order to determine the predictive capacity of the coupled model, a comparison of simulated groundwater level/storage against the observed groundwater level/storage is required. By changing model parameters such as hydraulic conductivity, a better agreement between the simulated and observed groundwater level can be achieved. This process is known as model calibration. The coupled land surface scheme and groundwater model applied over the ADA was calibrated by considering a one year time series of GRACE groundwater storage data (i.e a transient calibration). In order to compare the simulated groundwater storage with the monthly values of downscaled groundwater storage, the modeled groundwater level was averaged to a monthly time scale and subsequently converted to groundwater storage. Calibration targets were based on qualitative measures such as comparison of general trends and residuals (observed minus simulated) of groundwater storages and heads. Since the downscaled GRACE groundwater storage is available starting from April 2002, the data for the year 2003 was used to calibrate the model.

The hydraulic conductivity values from the 13 sub-basins were altered during the model calibration process. Initial values were estimated from previous pumping tests and then changed manually during calibration runs. Calibration was performed using a trial and error method in such a way that time series plots between the downscaled GRACE groundwater storage and the simulated groundwater storage at the selected well locations were matched. Once visual agreement between the observed

and simulated results were achieved, the residual values and statistical measures such as $RMSE$ and R^2 between the measured and the simulated groundwater levels were calculated. This procedure was repeated until the visual agreements and statistical parameter values were acceptable. The final hydraulic conductivity values used for modeling the ADA are shown in Table 6.2 and Figure 6.12. These values are within the range of the hydraulic conductivity values reported in Table 6.1. Differences are likely due to the estimation of effective parameters which will differ from well observations due to the larger areas involved and simplifications (i.e. simplified statigraphy, constant moisture storage properties, and constant aquifer bottom elevation) required to undertake the study.

Table 6.2: Calibrated and Initial Hydraulic Conductivity (K) values of the Assiniboine Delta Aquifer sub basins

Sub Basins	Calibrated K (m/hr)	Initial K (m/hr)	Differences %
Lower Whitemud East	3.18	2.55	25
Upper Whitemud East	2.83	2.12	33
Upper Whitemud West	3.61	3.61	0
Pine Creek North	0.89	0.99	10
Pine Creek South	0.76	0.76	0
Epinette Creek North	1.98	1.70	17
Squirrel Creek North	0.59	0.59	0
Squirrel Creek South	0.17	0.28	40
Epinette Creek South	1.70	2.04	17
Assiniboine West	1.70	2.04	17
Assiniboine East	0.64	0.51	25
Assiniboine Souris	1.91	2.55	25
Assiniboine South	0.76	0.76	0
Outside the ADA Domain	0.03	0.03	0

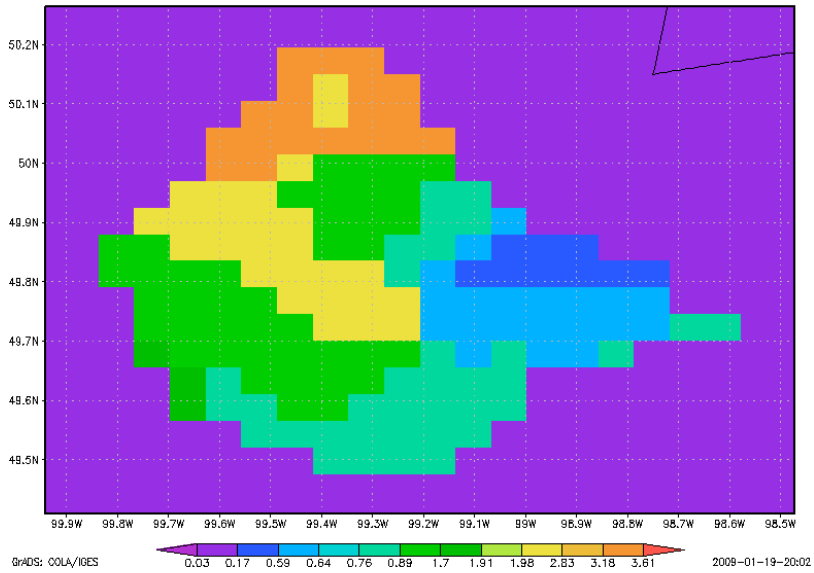

Figure 6.12: Calibrated Hydraulic Conductivity (K in m/hr) values over the Assiniboine Delta Aquifer sub basins

Figure 6.13 compares the spatially averaged simulated and downscaled-GRACE groundwater storage anomalies during the model calibration periods (January to December 2003). The average groundwater storage anomalies from the 59 observation wells where GRACE data was downscaled to groundwater storage anomalies were used in this plot. The figure shows that simulated results of the average groundwater storage anomaly agrees with the downscaled GRACE groundwater storage anomaly for the majority of the calibration period. The hydrological time series result as well as the amplitudes of the simulated result compares well with that of the downscaled GRACE measurements with the exception of April and May 2003 where a difference of about 5 cm is observed. The figure reveals that the model captured the groundwater storage anomalies with a reasonable accuracy for the purpose of this thesis. However, a single basin average result may lead to an incorrect conclusion regarding

model performance. Therefore, it is important to assess model performance using downscaled groundwater storage anomalies at other observation well locations.

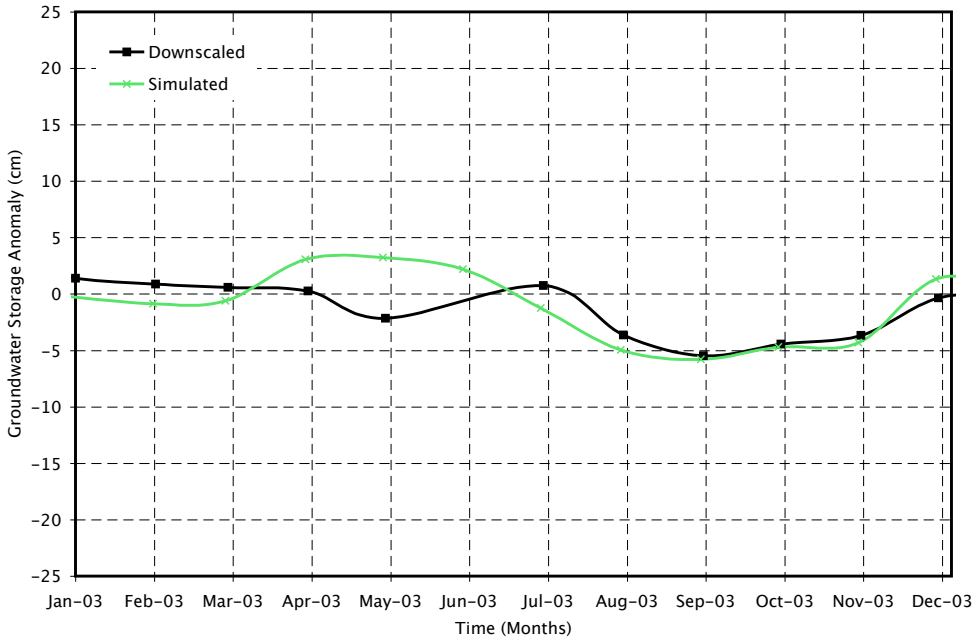

Figure 6.13: Average Modeled and Downscaled Groundwater Storage of the ADA during Model Calibration

Figure 6.14 shows the the downscaled and simulated groundwater storage anomalies of four observation wells for the model calibration period. As observed in this plot, a choice of different vertical scales has been made to better reveal the temporal patterns in the simulated and downscaled groundwater storage anomalies for the observation wells. The locations of these wells are shown in Figure 6.2. These locations were selected randomly to assess model performance during parameter estimation. As shown in the figure, the simulated and downscaled groundwater anomalies are in good agreement in these observation wells, however, there exist some discrepancies between the simulated and downscaled groundwater storage during part of the

calibration period. It should be noted that the simulated result represents a grid resolution of 5×5 km while the downscaled result represents a local point which could contribute significantly to the discrepancies observed. Over all, the simulated and downscaled groundwater storage anomalies agree reasonably well and the estimated parameters during this model calibration has been adopted for development of the groundwater model over the ADA.

Since measured groundwater level data exists throughout the study area (Figure 6.2) during the calibration period, a comparison was made between the simulated and measured groundwater level. In addition, statistical measure of fit are calculated to determine how well the calibrated model captures the dynamics of the measured groundwater levels. Figure 6.15 shows the simulated versus the measured groundwater level under transient conditions during the calibration period (January to December 2003). The simulated 3 hourly groundwater levels are averaged to a daily groundwater level since the measured data is availability only at a daily time step. The plot accounts for fifteen observation wells and contains 5475 points (15×365). It is assumed that these fifteen observation wells are sufficient to represent the study area. This correlation plot shows a very good agreement between the measured and simulated groundwater level with a good objective measure of $R^2 = 0.9932$, reasonable $RMSE$, AME and ME values of 1.439 m, 0.896 m and -0.296 m, respectively and statistically equal mean and variance at 95% confidence interval (p-values of 0.362 and 0.238, respectively). The R^2 value, however, decreases to 0.8549 and statistically significant differences of mean (p-value = 0.001) and variance (p-value = 0.001) are found when groundwater depths are considered.

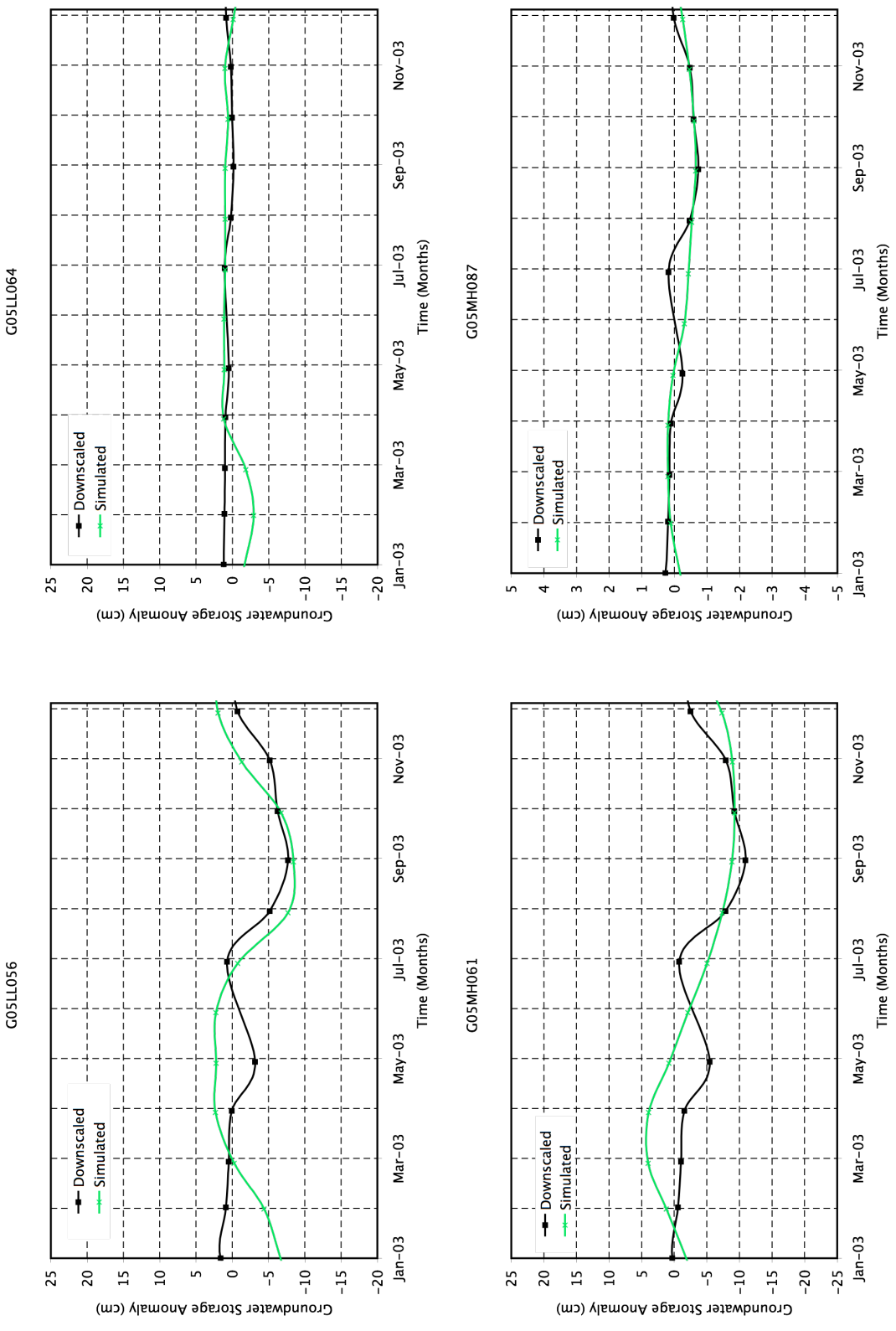

Figure 6.14: Modeled and Downscaled Groundwater Storages at four observation well locations in the ADA during Model Calibration

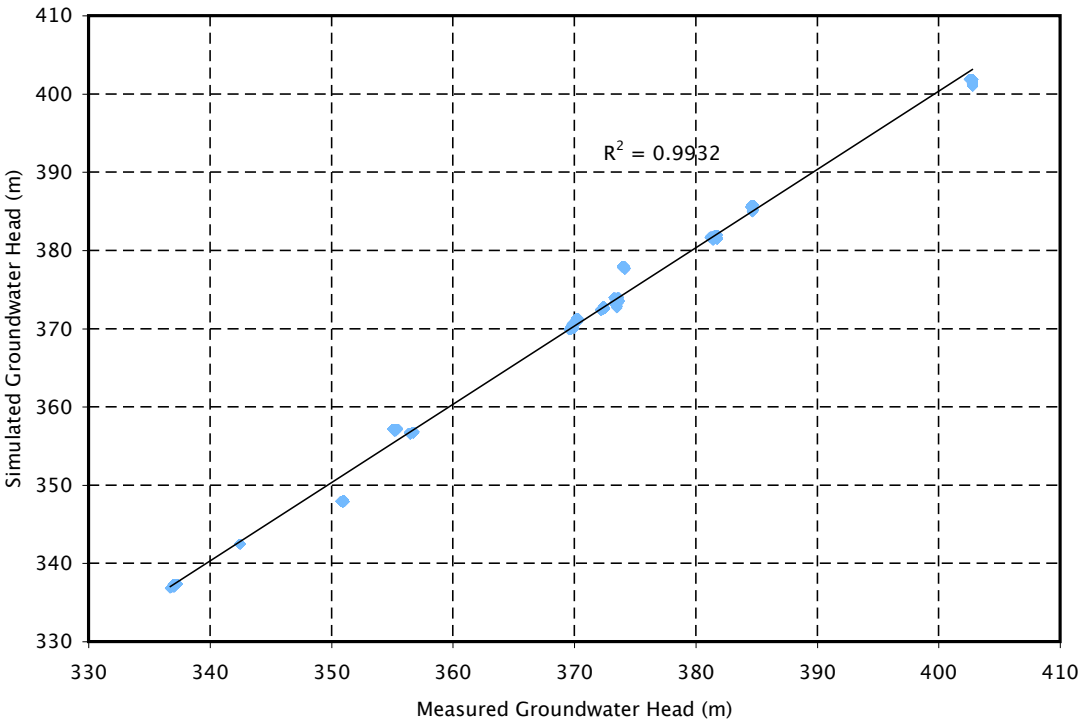

Figure 6.15: Simulated Vs. measured groundwater head from daily results from 15 wells (January to December 2003)

Although the coupled model calibration result presented here provides a relatively good fit between simulated and measured groundwater level and between the downscaled and measured groundwater storage, limitations exist. These limitations include the lack of detailed three-dimensional distributions of aquifer parameters, difficulties inherent in the interpretation and representation of the complex geometry and spatial variability of the hydrogeologic materials and geologic structures in the hydrogeologic framework, and the accuracy of the input data used to force the model during model calibration. Keeping in mind the scale of this model and the level of detail that were required to analyze the model at a regional scale grid (5×5 km), a reasonable level of accuracy is obtained during model calibration. Given the level of

uncertainties in setting up the model more testing would certainly be required before it could be recommended for general use. None-the-less, the next section presents detail model results based on continuous simulation from 1999 to 2006 over the ADA using the calibrated hydraulic conductivity parameters. It should be noted that the model remains forced with the NARR representation of meteorological observations which are known to contain significant error.

6.3.2 Groundwater Storage Anomalies

The model calibration provided a set of optimal hydraulic conductivity values estimated for each of the sub-basins. These parameters were used to run the model for eight years (1999 to 2006) using a three hour time step. The North American Regional Reanalysis (NARR) atmospheric data, which were mentioned in Section 6.2.7, were used to force the calibrated model during the simulation period. This and the following sections present some of the model outputs that are important and supportive of the thesis hypothesis presented in Section 1.2. Since the downscaled groundwater storage anomalies are only available at monthly time intervals, model computed anomalies are averaged from three hourly to monthly intervals.

Figure 6.16 shows the spatial distribution of the groundwater storage anomalies estimated from the model for the month of April 2003. The outline of the ADA sub-catchments is not shown in this image and in Figure 6.19 owing to a lack of an outline generating utility used in the image production. The selection of this month from the total simulation period is absolutely random and aims to show a typical spatial distribution of the estimated groundwater storage anomalies from the model. The

result indicates that groundwater storage anomalies over the ADA range from -50 to 50 *cm* for this particular month with the majority of the area being within ± 25 *cm* of water equivalent. The aquifer during this month is dominated by a positive storage anomaly. This is due to the depletion of winter snow accumulation which begins to melt during spring and results in increased groundwater recharge and thus storage. This subsequently contributes to positive groundwater storage anomalies over most of the aquifer. The larger outliers (≈ -200 *cm*) that are shown in the eastern part of the study area are likely due to the presence of the deeply incised Assiniboine River and the spatial resolution of the simulation.

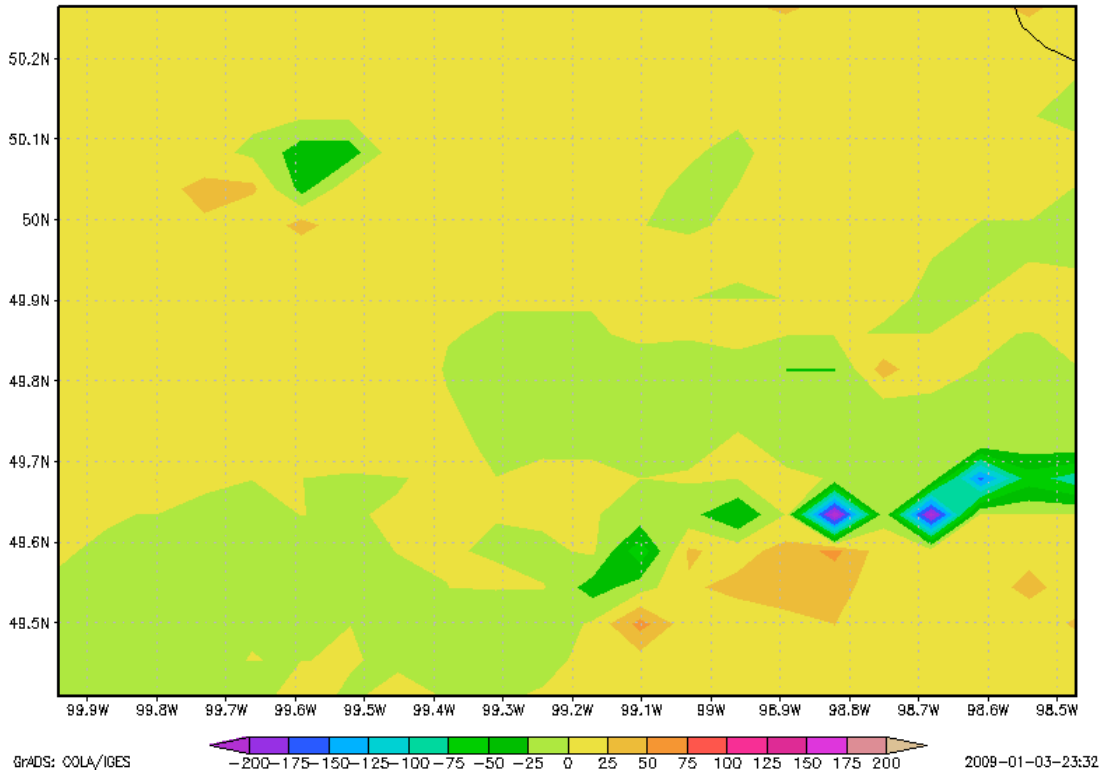

Figure 6.16: Spatial Distribution of Groundwater Storage Anomalies in units of *cm* over the ADA for the month of April 2003

In order to analyze the seasonal variation of the groundwater storage anomalies and compare these with downscaled and measured groundwater storage, time series outputs are required. Figure 6.17 shows a time series of basin-averaged, groundwater storage anomaly estimated from *i*) the measured groundwater head, *ii*) the downscaled GRACE groundwater storage anomalies and *iii*) the simulated groundwater head. A $1^o \times 1^o$ GRACE grid cell representing the total water storage anomaly from the ADA basin is also presented in the same figure. The monthly groundwater storage anomalies from the measured and simulated groundwater head were estimated by subtracting the long term mean measured and simulated groundwater head from average monthly groundwater head and multiplying by the specific yield that was used in the model. Since the downscaled groundwater storage anomalies are available starting from April 2002 to May 2006 with the exception of the months of May, June and July 2002 and June 2003, the groundwater storage anomaly result presented in this figure spans from April 2002 to May 2006.

As shown in Figure 6.17, the basin-average groundwater storage anomalies estimated from the model compare well with the corresponding downscaled groundwater storage anomalies through most of the simulation periods. The hydrological time series as well as the magnitude of the groundwater storage anomalies from the two results are within the same range. An exception occurs from August to November 2004 where the downscaled result shows monthly fluctuations while the model shows a gradual decrease in groundwater storage. The basin-average maximum groundwater storage anomaly from the model is approximately 5 *cm* and the corresponding anomaly from the downscaled result is as high as 7 *cm*. The basin-average mini-

mum groundwater storage anomaly estimated from the model and obtained from the downscaled GRACE total water storage is approximately -5 *cm* and occurs during the month of September 2003.

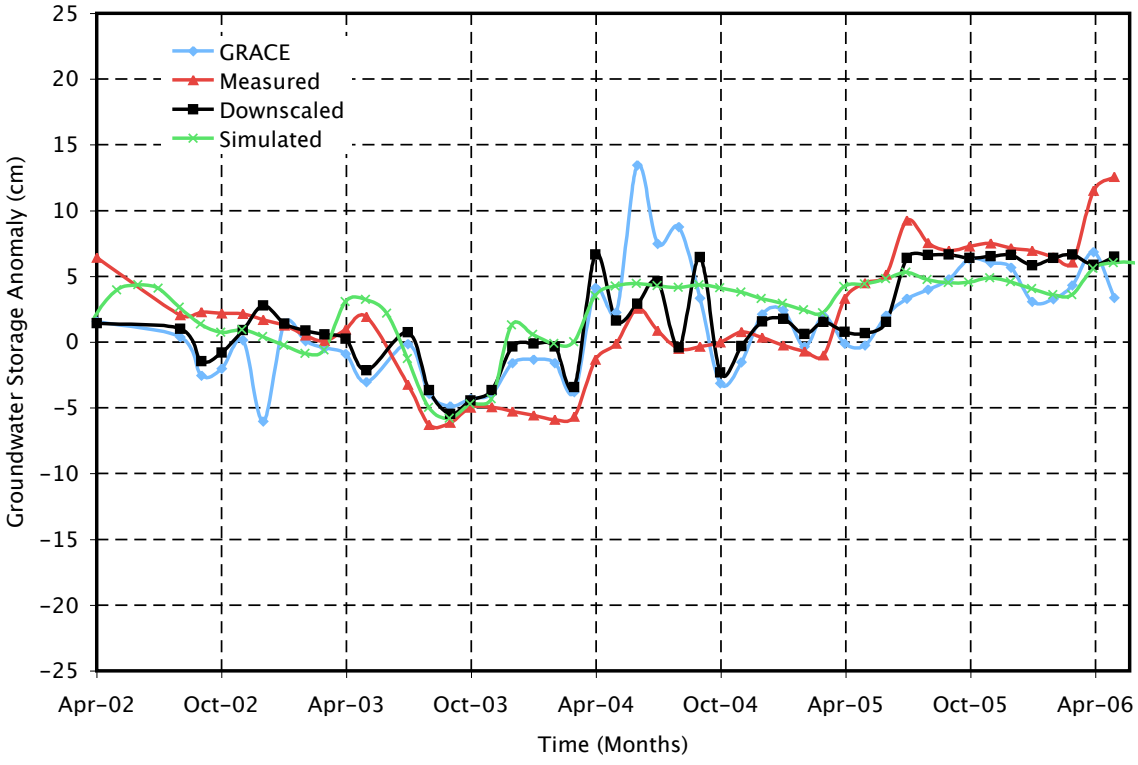

Figure 6.17: Average Groundwater Storage Anomalies over the ADA

Similarly, the comparison of the simulated groundwater storage anomalies with the measured groundwater storage anomalies and the GRACE total water storage anomalies show good agreement. Like that of the downscaled groundwater storage anomalies, the hydrological time series groundwater storage anomalies from these two methods compare well with the modeled groundwater storage anomalies. The maximum basin-averaged groundwater storage anomaly estimated from the measured

groundwater head is peaking at approximately 12 *cm* during the month May 2006, whereas the minimum measured basin-average groundwater storage anomaly remains at -5 *cm*. This is similar to that of the modeled and downscaled groundwater storage anomalies which occurs during the same month (September 2003). In general, the modeled groundwater storage anomalies are within the ranges of the corresponding estimates of the three approaches during most of the periods. This is surprising given the error present in the forcing data. However, this indicates how sensitive the model is to broad changes in hydraulic conductive such that the model can be calibrated to capture the dynamics of the groundwater storage anomalies in the aquifer.

Moreover, Figure 6.17 shows that all approaches (GRACE, Measured, Downscaled and Simulated) are all able to capture the negative groundwater storage anomalies that occurred in most of the months of 2003. This is likely the result of the extent of the effects of the recent Canadian Prairie drought, which started in 1999 and ended in early 2004 (Yirdaw et al., 2008), on the groundwater regime. A detailed explanation of this drought and its severity in the Saskatchewan River Basin are presented in Chapter 4. The result from these four approaches, however, reinforces the perception that this Canadian Prairie drought extended into southwestern Manitoba and included the ADA.

In addition to the time series plots of basin-average groundwater storage anomalies, these anomalies are computed at selected observation well locations. The results of the groundwater storage anomalies at four observation well locations are presented in Figure 6.18 with different vertical scales to reveal the temporal patterns in the groundwater storage anomalies. The modeled groundwater storage anomalies

in most of these observation well locations are in good agreement with the measured and downscaled groundwater anomalies except for the months of fall 2005 where the model underestimates the groundwater storage anomalies. The ranges (minimum and maximum) of the groundwater storage anomalies from the model, however, are within the ranges of that of the measured and downscaled groundwater storage anomalies. The comparison between the simulated and downscaled groundwater storage anomalies show good agreement compared to that of the the simulated versus the measured storage anomalies in most locations. For example, at observation well location G05MH087 (Figure 6.18), the groundwater storage anomalies of simulated and downscaled values compare better than the measured groundwater storage anomalies. This is because the model is calibrated based on the downscaled groundwater storage anomalies and it should be expected that a better comparison would be achieved between the model and the downscaled estimates. Generally the performance of the model in estimating the groundwater storage anomalies at the piezometer locations is satisfactory.

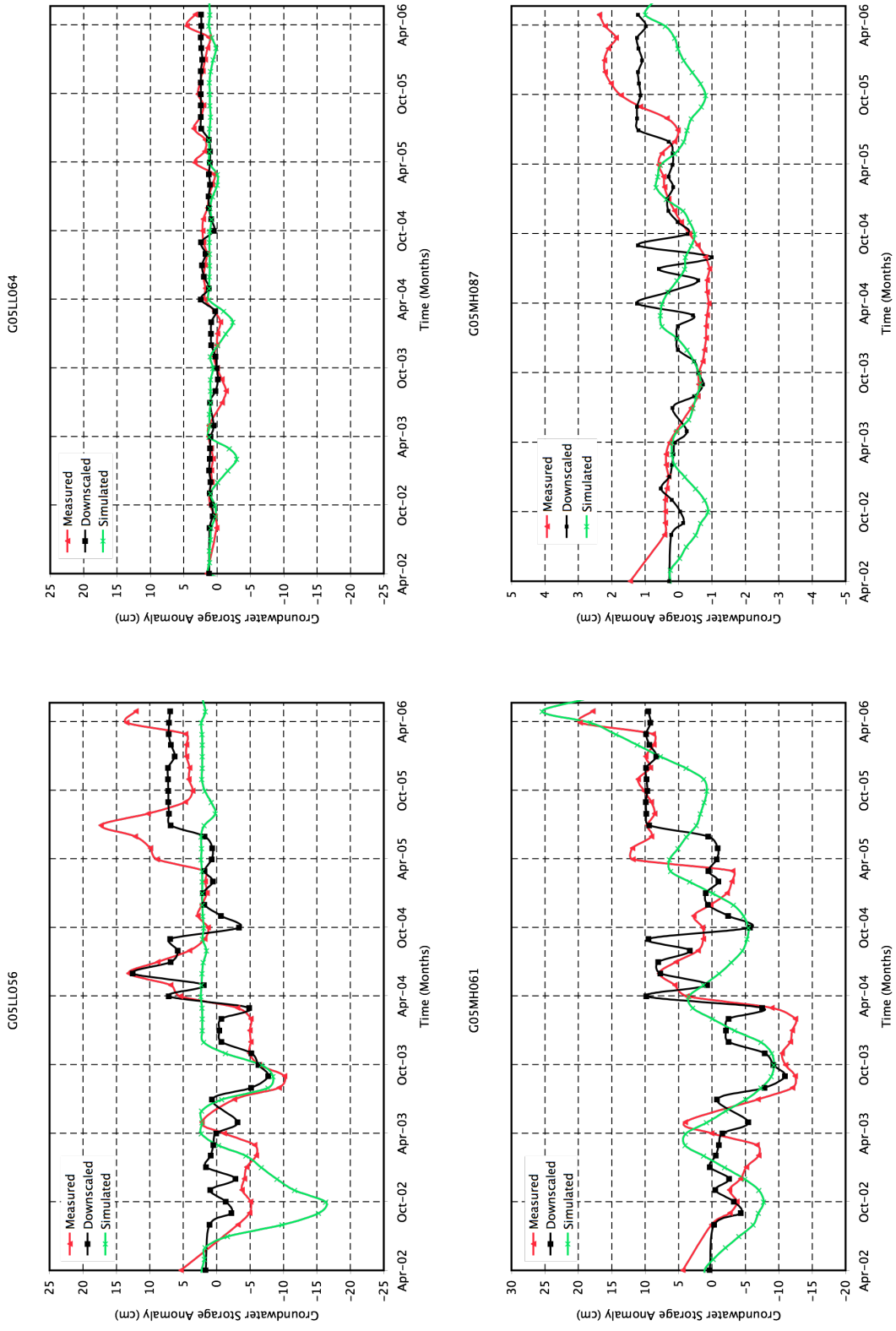

Figure 6.18: Groundwater Storages at four observation well locations in the ADA

6.3.3 Groundwater Head

In addition to the groundwater storage anomalies described in the previous section, the spatial and temporal groundwater head results are presented in this section. Figure 6.19 shows the spatial distribution of the groundwater head over the ADA. The groundwater varies from 240 to 540 m in the model domain, however, within the ADA boundary, the groundwater head variation ranges from 300 to 400 m. Note that the model domain is extended by about 10 km in each side of the ADA domain as shown in Figure 6.2. As a result, the groundwater head in the northwest corner of the model domain reaches as high as 540 m whereas near to Lake Manitoba (northeast corner) it falls as low as 240 m. Since there are no measured or downscaled groundwater head or storage data available to validate the performance of the model outside of the ADA boundary, the accuracy of the model result outside of the ADA domain may not be as good as those inside the ADA boundary, hence, the discussion of the different model outputs are limited to within the ADA domain.

From the spatial groundwater head plot, the groundwater flow directions can be determined. Generally, groundwater flows from higher to lower groundwater head. As shown in Figure 6.19, from a regional perspective, the groundwater flow direction over the ADA is towards the east. At a local level, however, the majority of the groundwater flows towards the Assiniboine River (a river which passes through the aquifer). The flow towards the Assiniboine River is delivered from the northwest, southwest and southeast directions through Whitemud, Assiniboine Souris and Assiniboine South sub-basins (Figure 6.3), respectively, and these rivers serve as a groundwater discharge zones. In addition, groundwater leaves the aquifer in the

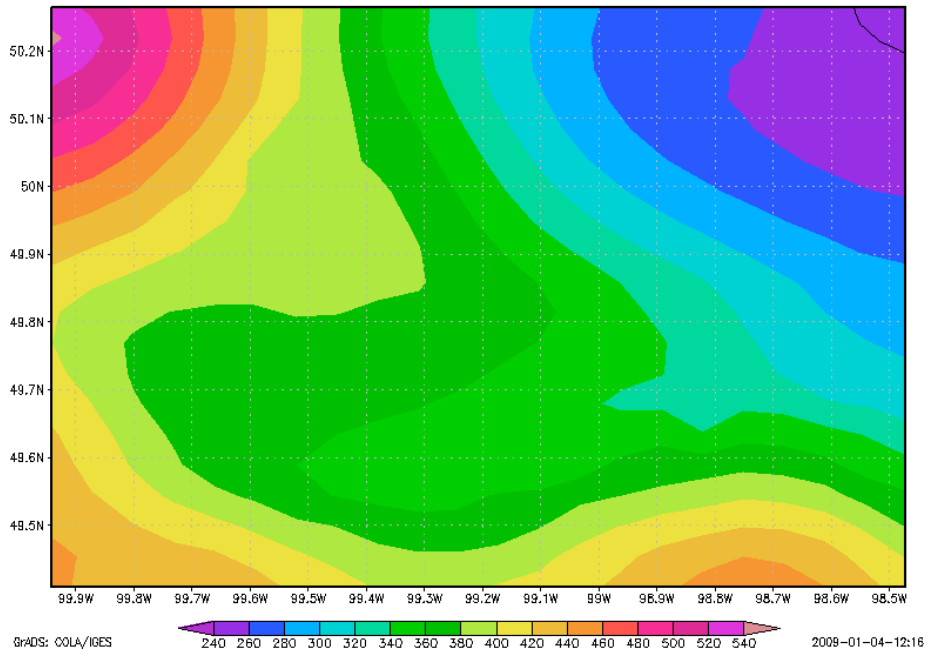

Figure 6.19: Spatial Distribution of Groundwater Head (m) over the ADA for the month of May 2000

northeast direction through Pine and Squirrel Creeks and eventually discharged into Lake Manitoba.

The simulated and measured time series of groundwater heads at eight observation wells are also presented in Figures 6.20 and 6.21. Since plotting all the simulated and measured groundwater head at the eight observation wells in one plot makes the plot unreadable, the results of these observation wells are plotted in two figures (Figures 6.20 and 6.21). The letters S and M in these figures stand for *Simulated* and *Measured* groundwater head respectively while the code (for example $G05MH061$) indicates the observation well name. Since the measured groundwater head is available at a daily time step, the three hourly simulated groundwater head is averaged to a daily time step. As shown in these two figures, the simulated and measured ground-

water head in those selected observation well locations agree. The seasonal groundwater fluctuations in some of the locations (G05MH006, G05MH061, G05MH060, G05MH034 and G05LL056) agree in both approaches (measured and simulated). For the remaining observation wells presented in Figures 6.20 and 6.21, the seasonal fluctuations in measured and simulated groundwater elevations are minimal. In both cases, whether there exist seasonal fluctuations or not, the model implemented over the basin captures the trend existing in the measured groundwater head.

All these results (groundwater storage anomalies and head) indicate how well the model is in simulating the groundwater dynamics of the region. The calibration of the groundwater model in this study is different from most traditional groundwater calibration approaches. The traditional calibration approach uses the measured groundwater head, however, this study uses the downscaled GRACE groundwater storage anomalies in calibrating the groundwater model. These results prove the usefulness of the GRACE total water storage anomalies in groundwater model parameterization. Given the uncertainties that exist in the downscaled groundwater storage anomalies, the atmospheric forcing data and the coarse resolution inherent in the model grid, the performance of the model in estimating the groundwater head at a local level is surprisingly good. Hence, a recommendation can be made to use the GRACE measurements for hydrological model calibration, especially in areas where ground measurements are limited or unavailable. Even for areas where measurements are available, the GRACE measurements could also be used to validate or assess the model as an independent dataset.

6.3.4 Unsaturated Soil Moisture Profile

One of the advantages of the CLM-PF model is the simulation of the unsaturated soil moisture with a feedback from the saturated groundwater reservoir. This is one of the unique parts of this model and it is also one of the few models that simulates the dynamically coupled saturated and unsaturated soil moisture. In addition to the unsaturated soil moisture profile, the model also simulates hydrological processes such as infiltration, evaporation, ground temperature and others. However, discussion here is limited to unsaturated soil moisture and groundwater level.

Figure 6.22 shows the vertical time series saturation profile for a grid located at 99.31^{o}W longitudinally and 49.81^{o}N latitudinally for the year 1999 at a three hourly time step. The saturation value ranges from 0 to 1 with 0 indicating dry condition while 1 indicates fully saturated condition. The first fully saturated layer beneath the unsaturated layer indicates the groundwater table location. Since the model is dynamically coupled, the saturated layer at a particular location is changing with time and results in the groundwater level varying accordingly.

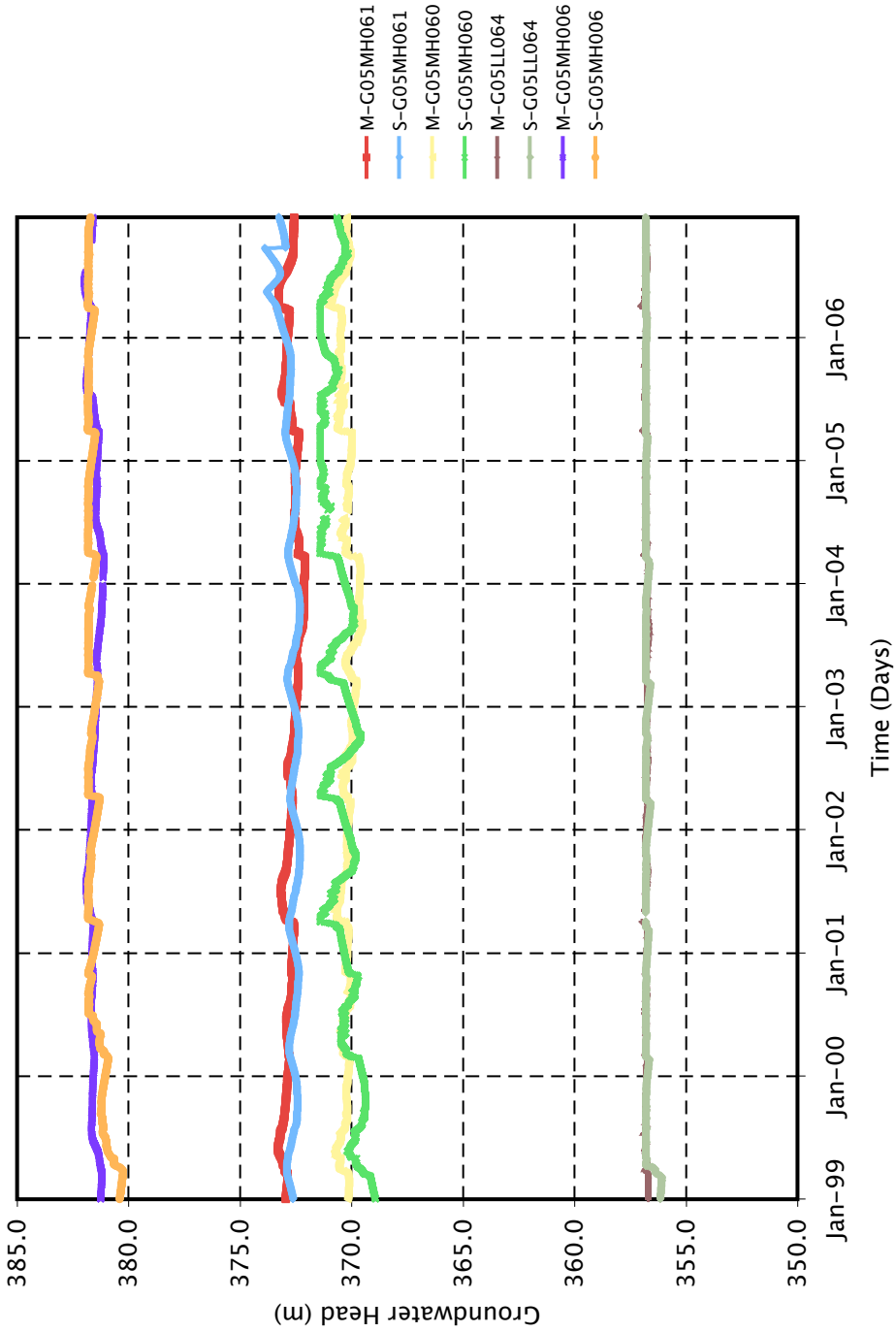

Figure 6.20: Groundwater Head at Selected well Locations in the ADA: Part 1

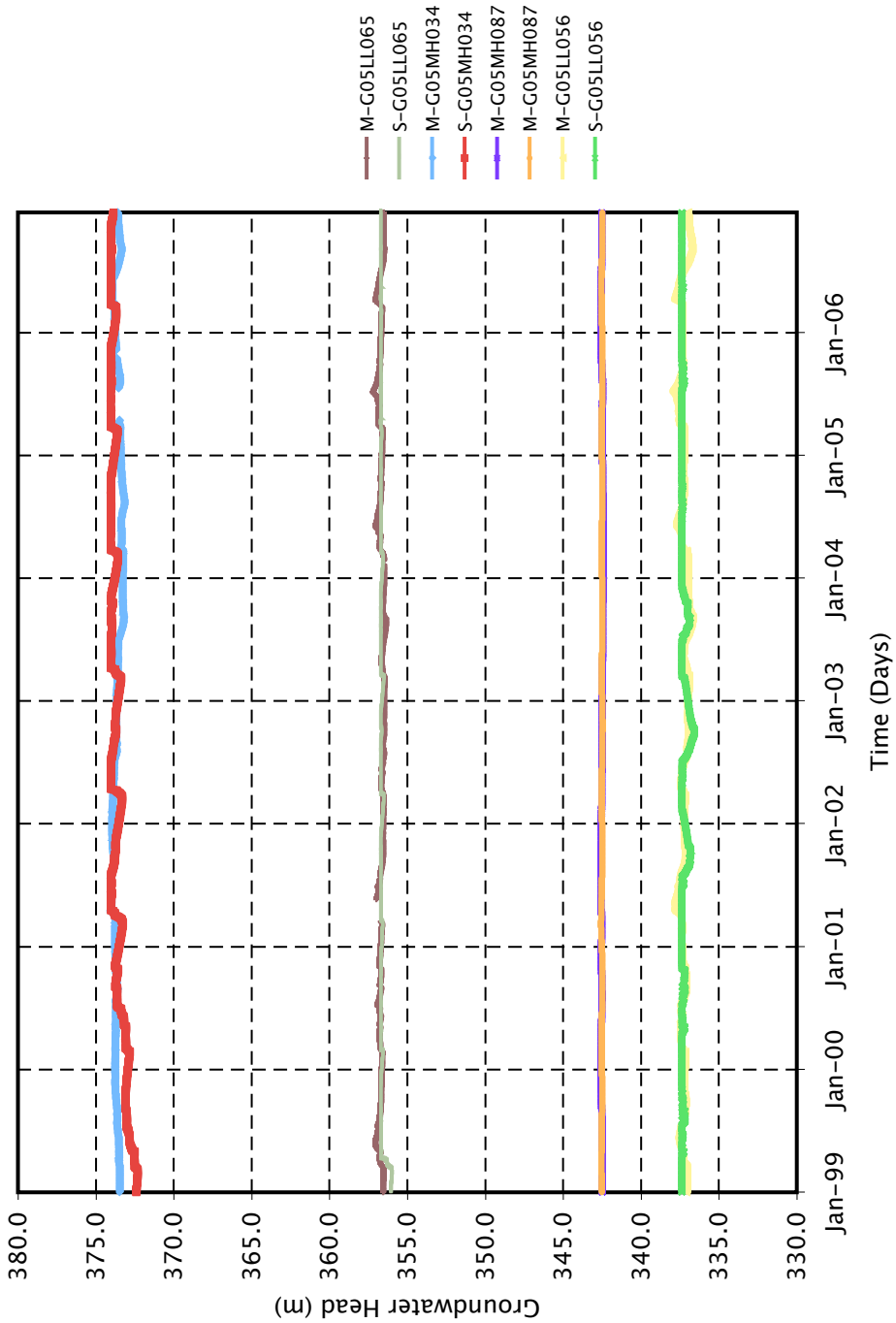

Figure 6.21: Groundwater Head at Selected well Locations in the ADA: Part 2

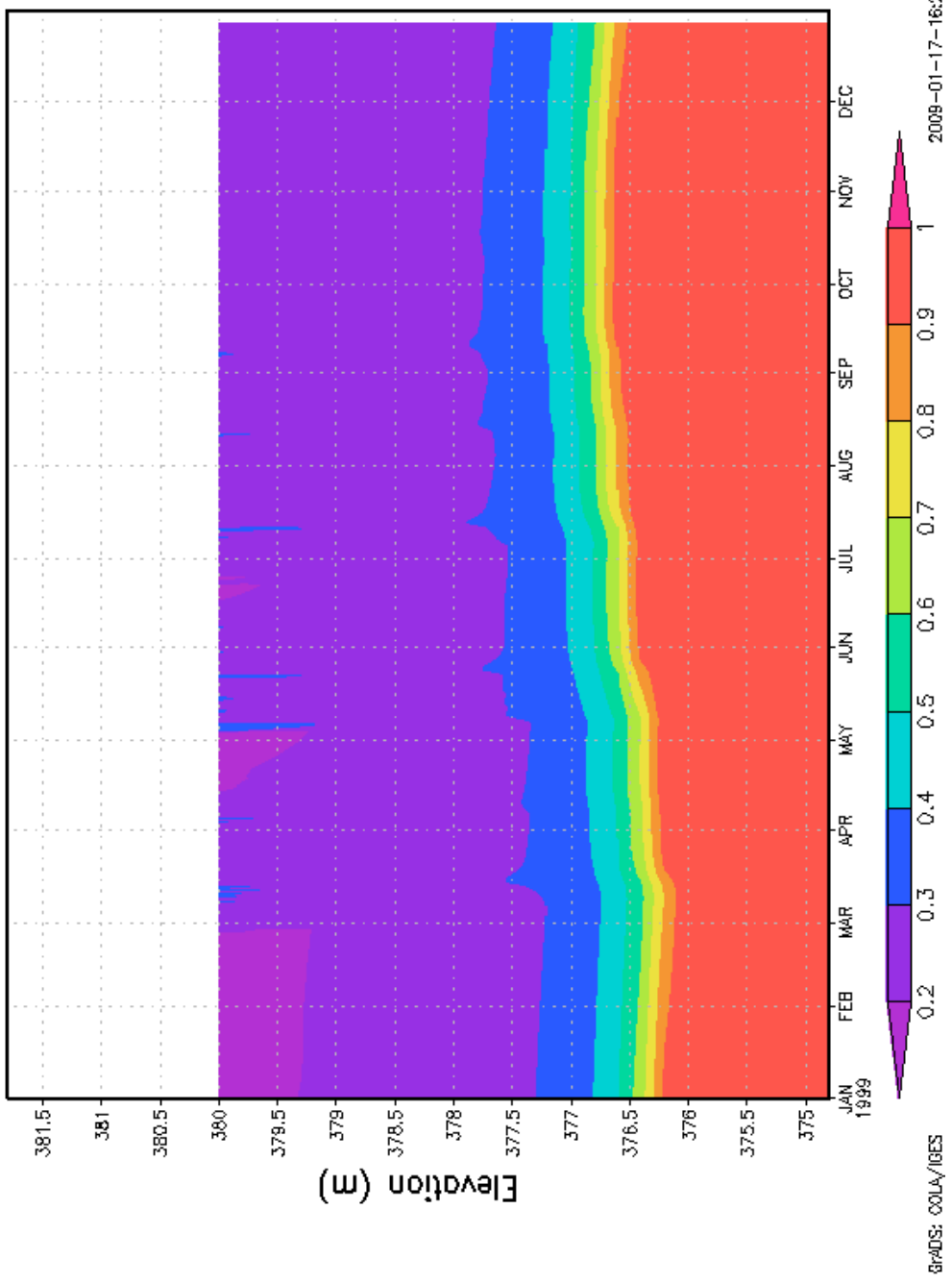

Figure 6.22: Time series Vertical Soil Saturation Profile at a Particular Location (99.31°W, 49.81°N)

The figure shows that the soil moisture profile varies temporally. During the winter season, for example, the saturated thickness decreased and caused the groundwater table to drop to approximately 376.0 m at this particular location. The saturated thickness, however, begins to expand starting from the middle of March and reaches a maximum groundwater elevation of approximately 376.80 m during the month of November. This increase in saturated thickness or groundwater elevation is associated with the spring snow melt and precipitation events that increases the recharge amount to groundwater and subsequently increases the saturated thickness. The effects of snow melt and precipitation are well reflected in the unsaturated thickness as well. For example, the spring snow melt contributes to the increase in soil moisture saturation during the month of March and April, while the precipitation events during the months of May, June and July contribute to increase in soil moisture during the corresponding months. Unfortunately, there are no measured data with which to validate these result. However, the qualitative analysis presented above would indicate that the processes are properly represented.

Figure 6.23 also shows the vertical soil moisture profile at a particular location. This figure is similar to Figure 6.22, except the former is for selected periods in time, while the latter is for a one year simulation period (01Jan1999 to 31Dec1999) at a three hourly time steps. The vertical saturation fields are computed following Equation 2.26 (Chapter 2), which gives the van Genuchten (1980) relationships used in the coupled model. Hence, Figure 6.23 presents the vertical soil moisture saturation profile for the time periods representing mid January, April, July and October 1999. For discussion purpose, the whole layer is divided into three zones namely: saturated,

mixed and unsaturated zones depending on saturation values during the periods from mid of January to mid of October (Figure 6.23). The saturated zone indicates the zone where the layers remain fully saturated, the mixed zone is the zone where the saturated fields changes from unsaturated to fully saturated while the unsaturated zone is the zone where the layers are unsaturated during the specified periods.

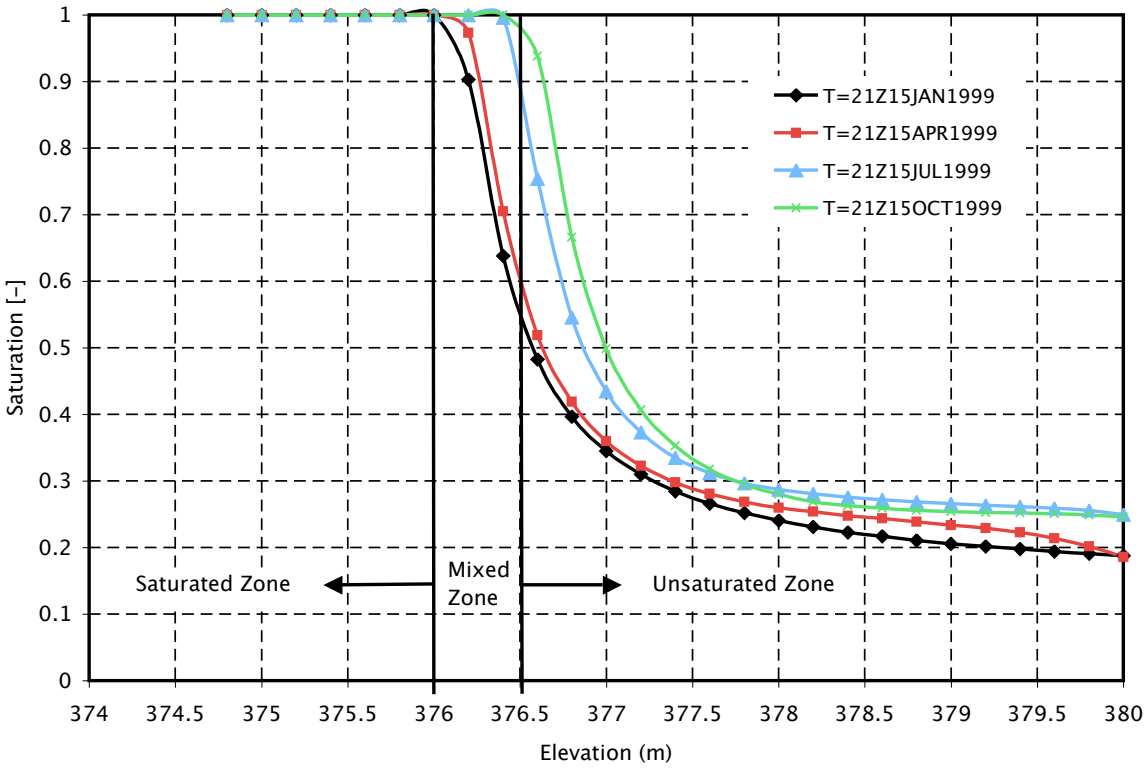

Figure 6.23: Vertical Soil Saturation Profile at a Particular Location (99.31^{o}W, 49.81^{o}N)

In the mixed zone, the saturation fields change from unsaturated to fully saturated with saturation values from about 0.55 to 1 between January and October. Subsequently, within the unsaturated zone, soil moisture ranges from as low as 0.2 to 0.9. However, the change in saturation between January and October varies from

layer to layer in this zone. For example, near the surface, the soil moisture values increase from 0.18 to 0.25, whereas near the mixed zone, these values increased from as low as 0.4 to 0.9 between January and October. The majority of the change in the saturation field in the mixed and unsaturated zones occurs between April and July. This change is well reflected near the boundary between mixed and unsaturated zones. The spring snowmelt and precipitation are responsible for this increase in saturation fields during the period. On the other hand, the change in saturation field between January and April in both zones are minimal; this is because of the winter snow accumulation on the surface that results in a minimum or some times zero recharge to the groundwater system, which subsequently reduce the saturation fields in the mixed and unsaturated zones. On the other hand, near the ground surface in the unsaturated zone, the soil moisture saturation decreases between the period of July and October. This indicates that during the summer periods the sub surface near the ground surface loses a significant amount of moisture in the form of evapotranspiration.

6.3.5 Moisture Fluxes

The fluxes of moisture (precipitation, surface runoff and evapotranspiration) into and out of the ADA are assessed at a monthly and annual time steps for the 8-year period of model simulation. The modeled surface runoff in mm of water thickness are summarized and plotted in Figure 6.24. The result indicates that within the 8-year simulation period, the majority of surface runoff occurs during the months of spring and fall with the maximum surface runoff occurring in 2005 with a runoff amount of

25 mm. This would be associated with the known 2005 flood event. On the other hand, minimal or less frequent runoff events are observed between the years 2001 to 2003. During these periods, the maximum simulated runoff is about 8 mm, but less than 5 mm in most of the months. The recent Canadian Prairie drought, which started in 1999 and ended in 2004, is responsible for the minimum surface runoff that occurred between 2001 to 2003.

The 2005 flood and 2001-2003 drought phenomena are reflected in the Pine Creek streamflow data that are measured at its outlet near Melbourne (99^{o}12'51" W, 49^{o}54'03" N). This basin has a gross drainage area of 225 km^2 and lies within the ADA. The Pine Creek streamflow data is obtained from Water Survey Canada (WSC), which is the only creek that maintains a continuous records of stremflow between 1999 and 2006. The measurements show that the maximum streamflow occurs in the spring months of 2001, 2005 and 2006 during the 8-year observation periods. However, streamflow remains low during the periods of 2001 to 2003, which is also observed in the model result. Moreover, a visual inspection of Figure 6.24 shows that the timing of peak flows between the modeled runoff and the measured streamflow data are reasonably matched but the magnitudes of the simulated runoff are greatly overestimated. It should be noted at this point that this comparison (between the modeled runoff over the ADA and the Pine Creek streamflow data) is not meant to validate the model result as the gross drainage area of the Pine Creek is very small compared to the ADA. This comparison, however, is to assess the model result with respect to the hydrological dynamics and moisture flux of the aquifer.

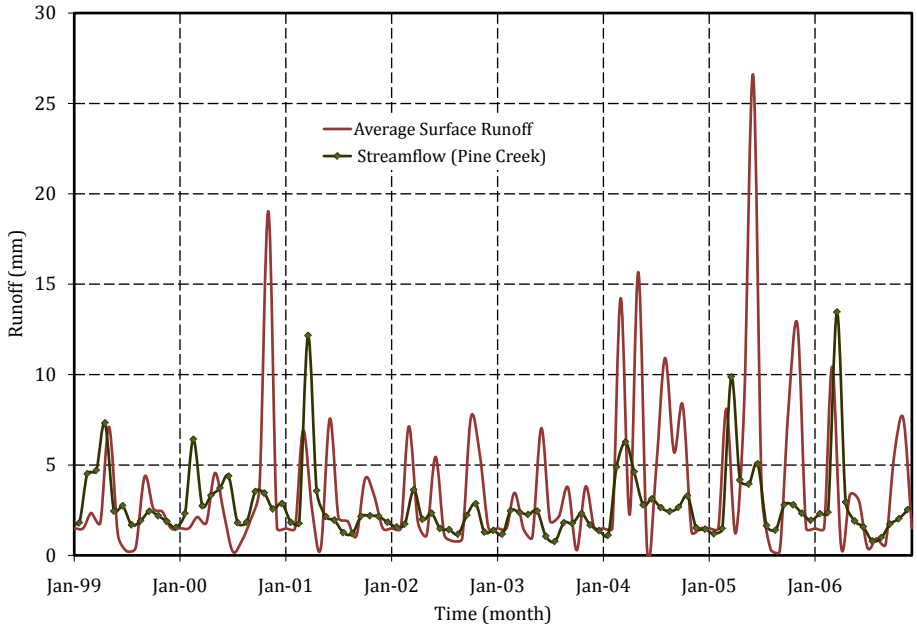

Figure 6.24: Simulated surface runoff over the ADA and measured streamflow records for the Pine Creek at its outlet near Melbourne

Moreover, the modeled monthly and annual evapotranspiration together with the forcing precipitation data (from NARR) and the simulated surface runoff and groundwater storage are presented in Figures 6.25 and 6.26, respectively. Evapotranspiration accounts for the largest portion of the moisture flux out of the ADA. On a monthly basis, most of the evapotranspiration events occur in summer and some months of spring and fall. Despite the fact that there are below average normal precipitation in the year 2001-2003, the moisture loss in the form of evapotranspiration accounts for between 70 to 80% of the precipitation and results in minimal surface runoff and reduction in groundwater storage in most of the months except during the spring period where the aquifer receives moisture from snow melt and spring precipitation. On an annual basis, the total evapotranspiration is consistent from year to year (Figure 6.26

and Table 6.3). Annually, the total evapotranspiration varies from about 250 *mm* to 315 *mm* while the total precipitation ranges from 370 *mm* to 610 *mm* with minimum precipitation observed in the years 2001, 2002, and 2003 and maximum precipitation observed in 2004 and 2005. The annual groundwater storage varies from as low as -3 *mm* in 2002 (moisture lost) to as high as 110 *mm* in 1999 (moisture gained). The moisture flux in the form of surface runoff ranges from about 25 *mm* to 75 *mm*.

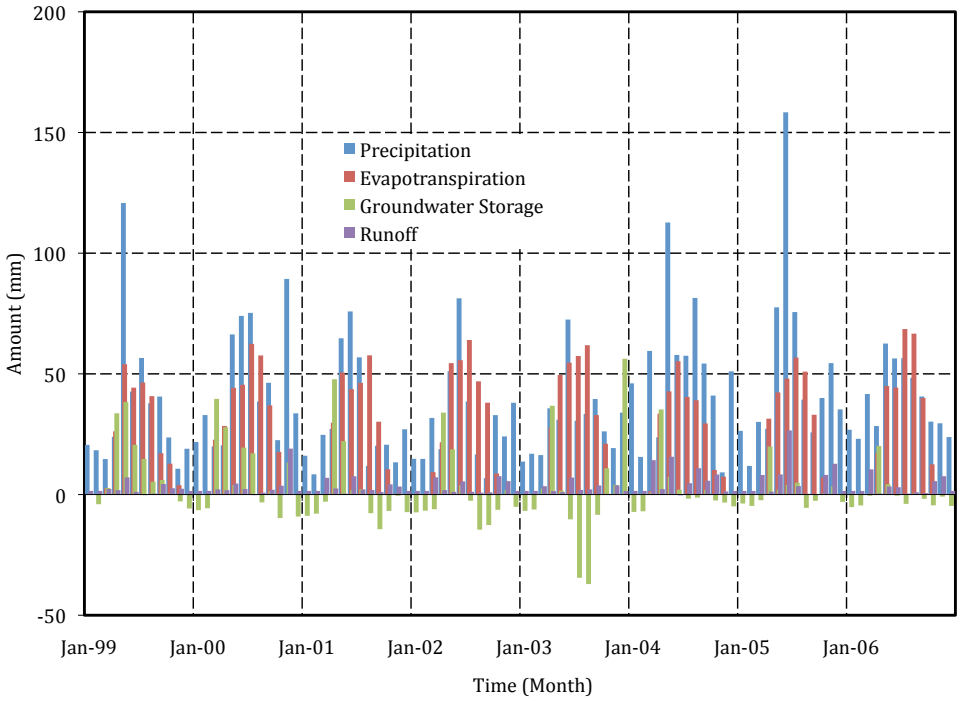

Figure 6.25: Monthly moisture fluxes (Precipitation from NARR, Evapotranspiration, Surface Runoff and Groundwater Storage) over the ADA

Table 6.3 summarizes annual moisture fluxes and percentage of evapotranspiration, surface runoff and groundwater storage with respect to total precipitation. The percentage of evapotranspiration varies from about 43% to 83%, with the 8-year average being about 60%. The percentage of groundwater storage varies from as low as

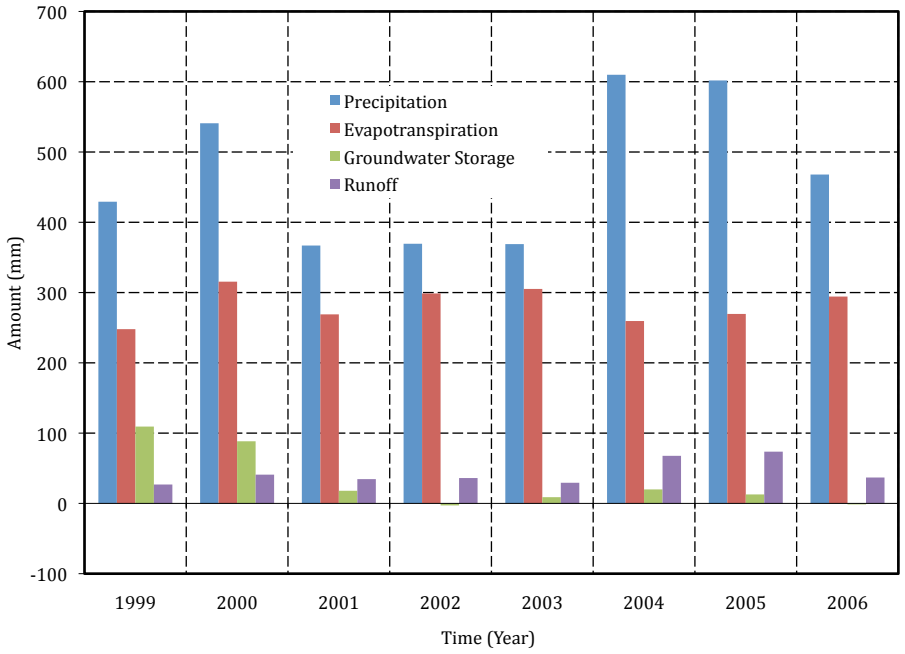

Figure 6.26: Annual moisture fluxes (Precipitation from NARR, Evapotranspiration, Surface Runoff and Groundwater Storage) over the ADA

-1% (moisture lost) to as high as 25%, with the 8-year average groundwater storage accounting for about 7% of the precipitation. Similarly, the percentage of moisture loss in the form of surface runoff ranges from 6% to 12%, with an average value of the percentage of surface runoff of about 9%. The remaining precipitated water may account for unsaturated moisture storage and snow stored on the ground.

6.4 Summary

The use of the GRACE total water storage anomalies for groundwater model calibration was explored in this study. The coupled groundwater and unsaturated model, known as CLM-PF, served to explore the use of the GRACE data for model

Table 6.3: Annual moisture fluxes (Precipitation (P) from NARR, Evapotranspiration (ET), Groundwater Storage (GWS) and Surface Runoff (R) and its percentage with respect to precipitation over the ADA

Year	P $(mm)(\%)$	ET $(mm)(\%)$	GWS $(mm)(\%)$	R $(mm)(\%)$
1999	429.26	247.93 (57.76)	109.32 (25.47)	26.88 (6.26)
2000	540.90	315.50 (58.33)	88.39 (16.34)	40.91 (7.56)
2001	366.92	268.99 (73.31)	17.97 (4.90)	34.54 (9.41)
2002	369.45	298.73 (80.86)	-2.88 (-0.78)	36.07 (9.76)
2003	368.95	305.16 (82.71)	8.84 (2.40)	29.36 (7.96)
2004	609.90	259.50 (42.55)	19.89 (3.26)	67.69 (11.10)
2005	601.82	269.58 (44.79)	12.76 (2.12)	73.62 (12.23)
2006	467.94	294.32 (62.90)	-0.53 (-0.11)	36.84 (7.87)
Average	469.39	282.46 (60.18)	31.72 (6.76)	43.24 (9.21)

calibration and to model the ADA. This study is the first of its kind to use this model over the ADA aquifer in order to quantify the availability of water for future management. The model was forced by atmospheric variables obtained from the NARR (North America Regional Reanalysis) data center at a time step of three hours. In addition, the geological and hydrological data that were available in the aquifer were used to set up the model. The measured groundwater level data, which were available at a daily time steps and collected from more than 100 observation wells, were used to assess to the validity of the model implementation in capturing the groundwater head dynamics.

A uniform vertical discretization of 0.2 m was used in both unsaturated and saturated zones. Similarly, a 5×5 km horizontal resolution was applied in the model. Then the coupled CLM-PF model was forced by the NARR data to simulate the 3D soil moisture saturation fields with a dynamically coupled approach. This means

that the unsaturated and saturated zones exchanged moisture simulated by the physically based moisture feedbacks between the two hydrological reservoirs (saturated and unsaturated zones). The groundwater model was then calibrated to match the downscaled GRACE groundwater water storage anomaly conditions with those simulated. During model calibration, adjustments were made to the aquifer hydraulic conductivities to match the monthly downscaled and simulated groundwater storage anomalies during the year 2003. Once a visual match was achieved, simulated groundwater heads were compared to the measured groundwater heads using statistical measures such as the root mean squared error ($RMSE$) and correlation of determination (R^2) between measured and simulated values at 15 observation wells locations that were used for model calibration.

Finally, the model was run for eight years (1999 - 2006) with a three hourly time step. The model simulation was computationally very expensive. With eight CPUs with 2GB of RAM per CPU, it took approximately 960 hours (40 days) to complete the 8 years simulation. Simulation output required disk space of approximately 700GB. The results obtained from this computationally expensive model clearly show the usefulness of the GRACE groundwater storage anomalies for groundwater model calibration. Using the calibrated model, it was possible to capture the groundwater head dynamics in the aquifer. The comparisons between the downscaled GRACE and simulated groundwater storage anomalies and the measured and simulated groundwater heads at selected observation wells were in good agreement during most periods. The simulated basin-average groundwater storage anomalies also compared well with the downscaled and measured groundwater storage anomalies. Similarly, even though

there is no data available to validate the simulated unsaturated soil moisture fields, it was possible to assess these fields with respect to the atmospheric conditions. The result shows a qualitative similarity between the unsaturated soil moisture response and the seasonal atmospheric simulations such as snow accumulation, snow melting, precipitation and summer temperature. Hence, from this study, it was possible to conclude that the GRACE gravity measurements will be an ideal dataset to calibrate hydrological models in areas where measured data is minimal or some times unavailable. Even in areas where hydrological models are calibrated using measured data, the GRACE gravity measurements can be used as an alternative dataset to assess or validate the developed models. In addition, the model developed over the ADA can be used as a tool to assess and manage the groundwater resource of the aquifer in a more effective way.

6.5 Future Modeling Work

This study provided valuable insight to the modeling of the ADA using a dynamically coupled physically based groundwater-surface water model. Nevertheless, it should be emphasized that even though the model result shows that there is sufficient flexibility in the model for it to exhibit behaviors that reflect observed storage changes over the ADA, these storage changes are achieved with the expense of other model fluxes. For example, forcing precipitation is underestimated by about 25% over the study period which represents approximately 780 mm over the 5-year period (see Figure 6.11), CLM-PF overestimates runoff flux as presented from Pine Creek streamflow comparison (Figure 6.24), and evapotranspiration estimated from the model is

not compared against order-of-magnitude estimates or other model results. Moreover, for the purpose of this study and the scale of the model, different assumptions were made. These assumptions include the representation of the aquifer, particularly the simplification of the saturated thickness and its structure, the non-representation of irrigation uses in the model and the utilization of few (15 out of about 100) well data to validate the model. Therefore, future-modeling task over the study area requires that the above assumptions and limitations need to be addressed before the model is put in place for general use. Additionally, the use of snow storage and intermittent streamflow measurements as an additional model validation dataset and seasonal precipitation measurements and crop yield as an input to the model could enhance the performance of the model in producing different hydrological fluxes over the ADA.

Chapter 7

Summary and Conclusions

The use of the GRACE satellite data for various hydrological applications has been explored in this thesis. Firstly, the GRACE gravity information has been analyzed and the total water storage anomalies have been determined for the Mackenzie River Basin and for the Saskatchewan River Basin. Before using the GRACE data for the various hydrological applications that are mentioned as part of the objectives of this thesis, the validation of the GRACE-based total water storages estimates using an independent technique was undertaken. This entailed retrieval of the spherical harmonic coefficients which are transformed into equivalent terrestrial water storage for the catchments and subsequently inter-compared with monthly estimates of basin total water storage derived from an atmospheric-based water balance approach. This step was necessary to enable the assessment of the quality of GRACE-based output prior to utilizing it for a number of applications.

As a result, this thesis has successfully compared two different techniques for the estimation of total water storage: the GRACE-based terrestrial water storage and

the hydrologically-based total water storage over two spatially varying catchments (Saskatchewan and Mackenzie River Basins), as a means of validation of the GRACE-based terrestrial water storage. The hydrologic storage is essentially derived from the atmospheric-based water balance $P - E$ in conjunction with the observed streamflow as recorded by the Water Survey of Canada for the chosen outlets in the respective basins. The result obtained from this study revealed a strong correlation between the GRACE-based and the hydrologically-derived total water storages over the studied basins. As evident in the time series plots displayed in Chapters 3 and 4, it is apparent that there is a good correlation between the estimated total water storage arising from the two techniques. A high value in the computed Pearson Product Moment Correlation (R) between the GRACE-derived and the atmospherically-derived total water storage provides a basis upon which the GRACE-retrieved total water storage can be used in constraining and assessing the accuracies of the simulated total water storage from a coupled land surface-hydrologic model. This is imperative as well as beneficial in that it provides an independent data source which are of highly desirable for the validation of output from a hydrologic model.

After successful validation, the GRACE-based total water storage was then utilized to assess the simulated total water storage from the WATCLASS hydrological model driven over the Mackenzie River Basin. The traditional approach of assessing the performance of a hydrological model is based solely on the goodness of fit between the simulated and observed streamflow result. However, use of streamflow alone may lead to inconclusive hydrologic model performance assessment in the studied area. Hence, as emphasized in this study, other model state variables or their derivatives

should be inter-compared with reliable data sources before any conclusion can be drawn as to the reliability of the model's outputs. The comparison of the terrestrial water storage derived from GRACE and that from the coupled land surface-hydrologic WATCLASS model over the Mackenzie River Basin and its six sub-catchments was undertaken in this study.

The principal outcome from this inter-comparison study using the terrestrial moisture storage from GRACE over the Mackenzie River Basin led to a recommendation to re-calibrate the WATCLASS hydrological model over a few of the sub-catchments within the larger Mackenzie River Basin. This has further corroborated the need for an alternative data source in addition to measured streamflow as a way of assessing a hydrological model's performance over a particular basin.

Owing to the recurrent nature of Prairie drought and the fact that the impact of drought on the different sectors of the economy is so devastating, a segment of the thesis was dedicated to the development of a robust drought index relying on the terrestrial storage from GRACE to arrive at a broader description of the severity of the last Canadian Prairie drought. The main accomplishment in this portion of this thesis led to the development of the Total Storage Deficit Index (TSDI). This index seemed more appropriate to characterize the recent Canadian Prairie drought domain since it synthesizes the various sub-surface and surface storages. The cumulative TSD provided a pictorial representation of the long-term dryness and wetness over the Saskatchewan River Basin and this resulted in the new finding that the recent Canadian Prairie drought actually terminated in May 2004. This differs from commonly held view that the cessation of this last drought occurred in mid-2003.

The outcome of this study therefore supports the pertinence and robustness of the GRACE satellite remote sensing data as a means of estimating basin total water storage necessary for drought studies in regions around the globe.

Furthermore, a downscaling technique to extract the regional ground water storage from the GRACE-based total water storage over the Assiniboine Delta Aquifer (ADA) was emphasized in one part of the thesis. The approach utilized was based on the artificial neural network (ANN) methodology to extract the groundwater storages at points and regional scales (approximately 4,000 km^2) from the large scale, GRACE-based terrestrial moisture storage. An inter-comparison of the downscaled and measured groundwater storages resulted in a high correlation coefficient value. This essentially signals a very promising prospect of wider use of the GRACE terrestrial water storage in the hydrologic community. From the analysis done in this study segment, it has been found that there is a strong agreement between the terrestrial moisture storage (output from a coarse resolution GRACE data) and the spatially averaged groundwater storage observed over the ADA. Interestingly, it can be concluded therefore that the groundwater storage component from the integrated GRACE terrestrial moisture storage represents a greater proportion of the integral storage over this deltaic aquifer. Moreover, it can be inferred from this line of investigation that with the choice of either statistical or dynamic downscaling techniques, it is possible to extract any of the sub-component storages from the GRACE integrated total water storage, on the condition that there is sufficient data to train and validate the downscaling method.

Finally, this thesis explores the potential utilization of the downscaled GRACE-based groundwater storage for the calibration and validation of a coupled land surface-groundwater hydrologic model. This model, generally known as the CLM-PF model (Common Land Model-ParFlow), was driven at 5×5 km spatial resolution with a sub-daily temporal resolution over the ADA. The results obtained from the groundwater modeling over this domain indicates that the downscaled GRACE groundwater storage is a useful data source for groundwater model parameterization. The simulated and downscaled groundwater storage anomalies as well as the simulated and measured groundwater heads showed an agreement during a large proportion of the simulation period. As seen in some of the figures presented in the thesis, there exist some discrepancies between the modeled and downscaled groundwater storage anomalies and heads during some of the runs. Expectedly, uncertainties exist in the meteorological forcing and in the model's structure. These to a large extent could account for these discrepancies. However, even with these discrepancies, this study has demonstrated how pertinent and useful the GRACE data is for hydrological studies especially in terrain types or basins where measured data is unavailable. This is especially true for areas on the globe where availability of data is sparse or unavailable for hydrological modeling owing to harsh climatic conditions and due to potential restriction resulting from geopolitical boundaries. In these scenarios, the GRACE data, which is available globally would serve as an alternate dataset that could be put to numerous uses for hydrological modeling necessary for the assessment and management of future water resources.

In addition, modeling of the ADA will help to better understand long term sustainability of the aquifer water resources and to incorporate climatic variability that can influence or alter its sustainable yield and allocation limits for future water use. This could influence alternative adaptation and management strategies. To date and to the author's best knowledge, no groundwater model has been developed for the ADA area and this work appears to be one of the first efforts along this direction. Although the developed model has a relatively coarse spatial resolution (5×5 km), it is sufficient to quantify the groundwater resource in this aquifer and this will serve as a benchmark for future detailed groundwater modeling studies.

In conclusion, this thesis has demonstrated the diverse applications of the GRACE gravity measurements for hydrological studies over spatially varying basins in Canada. As discussed in the thesis, it has been demonstrated that the GRACE data can be used for terrestrial hydrological studies such as drought characterization and regional hydrological model calibration. At continental and regional scales, the GRACE measurements can be employed in the estimation of the total water storage distribution over basins as depicted in the case of the Mackenzie River Basin and its associated sub-catchments, and for drought characterization and hydrological model calibration as in the case of the Saskatchewan River Basin and the Assiniboine Delta Aquifer, respectively.

References

[] Abart, C., 2005: Assessment of solution strategies for GRACE gravity field processing. M.Sc. Thesis, Institute of Navigation and Satellite Geodesy, Graz University of Technology, Austria.

[] Alberto, M. M., C. Zhang and D. B. Enfield, 2005: Uncertainties in estimating moisture fluxes over the Intra-Americas Sea. J. Hydrometeor, 6: 696-709.

[] Andersen, O. B. and J. Hinderer, 2005a: Global inter-annual gravity changes from GRACE: Early results. Geophys. Res. Lett, 32, L01402, doi:10.1029/2004GL020948.

[] Andersen, O. B., S.I. Seneviratne, J. Hinderer and P. Viterbo, 2005b: GRACE-derived terrestrial water storage depletion associated with the 2003 European heat wave. Geophys. Res. Lett., 32, L18405, doi:10.1029/2005GL023574.

[] Ashby, S. F., and R.D. Falgout, 1996: A parallel multigrid preconditioned conjugate grandient algorithm for groundwater flow simulations. Nucl. Sci. Eng., 124: 145-159.

[] Becker, A. and P. Braun, 1999: Disaggregation, aggregation and spatial scaling in Hydrological Modeling. J. Hydrology, 217: 239-252.

[] Beven, K.J. and J. Freer, 2001: Equifinality, data assimilation, and uncertainty estimation in mechanistic modelling of complex environmental systems. J. Hydrology, 249: 11-29.

[] Bonan, G. B., 1998: A Land Surface Model (LSM version 1.0) for Ecological, Hydrological, and Atmospheric Studies: Technical Description and Users Guide. NCAR Tech. Note NCAR/TN-4171STR. National Center for Atmospheric Research, Boulder, CO, 150 pp.

[] Boronina, A., and G. Ramillien, 2007: Application of AVHRR imagery and GRACE measurements for calculation of actual evapotranspiration over the Quaternary aquifer (Lake Chad basin) and validation of groundwater models. J. Hydrology. 348: 98-109, doi:10.1016/j.jhydrol.2007.09.061.

[] Bosilovich, M. G. and S. D. Schubert, 2002: Water vapor tracers as diagnostics of the regional hydrologic cycle. J. Hydrometeor. 3: 149-165.

[] Brubaker, K.L., D. Entekhabi and P.S. Eagleson, 1994: Atmospheric water vapor transport and Continental Hydrology over the Americas. J. Hydrology. 155: 407-428.

[] Chen, J.L., C.R. Wilson, J.S. Famiglietti and M. Rodell, 2005a: Spatial sensitivity of GRACE time-variable gravity observations. J. Geophys. Res., 110, B08408.

[] Chen, J.L., M. Rodell, C.R. Wilson and J.S Famiglietti, 2005b: Low degree spherical harmonic influences on GRACE water storage estimates. Geophys. Res. Lett, 32, L14405, doi: 10.1029/2005GL022964.

[] Chow, V.T, D.R. Maidment and L.W. Mays, 1988: Applied Hydrology, McGraw-Hill series in water resources and environmental engineering. McGraw-Hill, Inc., p. 572.

[] Cihlar, J., and J. Beaubien, 1998: Land Cover of Canada 1995 Version 1.1. Digital dataset Documentation, Natural Resources Canada, Ottawa, Ontario.

[] Clapp, R. B. and G.M Hornberger, 1978: Empirical equations for some soil hydraulic properties. Water Resour. Res., 14: 601-604.

[] Cosby, B. J., G.M Hornberger, R.B. Clapp and T.R. Ginn, 1984: A statistical exploration of the relationships of soil moisture characteristics to the physical properties of soils. Water Resour. Res., 20: 682-690.

[] Cote, J., S. Gravel, A. Methot, A. Patoine, M. Roch and A. Staniforth, 1998: The Operational CMC-MRB Global Environmental Multiscale (GEM) Model. Part I: Design Considerations and Formulation, Monthly Weather Review, 126: 6, 1373-1395.

[] Dai, Y. J. and Coauthors, 2003: The Common Land Model. Bull. Amer. Meteor. Soc., 84: 1013-1023.

[] Dai, Y. J., and Q.C. Zeng, 1997: A land surface model (IA94) for climate studies. Part I: Formulation and validation in of-line experiments. Adv. Atmos. Sci., 14, 433-460.

[] Dibike, Y. B. and P. Coulibaly, 2006: Temporal neural networks for downscaling climate variability and extremes. Neural Networks, 19: 135-144.

[] Dibike, Y. B. and P. Coulibaly, 2004: Hydrologic Impact of Climate Change in the Saguenay Watershed: Comparison of Downscaling Methods and Hydrologic Models, J ournal of Hydrology, 307, 145-163.

[] Dickinson, R. E., P.J Kennedy, A. Henderson-Sellers and M. Wilson, 1993: Biosphere-Atmosphere Transport Scheme (BATS) for the NCAR Community Climate Model. NCAR Tech. Note NCAR/TN-275STR, 69 pp.

[] Fassnacht, S.R., 1997: A Multi-channel suspended sediment transport model for the Mackenzie Delta, Northwest Territories. J. Hydrology, 197: 128-145.

[] Filmon, P.C., 2004: Firestorm 2003 Provincial Review, Province British Colombia, Vancouver, B.C.

[] Frost, L.H. and F.W. Render, 2002: Hydrogeological Summary of the Assiniboine Delta Aquifer, Manitoba Conservation, Winnipeg, MB.

[] Govindaraju, R.S, 2000: Artificial neural networks in hydrology, I: Preliminary Concepts. J. Hydrologic Engineering (ASCE), 5(2): 115-123.

[] Hay, L.E. and M.P. Clark, 2003: Use of statistically and dynamically downscaled atmospheric model output for hydrologic simulations in three mountainous basins in the Western United States. J. Hydrology, 282: 56-75.

[] Haykin, S., 1994: Neural Networks. Macmillan College Publishing Company, Inc, New York.

[] Heiskanen, W. A. and H. Moritz, 1967: Physical Geodesy. San Francisco: W.H. Freeman and Company.

[] Hu, Q. and S. Feng, 2001: Climatic role of the southerly flow from the Gulf of Mexico in interannual variations in summer rainfall in the central United States. J. Climate. 14: 3156-3170.

[] Jackson, T.J., D.M. LeVine, A.Y. Hsu, A. Oldak, P.J. Starks, C.T. Swift, J.D. Isham and M. Haken, 1999: Soil Moisture Mapping at Regional Scales using Microwave Radiometry: The Southern Great Plains Hydrology Experiment. IEEE Trans. Geosci. Rem. Sens., 37: 2136-2151.

[] Jain, S. K., V.P. Singh and M.T. Van Genuchten, 2004: Analysis of soil water retention data using artificial neural networks. J. Hydraulic Engineering (ASCE), 9(5): 415-420.

[] Jain, S. K., A. Das and D.K. Srivastava, 1999: Application of ANN for reservoir inflow prediction and operation. J. Water Resour. Plan. Manage., 125(5): 263-271.

[] Jones, J. E. and C.S. Woodward, 2001: Newton-Krylov-multigrid solvers for large-scale, highly heterogeneous, variably saturated flow problems. Adv. Water Resour., 24, 763-774.

[] Khan, M.S. and P. Coulibaly, 2006: Bayesian Neural Network for rainfall-runoff modeling. Water Resour. Res., doi:10.1029/2005WR003971.

[] Kim, G., and Ana P. Barros, 2002: Downscaling of Remotely Sensed Soil Moisture with a Modified Fractal Interpolation Method Using Contraction Mapping and Ancillary Data. Remote Sensing of Environment, 83: 400-413.

[] Kite, G. W., A. Dalton and K. Dion, 1994: Simulation of stream flow in a marcoscale watershed using general circulation model data. Water Resour. Res. 30(5): 1547-1559.

[] Kite, G. W. and U. Haberlandt, 1999: Atmospheric model data for macroscale hydrology. J. of Hydrology, 217(3-4): 169-338.

[] Kollet, S. J. and R. M. Maxwell, 2008: Capturing the influence of groundwater dynamics on land surface processes using an integrated, distributed watershed model, Water Resour. Res., 44: W02402, doi:10.1029/2007WR006004.

[] Kollet, S.J. and R. M. Maxwell, 2006: Integrated surface-groundwater flow modeling: a free-surface overland flow boundary condition in a parallel groundwater flow model. Adv Water Resour., 29: 945-58.

[] Kouwen, N., E. D. Soulis, A. Pietroniro, J. Donald and R. A. Harrington, 1993: Grouped response units for distributed hydrologic modeling. J. Water Resources Planning and Management (ASCE), 119(3): 289-305.

[] Kreyszig, E, 1993: Advanced Engineering Mathematics. 7^{th} Edition, John Wiley and Sons, Inc.

[] Kumar, M., N. S. Raghuwanshi, R. Singh, W. W. Wallender and W. O. Pruitt , 2002: Estimating evapotranspiration using artificial neural network. J. Irrig. Drain. Eng., 128(4): 224-233.

[] Lavado Contador, J., M. Maneta and S. Schnabel, 2006: Prediction of near-surface soil moisture at large scale digital terrain modeling and neural networks. Environmental Monitoring and Assessment, 121: 213-232.

[] Louie, P.Y.T., W. D. Hogg, M. D. MacKay, X. Zhang and R. F. Hopkinson, 2002: The water balance climatology of the Mackenzie Basin with reference to the 1994/95 Water year. Atmosphere-Ocean, 40 (2): 159-180.

[] Loukili, Y., A. D. Woodbury and K. R. Snelgrove, 2008: SABAE-HW: An enhanced water balance prediction in the Canadian Land Surface Scheme compared with existing models. Vadose Zone J., 7: 865-877.

[] Maxwell, R. M., F. K. Chow and S. Kollet, 2007: The groundwater-land-surface-atmosphere connection: Soil moisture effects on the atmospheric boundary layer in fully-coupled simulations. Adv Water Resour., 30:2447-2466.

[] Maxwell, R.D and N.L Miller, 2005: Development of a Coupled Land Surface and Groundwater Model. J. Hydrometeo., 6: 233-247.

[] Mesinger, F. and Co-authors, 2006: North American Regional Reanalysis. Bull. Amer. Meteor. Soc., 87: 343-360.

[] Milly, P. C. D.,1994: Climate, soil water storage, and the average annual water balance. Water Resour. Res., 30: 2143-2156.

[] Milly, P. C. D. and K. A. Dunne, 1994: Sensitivity of the global water cycle to the water holding capacity of land. J. Clim. 7: 506-526.

[] Montgomery, D. and G. Runger, 2002: Applied Statistics and Probability for Engineers. 3^{rd} Ed, USA, John Wiley and Sons, Inc.

[] Narasimhan, R. and R. Srinivasan, 2005: Development and evaluation of Soil Moisture Deficit Index (SMDI) and Evapotranspiration Deficit Index (ETDI) for agricultural drought monitoring, Agricultural and Forest Meteorology, 133: 69-88.

[] Njoku, E.G. and N.-A. Kong, 1977: Theory for passive microwave remote sensing of near-surface soil moisture. J. Geophys. Res., 82: 3108-3118.

[] Nijssen, B., Bowling, L.C., Lettenmaier, D.P., Clark, D.B., El Maayar, M., Essery, R., Goers, S., Gusev, Y.M., Habets, F., van den Hurk, B., Jin, J.M., Kahan, D., Lohmann, D., Ma, X.Y., Mahanama, S., Mocko, D., Nasonova, O., Niu, G.Y., Samuelsson, P., Schmakin, A.B., Takata, K., Verseghy, D., Viterbo, P., Xia, Y.L., Xue, Y.K. and Yang, Z.L., 2003. Simulation of high latitude hydrological processes in the Torne-Kalix basin: PILPS phase 2(e) - 2: Comparison of model results with observations. Global and Planetary Change, 38(1-2): 31-53.

[] Oki, T., K. Musiake, H. Matsuyama and K. Masuda, 1995: Global atmospheric water balance and runoff from large river basins. Hydrological Processes, 9: 655-678.

[] Palmer, W.C., 1965: Meteorological drought, Research Paper 45. U.S Department of Commerce, Weather Bureau, Washington, D.C.

[] Pellenq J., J. Kalma, G. Boulet, G.M. Saulnier, S. Wooldridge, Y. Kerr and A.

Chehbouni, 2003: A disaggregation scheme for soil moisture based on topography and soil depth. J. Hydrology, 276: 112-127.

[] Ramillien, G., A. Cazenave and O. Brunau, 2004: Global time variations of hydrological signals from GRACE satellite gravimetry. Geophys. J. Int., 158: 813-826.

[] Rasmusson, E.M, 1997: Atmospheric water vapor transport and the water balance of North America: Part 1. Characteristics of the water vapor flux field. Monthly Weather Review, 7: 403-426.

[] Reed, S., D. Maidment and J. Patoux, 1997: Spatial water balance of Texas, Center for Research in Water Resources, University of Texas at Austin, Texas.

[] Reichle, R. H., D. Entekhabi and D. B. McLaughlin, 2001: Downscaling of radio brightness measurements for soil moisture estimation: A Four-dimensional variational data assimilation approach. Water Resour. Res., 37(9): 2353-2364.

[] Reigber, C., R. Schmidt, F. Flechtner, R. Konig, U. Meyer, K.-H. Neumayer, P. Schwintzer and S. Y. Zhu, 2005: An Earth gravity field model complete to degree and order 150 from GRACE: EIGEN:GRACE02S. Journal of Geodynamics, 39: 1-10.

[] Richard, L. A., 1931: Capillary conduction of liquids through porous mediums. Physics, 1: 318-333.

[] Rodell, M. and J. S. Famiglietti, 1999: Detectability of variations in continental water storage from satellite observations of the time dependent gravity field. Water Resour. Res., 35: 2705-2723.

[] Rodell, M. and J. S. Famiglietti, 2002: The potential for satellite-based monitoring of groundwater storage changes using GRACE: The high plains aquifer, central U.S. J. Hydrology, 263: 245-256.

[] Rodell, M., J. S. Famiglietti, J. Chen, S. I. Seneviratne, P. Viterbo, S. Holl and C. R. Wilson, 2004: Basin scale estimates of evapotranspiration using GRACE and other observations. Geophys. Res. Lett., 31: L20504, doi:10.1029/2004GL020873.

[] Ronald, S., 2002: Towards understanding water and energy processes within the Mackenzie River Basin. Atmosphere-Ocean, 40(2): 91-94.

[] Schoof, J.T. and S. C. Pryor, 2001: Downscaling temperature and precipitation: A comparison of regression-based methods and artificial neural networks. International Journal of Climatology, 21: 773-790.

[] Seo, K.-W., C. R. Wilson, J. S. Famiglietti, J. L. Chen and M. Rodell, 2006: Terrestrial water mass load changes from Gravity Recovery and Climate Experiment (GRACE), Water Resour. Res., 42: W05417, doi:10.1029/2005WR004255.

[] Snelgrove, K. R., 2002: Implications of lateral flow generation on land-surface scheme fluxes. Ph.D. Thesis, University of Waterloo, Ontario, Canada.

[] Snelgrove, K.R., E. D. Soulis, F. R. Seglenieks and N. Kouwen, 2005: The application of hydrological models in MAGS: lessons learned for PUB. In prediction in ungauged basins: Approaches for Canadas cold regions. Spence, C., J.W. Pomeroy and A. Pietroniro (eds.). Canadian Water Resources Association. 139-164.

[] Snelgrove, K.R., S. Z. Yirdaw and E. D. Soulis, 2004: GRACE (Gravity Recovery And Climate Experiment) measurements of the Mackenzie River Basin water balance. Eos Trans. AGU, 85(47): Fall Meet. Suppl., F780.

[] Solomon, S.I., C. F. Cadou, J. P. Jolly and E. D. Soulis, 1977: Regional flood analysis for proposed Arctic gas pipeline route. Proceedings Canadian Hydrology Symposium: 77, Edmonton, Alberta, 11 p.

[] Soulis, E.D. and F. Seglenieks 2007: The MAGS integrated modeling system. Cold regions atmospheric and hydrologic studies: the Mackenzie GEWEX experience. Vol. II: Hydrologic Processes, Ed. M.K. Woo, Springer-Verlag, 445-474.

[] Soulis, E.D., N. Kouwen, A. Pietroniro, F.R. Seglenieks, K.R. Snelgrove, P. Pellerin, D.W. Shaw and L.W. Martz, 2005: A framework for hydrological modelling in MAGS. In prediction in ungauged basins: Approaches for Canadas cold regions. Spence, C., J.W. Pomeroy and A. Pietroniro (eds.), Canadian Water Resources Association, 119-138.

[] Soulis, E.D. and D. G. Vincent, 1977: Statistics of individual storm events from daily rainfall records. Proceedings, Second Hydrometeorology Conference, Toronto, Ontario, October, 6 p.

[] Strong, G. S., B. Proctor, M. Wang, E. D. Soulis, C. D. Smith, F. R. Seglenieks and K.R. Snelgrove, 2002: Closing the Mackenzie basin water budget, water years 1994-95 through 1996-97. Atmosphere-Ocean, 40(2): 113-124.

[] Swenson, S., J. Wahr and P. C. D. Milly, 2003: Estimated accuracies of regional water storage variations inferred from the Gravity Recovery and Climate Experiment (GRACE). Water Resour. Res., 39(8): 1223, doi:10.1029/2002WR001808.

[] Syed, T. H., J. S. Famiglietti, J. Chen, M. Rodell, S. I. Seneviratne, P. Viterbo and C. R. Wilson, 2005: Total basin discharge for the Amazon and Mississippi River Basins from GRACE and a land-atmosphere water balance. Geophys. Res. Lett., 32: L24404, doi:10.1029/2005GL024851

[] Syed, T. H., J. S. Famiglietti, V. Zlotnicki and M. Rodell, 2007: Contemporary estimates of Pan-Arctic freshwater discharge from GRACE and reanalysis. Geophys. Res. Lett., 34: L19404, doi:10.1029/2007GL031254.

[] Talagrand, O., 1997: Assimilation of Observations, an Introduction. J. Meteorological Society of Japan, 75: 191-209.

[] Tapley, B. D., S. Bettadpur, M. Watkins and C. Reigber, 2004a: The Gravity Recovery and Climate Experiment: Mission overview and early results. Geophys. Res. Lett., 31: L09607, doi:10.1029/2004GL019920.

[] Tapley, B. D., S. Bettadpur, J. Ries, P. F. Thompson and M. M. Watkins, 2004b: GRACE measurements of mass variability in the Earth system. Science, 305: 503-505.

[] Van Genuchten, M. T., 1980: A closed form equation for predicting the hydraulic conductivity of unsaturated soils. Soil Sci. Soc. Amer. J., 44: 892-898.

[] Verseghy, D.L., 1991: CLASS - A Canadian Land Surface Scheme for GCMs, I. Soil model, International Journal of Climatology, 11: 111-133.

[] Von Storch, H., H. Langenberg and F. Feser, 2000: A spectral nudging technique for dynamical downscaling purposes. Mon. Wea. Rev., 128: 3664-3673.

[] Wagner, W., G. Lemoine and H. Rot, 1999: A method for estimating soil moisture from ERS scatterometer and soil data. Remote Sens. Environ., 70: 191-207.

[] Wahr, J., M. Molenaar and F. Bryan, 1998: Time-variability of the Earths gravity field: Hydrological and oceanic effects and their possible detection using GRACE. J. Geophys. Res., 103 (30): 205-230.

[] Wahr, J., S. Swenson, V. Zlotnicki and I. Velicogna, 2004: Time-variable Gravity from GRACE: First Results. Geophys. Res. Lett., 31: L11501, doi:10.1029/2004GL019779.

[] Walsh, J. E., X. Zhou, D. Portis and M. C. Serreze, 1994: Atmospheric contribution to hydrologic variations in the arctic. Atmosphere-Ocean, 32(4): 733-755.

[] Weichert, A., and G. Burger, 1998: Linear versus nonlinear techniques in downscaling. Climate Research, 10: 83-93.

[] Western, A.W. and G. Bloschl, 1999: On spatial scaling of soil moisture. J. Hydrology, 217: 203- 224.

[] Wheaton, E., V. Wittrock, S. Kulshreshtha, G. Koshida, C. Grant, A. Chipanshi and B. Bonsal, 2005: Lessons learned from the Canadian drought years of 2001 and 2002. Agriculture and Agri-Food Canada. Smart Science Solution, 11602-46E03.

[] Wilson, B., I. Trpanier and M. Beaulieu, 2002: The western Canadian drought of 2001-how dry was it?. Statistics Canada., 21-004-XIE.

[] Yeh, P. J.-F., S. C. Swenson, J. S. Famiglietti and M. Rodell, 2000: Remote sensing of groundwater storage changes in Illinois using the Gravity Recovery and Climate Experiment (GRACE). Water Resour. Res., 42: W12203, doi:10.1029/2006WR005374.

[] Yirdaw, S. Z. and K. R. Snelgrove, 2006: Validation of regional precipitation minus evaporation using a coupled GRACE driven moisture storage and measured basin runoff, Eos Trans. AGU, 87(52): Fall Meet. Suppl., GC41A-1031.

[] Yirdaw, S. Z., K. R. Snelgrove and C. O. Agboma, 2008: GRACE satellite observations of terrestrial moisture changes for drought characterization in the Canadian Prairie. J. Hydrology, 356 (1-2): 84-92.

[] Yirdaw, S.Z., K. R. Snelgrove, F. R. Seglenieks, C. O. Agboma and E. D. Soulis, 2009: Assessment of the WATCLASS hydrological model result of the Mackenzie River Basin using the GRACE satellite total water storage measurement. Hydrological Processes, 23:23, 3391-3400.